CAPITAL UNIVERSITY OF SCIENCE AND TECHNOLOGY, ISLAMABAD


# A study on Anti-diabetic Attributes of *Astragalus membranaceus* against Type 2 Diabetes Mellitus

by

Haseeb Ul Hassan

A thesis submitted in partial fulfillment for the degree of Master of Science

in the

Faculty of Health and Life Sciences
Department of Bioinformatics and Biosciences

2026

## CERTIFICATE OF APPROVAL

# A study on Anti-diabetic Attributes of *Astragalus membranaceus* against Type 2 Diabetes Mellitus

by

Haseeb Ul Hassan

(MBS243015)

### THESIS EXAMINING COMMITTEE

| S. No. | Examiner | Name | Organization |
|---|---|---|---|
| (a) | External Examiner | Dr. Muhammad Imran | QAU, Islamabad |
| (b) | Internal Examiner | Dr. Syeda Marriam Bakhtiar | CUST, Islamabad |

Dr. Rizwan ur Rehman
Thesis Supervisor
April, 2026

Dr. Syeda Marriam Bakhtiar
Head
Dept. of Bioinfo. & Biosciences
April, 2026

Dr. Sahar Fazal
Dean
Faculty of Health & Life Sciences
April, 2026

# *Author's Declaration*

I, **Haseeb Ul Hassan** hereby state that my MS thesis titled "**A study on Anti-diabetic Attributes of *Astragalus membranaceus* against Type 2 Diabetes Mellitus**" is my own work and has not been submitted previously by me for taking any degree from Capital University of Science and Technology, Islamabad or anywhere else in the country/abroad.

At any time if my statement is found to be incorrect even after my graduation, the University has the right to withdraw my MS Degree.

**(Haseeb Ul Hassan)**

Registration No: MBS243015

# *Plagiarism Undertaking*

I solemnly declare that research work presented in this thesis titled "**A study on Anti-diabetic Attributes of *Astragalus membranaceus* against Type 2 Diabetes Mellitus**" is solely my research work with no significant contribution from any other person. Small contribution/help wherever taken has been duly acknowledged and that complete thesis has been written by me.

I understand the zero tolerance policy of the HEC and Capital University of Science and Technology towards plagiarism. Therefore, I as an author of the above titled thesis declare that no portion of my thesis has been plagiarized and any material used as reference is properly referred/cited.

I undertake that if I am found guilty of any formal plagiarism in the above titled thesis even after award of MS Degree, the University reserves the right to withdraw/revoke my MS degree and that HEC and the University have the right to publish my name on the HEC/University website on which names of students are placed who submitted plagiarized work.

**(Haseeb Ul Hassan)**
Registration No: MBS243015

# *Acknowledgement*

All praise and gratitude to Allah Almighty, the Most Merciful and Beneficent, whose blessings and guidance have enabled me to complete this work. I send my humble salutations to the Holy Prophet Muhammad (PBUH), the epitome of guidance and knowledge.

"I extend my heartfelt gratitude to my esteemed supervisor, Dr. Rizwan Ur Rehman, for their invaluable guidance, expertise, and unwavering support throughout this journey. I would like to express my sincere appreciation to Asadullah Nasir and Dr. Maliha, for their valuable input, encouragement, and support.

My deepest gratitude goes to my family: my grandparents, especially Dada Raja Muhammad Arif; my beloved mother, Shaista Farhat; and my dear father, Raja Muhammad Shawaiz, whose unwavering support and sacrifices have brought me here. My siblings, Anees Raja and Anusha Eman, have been a constant source of motivation.

My loving aunts, Rashida Khatoon, Razia Afreen, Ismat Ara, and Tanveer BiBi, your encouragement and care mean a lot to me. My uncles, Shahid Liaqat and Sahadat Hussain Raja, your guidance and support have been invaluable. And especially to Uncle Sahadat Hussain Raja, who has been my rock throughout this journey, providing financial and moral support – thank you for believing in me, Forever grateful. To all my teachers, mentors, and well-wishers who have contributed to my growth and learning, I am forever grateful."

Meanwhile, I am highly thankful to Higher Education Commission of Pakistan, who provided the research funding under the project **#NRPU 16186 Title "Isolation and Identification of therapeutic agents involved in the activation of PPAR-$\gamma$ to ameliorate Type 2 Diabetes"** for the accomplishment of the thesis.

**(Haseeb Ul Hassan)**

# *Abstract*

Type 2 Diabetes Mellitus (T2DM) is a widespread metabolic disorder that is associated with insulin resistance and an abnormality in glucose metabolism, resulting in chronic hyperglycemia and severe health complications globally. The increasing prevalence of T2DM necessitates the need for effective, safe, and cost-effective treatment options, thereby emphasizing the need for the use of traditional medicinal plants such as *Astragalus membranaceous*. This medicinal plant has been employed for several centuries in Ayurvedic medicine and traditional practices due to its high phytochemical composition, such as phenols, flavonoids, and alkaloids, which are well known for their antioxidant properties. This research aims to explore the fractionation of the methanolic leaf extract of *A. membranaceous* through column chromatography. These fractions were analyzed through thin-layer chromatography and combined to form three super-fractions i.e., AF1, AF2 and AF3. These were further evaluated for their antioxidant and antidiabetic potential through different bioactivity assays. The findings revealed the presence of strong antioxidant properties and potent inhibitory action of $\alpha$-glucosidase and $\alpha$-amylase enzymes in AF2. The phytochemical screening of super-fractions through LC-MS indicated the presence of aristolone, medicarpin, riboflavin and vasicine. These compounds were docked against T2DM target proteins i.e., Akt2, PI3K-$\alpha$, PPAR-$\gamma$, IRS-2 and PDX-1. Riboflavin from super-fraction AF2 was selected as lead compound because of high docking score i.e., -9.1 against Akt2 and good ADMET and interaction profile. To test the additional efficiency of riboflavin, it was evaluated against the commercial anti-diabetic drug metformin. Comparing riboflavin with metformin with respect to ADMET analysis, which was comparable, though the docking score and interaction profile of riboflavin are better than those of metformin. Thus, it is concluded at this stage that AF2 proved to be a good fraction in the context to anti-oxidative and anti-diabetic activities. Moreover, the lead compound riboflavin from AF2 possesses the ability to be a potential anti-diabetic drug of the future.

**Keywords:** Type 2 diabetes mellitus, riboflavin, ADMET profile, anti-diabetic, super-fractions, anti-oxidative

# Contents

# List of Figures

# List of Tables

# Abbreviations

| | |
|---|---|
| **AMPK** | AMP-activated protein kinase |
| **APS** | Astragalus polysaccharides |
| **ATP** | Adenosine triphosphate |
| **BCAAs** | Branched-chain amino acids |
| **CGM** | Continuous glucose monitor |
| **CKD** | Chronic kidney disease |
| **CRISPR** | Clustered Regularly Interspaced Short Palindromic Repeats |
| **DAG** | Diacylglycerol |
| **DM** | Diabetes mellitus |
| **DPP-4** | Dipeptidyl peptidase-4 |
| **ER** | Endoplasmic reticulum |
| **FDA** | Food and Drug Administration |
| **FOXO1** | Forkhead box protein O1 |
| **G6Pase** | Glucose-6-phosphatase |
| **GLP-1** | Glucagon-like peptide-1 |
| **GLUT4** | Glucose transporter type 4 |
| **GSK3** | Glycogen synthase kinase 3 |
| **HFrEF** | Heart failure with reduced ejection fraction |
| **HSL** | Hormone-sensitive lipase |
| **HbA1c** | Hemoglobin A1c |
| **IDF** | International Diabetes Federation |
| **IKK** | Inhibitor of kappa B kinase |
| **IL-6** | Interleukin-6 |
| **INSR** | Insulin receptor |

| | |
|---|---|
| **iPSCs** | Induced pluripotent stem cells |
| **IRS** | Insulin receptor substrate |
| **JNK** | c-Jun N-terminal kinase |
| **LC-MS/MS** | Liquid chromatography–mass spectrometry/mass spectrometry |
| **mTORC1** | Mechanistic target of rapamycin complex 1 |
| **mTOR** | Mechanistic target of rapamycin |
| **NCCIH** | National Center for Complementary and Integrative Health |
| **PDK1** | Phosphoinositide-dependent kinase 1 |
| **PEPCK** | Phosphoenolpyruvate carboxykinase |
| **PI3K** | Phosphoinositide 3-kinase |
| **PKB** | Protein kinase B (Akt) |
| **PKC** | Protein kinase C |
| **PPAR-$\gamma$** | Peroxisome proliferator-activated receptor gamma |
| **PTEN** | Phosphatase and tensin homolog |
| **PTP1B** | Protein tyrosine phosphatase 1B |
| **RNAi** | RNA interference |
| **ROS** | Reactive oxygen species |
| **S6K** | Ribosomal protein S6 kinase |
| **SGLT2** | Sodium-glucose cotransporter 2 |
| **SH2** | Src homology 2 domain |
| **SOCS** | Suppressor of cytokine signaling |
| **T1DM** | Type 1 diabetes mellitus |
| **T2DM** | Type 2 diabetes mellitus |
| **TNF-$\alpha$** | Tumor necrosis factor-alpha |
| **TNFR** | Tumor necrosis factor receptor |
| **TZDs** | Thiazolidinediones |
| **UTI** | Urinary tract infection |

# Chapter 1

# Introduction

Diabetes mellitus (DM) is a chronic metabolic condition marked by sustained hyperglycemia resulting from impairments in insulin secretion, insulin action, or both. It has become one of the most urgent public health challenges globally due to its swiftly rising prevalence and significant impact on morbidity, mortality, and economic burden [1]. The disease includes a diverse array of metabolic disorders that disrupt glucose homeostasis by impairing carbohydrate, lipid, and protein metabolism. Type 1 diabetes mellitus (T1DM) and type 2 diabetes mellitus (T2DM) are the two most common forms, differing in their aetiology yet exhibiting analogous pathophysiological outcomes of hyperglycemia and related complications. Type 1 diabetes mellitus (T1DM) arises from the autoimmune destruction of pancreatic $\beta$-cells, resulting in complete insulin deficiency, whereas type 2 diabetes mellitus (T2DM), which constitutes about 90% of worldwide diabetes cases, primarily develops due to insulin resistance coupled with relative insulin deficiency [2, 3].

The International Diabetes Federation (IDF) reports that the adult population with diabetes reached 589 million in 2025, accounting for nearly one in nine adults globally, with projections estimating an increase to 853 million by 2050. Regional trends demonstrate significant increases in Africa (134%), South-East Asia (68%), and the Middle East (62%), indicative of lifestyle transitions, urbanisation, and ageing demographics [4, 5]. In Pakistan, the burden has escalated to concerning

levels, with around 34.5 million adults impacted, constituting 31.4% of the adult population—the third-highest prevalence worldwide, following China and India. This epidemiological transition highlights diabetes as a medical and socioeconomic emergency. Global annual healthcare expenditures related to diabetes now surpass USD 1 trillion, with over 81% of affected adults living in low- and middle-income countries, where access to healthcare and medication affordability are constrained [6, 7].

The disease's complexity stems from multifactorial influences, including genetic, environmental, and lifestyle factors. The dysregulation of glucose metabolism, driven by abnormalities in insulin secretion and peripheral insulin action, is central to its pathogenesis [8]. Under typical physiological conditions, glucose metabolism guarantees energy provision and homeostasis via coordinated hormonal regulation. Subsequent to nutrient consumption, pancreatic $\beta$-cells release insulin, promoting cellular glucose absorption and its storage as glycogen, while inhibiting hepatic glucose synthesis [9]. Conversely, glucagon released by pancreatic $\alpha$-cells during fasting promotes glycogenolysis and gluconeogenesis to sustain normoglycemia [10]. This equilibrium is sustained by a closely regulated hormonal interaction involving insulin, glucagon, glucagon-like peptide-1 (GLP-1), and glucose-dependent insulinotropic polypeptide (GIP) [11].

In diabetes, impairments in insulin signalling pathways result in diminished glucose uptake by insulin-sensitive tissues, notably skeletal muscle, liver, and adipose tissue [12]. Skeletal muscle accounts for approximately 80% of postprandial glucose disposal, thereby playing a crucial role in glucose regulation [13]. The insulin receptor (INSR) is a heterotetrameric transmembrane protein consisting of two alpha and two beta subunits. Following insulin binding, autophosphorylation of the receptor transpires on the tyrosine residues (Y972, Y1158, Y1162, Y1163) of the $\beta$-subunit, thereby activating downstream signalling pathways that encompass insulin receptor substrate (IRS) proteins, phosphoinositide 3-kinase (PI3K), and protein kinase B (Akt/PKB) [14]. The activation of PI3K transforms phosphatidylinositol 4,5-bisphosphate (PIP2) into phosphatidylinositol 3,4,5-trisphosphate (PIP3), subsequently recruiting phosphoinositide-dependent

kinase-1 (PDK1) and Akt to the plasma membrane for phosphorylation and activation [15]. Akt phosphorylates various substrates involved in glucose transport, glycogen synthesis, lipogenesis, and the inhibition of gluconeogenic genes, including phosphoenolpyruvate carboxykinase (PEPCK) and glucose-6-phosphatase (G6Pase) [16, 17].

The translocation of glucose transporter 4 (GLUT4) vesicles from intracellular compartments to the plasma membrane mediates insulin-stimulated glucose uptake in skeletal muscle and adipose tissue. Activated Akt phosphorylates AS160 (TBC1D4), thereby alleviating the inhibition of Rab proteins that govern GLUT4 trafficking. Insulin signalling in the liver inhibits gluconeogenesis through Akt-mediated phosphorylation and nuclear exclusion of the transcription factor FOXO1, while facilitating glycogen synthesis by inhibiting glycogen synthase kinase - 3 (GSK3). Insulin stimulates lipid synthesis in adipose tissue by activating the mTORC1-SREBP1 pathway and inhibiting lipolysis via PDE3B-induced decrease of cAMP levels [18, 19]. These integrated pathways facilitate effective glucose clearance and energy storage during fed states. In T2DM, impairments in IRS phosphorylation, PI3K activity, and Akt signalling lead to insulin resistance, hyperglycemia, and dyslipidemia [20].

The nuclear receptor peroxisome proliferator-activated receptor-gamma (PPAR-$\gamma$) regulates glucose and lipid metabolism by influencing insulin sensitivity, adipogenesis, and fatty acid storage. PPAR-$\gamma$ agonists, including thiazolidinediones (TZDs), augment insulin sensitivity by facilitating glucose absorption and elevating adiponectin concentrations; however, they are linked to negative effects such as weight gain, edoema, and heart failure [21, 22]. The activation of PPAR-$\gamma$ by natural ligands, including polyunsaturated fatty acids, flavonoids, and triterpenoids, has shown enhanced insulin signalling through elevated IRS-1 tyrosine phosphorylation and Akt activation [23]. Thus, plant-derived PPAR agonists serve as promising alternatives for the management of insulin resistance, exhibiting fewer side effects than synthetic medications [24].

Insulin resistance, a characteristic of type 2 diabetes mellitus, arises from both

extrinsic and intrinsic mechanisms. Extrinsic factors encompass overnutrition, elevated circulating fatty acids, and chronic inflammation, which activate protein kinase C (PKC), c-Jun N-terminal kinase (JNK), and inhibitor of $\kappa$B kinase (IKK), leading to serine phosphorylation of IRS proteins and suppression of insulin signalling [25]. The accumulation of diacylglycerols (DAG) and ceramides further hinders Akt activation, worsening metabolic dysfunction [26].

Proinflammatory cytokines, including tumour necrosis factor-alpha (TNF-$\alpha$) and interleukin-6 (IL-6), released by adipose tissue macrophages, exacerbate insulin resistance by inducing suppressor of cytokine signalling (SOCS) proteins that facilitate IRS degradation [26, 27]. Intrinsic mechanisms encompass epigenetic and post-transcriptional modifications that influence insulin signalling genes, mitochondrial dysfunction, and modified miRNA regulation of essential signalling molecules [28]. Molecular disruptions lead to reduced glucose uptake, increased hepatic glucose production, and $\beta$-cell dysfunction, resulting in chronic hyperglycemia [29].

Chronic hyperglycemia results in microvascular and macrovascular complications, such as neuropathy, nephropathy, retinopathy, cardiovascular diseases, and peripheral arterial disease [30]. Oxidative stress, advanced glycation end-products (AGEs), and persistent low-grade inflammation are fundamental to these pathological mechanisms [31]. Diabetic nephropathy constitutes a substantial percentage of end-stage renal disease, whereas cardiovascular diseases are responsible for more than 65% of fatalities associated with diabetes [32, 33].

Standard therapeutic approaches for T2DM emphasise the regulation of hyperglycemia via pharmacological agents, including insulin, metformin, sulfonylureas, meglitinides, $\alpha$-glucosidase inhibitors, incretin-based therapies, and sodium-glucose cotransporter-2 (SGLT2) inhibitors [34]. Metformin, a biguanide, continues to be the primary treatment, enhancing hepatic insulin sensitivity through the activation of AMP-activated protein kinase (AMPK) and the inhibition of gluconeogenesis [35, 36]. Nonetheless, prolonged administration of these agents may result in complications including hypoglycemia, lactic acidosis, gastrointestinal distress, hepatotoxicity, and weight gain [37, 38]. Moreover, numerous medications do not

target the fundamental pathophysiological mechanisms of insulin resistance and $\beta$-cell degeneration.

In light of these challenges, there is a growing focus on investigating natural products as safer, more economical alternatives for diabetes management [39]. Medicinal plants abundant in bioactive compounds have been employed in traditional medicine systems globally and are currently undergoing scientific validation for their antidiabetic efficacy. Over 410 medicinal herbs have been recognised for their hypoglycemic properties, functioning through mechanisms including the enhancement of insulin secretion, modulation of glucose transporters, inhibition of carbohydrate-hydrolyzing enzymes, and improvement of lipid metabolism [40].

Phytochemicals, including flavonoids, tannins, phenolics, alkaloids, and saponins, enhance pancreatic $\beta$-cell function, bolster antioxidant defences, and restore insulin sensitivity [41].

Empirical evidence substantiates the effectiveness of phytochemical compounds in regulating insulin signalling. Rutin, morin, and gallic acid have shown the capacity to augment glucose uptake through the activation of the PI3K/Akt pathway and the promotion of GLUT4 translocation [42]. Mangiferin, berberine, lupeol, and ursolic acid have demonstrated the ability to enhance glucose absorption and diminish oxidative stress by modulating AMPK and PPAR-$\gamma$ signalling pathways [43]. Likewise, compounds like naringenin, kaempferol, and derivatives of resveratrol enhance lipid profiles, inhibit hepatic glucose production, and mitigate inflammatory damage [44]. These findings collectively affirm that phytochemicals have diverse antidiabetic effects via direct interaction with molecular targets in insulin signalling.

The emergence of computational biology and molecular docking techniques has transformed the identification of natural compounds that can target insulin-related proteins. In silico docking analyses of bioactive phytochemicals from Ficus racemosa, Pinus roxburghii, and Solanum xanthocarpum have demonstrated significant binding affinities with critical targets including insulin receptor substrate, PI3K, Akt, and GLUT4 [45][. These studies have yielded structural insights into

ligand-protein interactions, facilitating the systematic identification of effective natural inhibitors or activators of insulin signalling components.

*Astragalus membranaceus*, also referred to as *Astragalus propinquus* or "Huang Qi," has garnered considerable interest among antidiabetic medicinal plants due to its various pharmacological properties [46]. *A. membranaceus*, a member of the Fabaceae family, is indigenous to northern China and extensively utilised in traditional Chinese medicine for its immunomodulatory, antioxidant, and anti-inflammatory properties. The roots contain abundant bioactive compounds, particularly polysaccharides (Astragalus polysaccharides, APS), triterpenoid saponins (astragalosides I–IV), flavonoids (formononetin, calycosin), and isoflavones, all of which enhance its therapeutic efficacy. APS have demonstrated the ability to augment immune function, elevate cytokine production, and modulate oxidative stress through the regulation of the Nrf2/antioxidant pathway [6]. Astragalus extracts demonstrate vasoprotective and hepatoprotective properties by downregulating NF-$\kappa$B and proinflammatory mediators, including TNF-$\alpha$, IL-6, and COX-2.

*A. membranaceus* demonstrates hypoglycemic and insulin-sensitizing effects in diabetes by modulating the PI3K/Akt and AMPK pathways [47]. The bioactive constituents, specifically APS and astragaloside IV, enhance glucose tolerance, promote $\beta$-cell viability, and inhibit oxidative stress-induced apoptosis [48]. Research indicates that *Astragalus* treatment enhances insulin-mediated GLUT4 translocation, reinstates PI3K activity, and elevates Akt phosphorylation in skeletal muscle, consequently improving insulin sensitivity [49]. Moreover, its antioxidant and anti-inflammatory properties alleviate complications like nephropathy and retinopathy by diminishing oxidative damage and the expression of inflammatory cytokines [50]. Clinical evaluations indicate that *Astragalus*, when used in conjunction with standard hypoglycemic medications such as metformin, can enhance fasting glucose, HbA1c, and lipid profiles more effectively than pharmacotherapy alone [51].

The diverse effects position *Astragalus membranaceus* as a potential adjunctive treatment for diabetes. The phytoconstituents interact with various molecular targets associated with insulin resistance and $\beta$-cell dysfunction, providing a comprehensive strategy for disease management with minimal side effects. Despite

extensive traditional use and emerging scientific validation, the exact molecular mechanisms underlying the antidiabetic effects of *A. membranaceus* remain inadequately understood. Consequently, integrating in silico molecular docking with in vitro and *in vivo* analyses can yield enhanced understanding of its bioactive compounds and their prospective interactions with insulin signalling proteins [52].

This study aims to examine the bioactive compounds of *Astragalus membranaceus* using computational docking and biochemical assessment to identify effective antidiabetic agents targeting the insulin signalling pathway. This research aims to clarify these interactions to aid in the creation of innovative, plant-derived therapeutic agents for the effective treatment of type 2 diabetes mellitus.

## 1.1 Aims and Objectives

The present study is aimed to explore natural therapeutic compounds of *Astragalus membranacous* leaf extract to ameliorate Type 2 Diabetes that could provide both symptomatic relief as well as exhibit potential to treat disease.

### 1.1.1 Objectives

i. To isolate the bioactive compounds from *Astragalus membranacous* leaf extract through different chromatography techniques.

ii. To elucidate the antioxidant, total polyphenol and invitro antidiabetic attributes of the isolated bioactive compounds fractions.

iii. To characterize different fractions through LC-MS technique.

iv. To conduct the molecular docking of identified compounds with Insulin pathway proteins including Akt2, PI3K- $\alpha$, PPAR-$\gamma$, IRS-2 and PDX-1.

# Chapter 2

# Literature Review

## 2.1 Diabetes

Diabetes mellitus is a chronic, metabolic disorder characterized by elevated blood glucose levels, resulting from the body's inability to produce or effectively utilize insulin, a hormone crucial for regulating glucose homeostasis. This complex and multifactorial disease has become a global health concern, with its prevalence steadily increasing worldwide [1]. It is mainly classified into two types. In type 1 diabetes, an autoimmune response leads to the destruction of insulin-producing beta cells in the pancreas, resulting in the body's inability to produce insulin [2]. In type 2 diabetes, the body becomes resistant to the effects of insulin, leading to a gradual decline in insulin sensitivity and the inability to maintain normal blood glucose levels. T2DM accounts for 90% of diabetic cases and is predominantly linked to lifestyle factors such as obesity, physical inactivity, and poor dietary habits, leading to the disease's growing cases worldwide [3].

## 2.2 Etiology

The pathogenesis of diabetes mellitus involves complex interactions between genetic, environmental, and lifestyle factors. At the core of this complex disease

is the dysregulation of glucose metabolism, which is primarily driven by impairments in insulin production and action. Frequent urination, excessive thirst, intense hunger, fatigue, and ketoacidosis are the most common symptoms of diabetes mellitus. While diabetes was once categorized by age of onset or treatment type, current classification primarily focuses on the pathogenic processes leading to hyperglycemia. The terms insulin-dependent and noninsulin-dependent are usually used to identify the pathophysiological conditions of diabetes [28, 32].

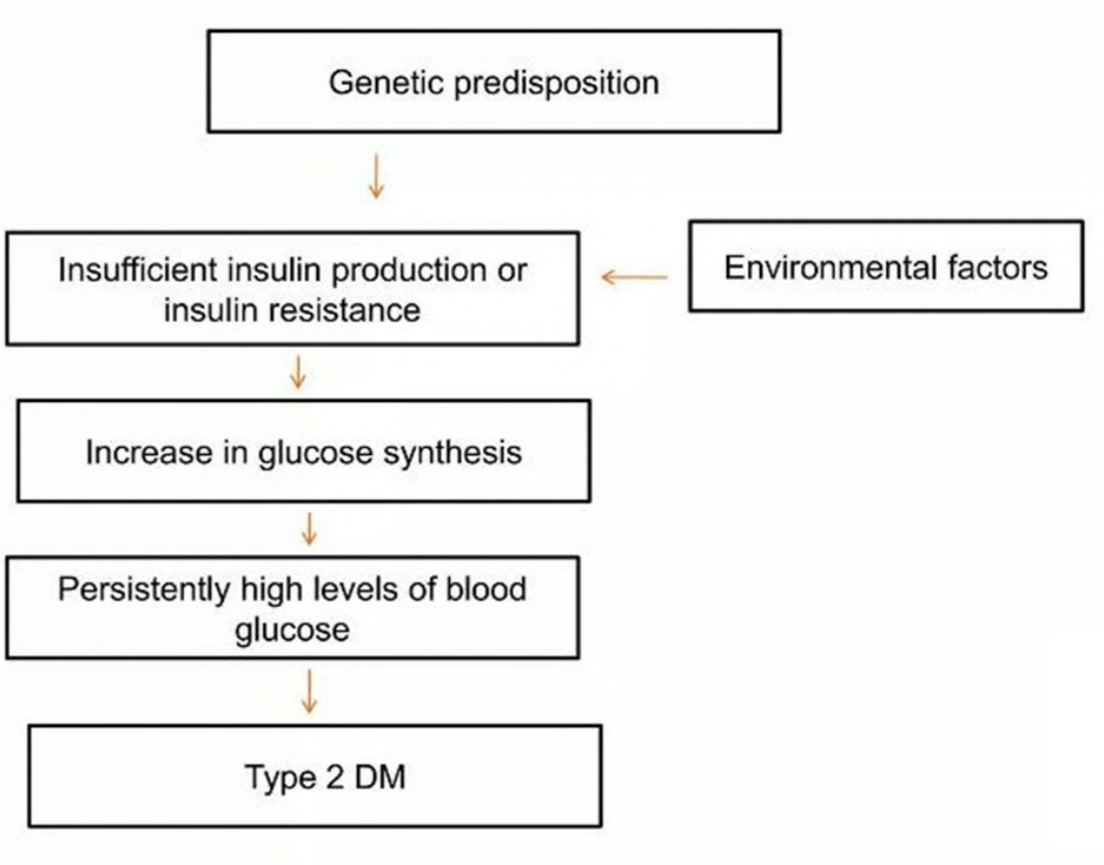


FIGURE 2.1: Pathogenesis of Diabetes mellitus [32].

## 2.3 Classification of Diabetes

### 2.3.1 Type 1 Diabetes

Type 1 diabetes is an autoimmune condition leading to the destruction of insulin-producing beta cells. It is less common, accounting for about 5-10% of all diabetes

cases, and typically begins in childhood or adolescence. Due to insufficient insulin production, type 1 diabetes is frequently referred to as insulin-dependent diabetes. To survive, individuals with diabetes classified as type 1 require insulin shots every day, a particular diet, and frequent blood glucose checks [29].

### 2.3.2 Type 2 Diabetes

T2DM is also known as adult-onset diabetes and it usually affects middle-aged and elderly individuals and occurs because of both insufficient insulin secretion and insulin resistance. It is more prevalent and represents the majority of diabetes cases worldwide. Approximately 90% of the 800 million persons who have diabetes around the world have T2DM. Risk factors for T2DM include obesity, physical inactivity, genetic predisposition, and advancing age. It is a metabolic ailment that invites other illnesses and is mostly to blame for lower limb amputation, heart attacks, strokes, blindness, and renal failure. Managing type 2 diabetes usually includes making lifestyle changes like adjusting diet and increasing physical activity, in addition to using medications to help control blood sugar levels [30].

### 2.3.3 Gestational Diabetes

Diabetes that was not evident before pregnancy but was discovered during the second or third trimester is known as gestational diabetes mellitus. Approximately 13% of all infants are affected by it. GDM typically resolves after childbirth, but around 50% of affected women may develop type 2 diabetes mellitus later in life. During pregnancy, the placenta produces hormones that can reduce the effectiveness of insulin, leading to the development of GDM. While many symptoms of T2DM are present in GDM, diagnosis usually relies on prenatal screening such as fasting glucose tests rather than symptoms reported by the patient. Management of gestational diabetes involves strategies such as adopting a healthy diet, engaging in physical exercise, monitoring blood glucose levels, and sometimes using oral medications [31].

### 2.3.4 Maturity Onset Diabetes of the Young

It is a non-autoimmune type of diabetes caused by a single gene mutation. It is often misdiagnosed as T1DM or T2DM. The diagnosis criteria include $\beta$-cell malfunction without autoantibodies, a family history of autosomal dominant diabetes, and onset between adolescence and early adulthood. In MODY, insulin production disruption leads to hyperglycemia, potentially damaging kidneys, nerves, eyes, and blood vessels [33].

### 2.3.5 Neonatal Diabetes

It is a rare condition characterized by mutations in proteins essential for pancreatic $\beta$-cell function. It typically occurs before 6 months and arises from pancreatic abnormalities that impact the ability of cells that secrete insulin to survive or aberrant activity of the pancreatic $\beta$-cells that are already there.

Mutations in the genes ATP-binding cassette subfamily C member 8 (ABCC8) or potassium inwardly rectifying channel subfamily J member 11 (KCNJ11), which regulate the potassium channel in pancreatic $\beta$-cells, are the main genetic reasons. Patients with these mutations can successfully switch from insulin injection to oral sulfonylureas [34].

### 2.3.6 Type 3c DM

It occurs due to cystic fibrosis, chronic pancreatitis, and other diseases that impact the exocrine pancreas, which is why also referred to as pancreatic DM. Pancreatic exocrine insufficiency is common in T3cDM patients, which can result in undernutrition and fat malabsorption.

The pathophysiology involves a reduction in insulin synthesis, reduced islet functional capacity and extensive sclerosis and fibrosis. Controlling hyperglycemia is the primary target for minimizing complications [35].

### 2.3.7 Latent Autoimmune Diabetes in Adults

This type 1 diabetes subtype serves as a link between type 1 and type 2 diabetes. It displays immunological signs resembling those of type 1 diabetes and progresses slowly, but is diagnosed without the need for insulin therapy. Diagnosis is more common in secondary care settings, with critical criteria including adult-onset, presence of autoantibodies, and no immediate insulin therapy requirement. LADA patients retain functioning $\beta$-cells, so therapeutic strategies are crucial to improve metabolic control and preserve insulin-secreting capacity [36].

TABLE 2.1: Prevalence of Different Types of Diabetes

| **Type of Diabetes** | **Approximate Occurrence / Prevalence** | **Ref** |
|---|---|---|
| Type 1 Diabetes | 5–10% of all diabetes cases | [29] |
| Type 2 Diabetes (T2DM) | ∼90% of all diabetes cases worldwide | [30] |
| Gestational Diabetes (GDM) | Affects ∼13% of all pregnancies globally | [31] |
| Maturity Onset Diabetes of the Young (MODY) | 1–2% of all diabetes cases | [33] |
| Neonatal Diabetes | 1 in 100,000 to 260,000 live births | [34] |
| Type 3c Diabetes (Pancreatogenic) | ∼1–5% of all diabetes cases in Western populations | [35] |
| Latent Autoimmune Diabetes in Adults (LADA) | ∼2–12% of all diabetes cases | [36] |

## 2.4 Prevalence

According to the International Diabetes Federation, approximately 589 million adults (aged 20-79 years) were living with diabetes worldwide in 2025, equivalent to nearly one in nine adults globally. Projections indicate that this number will rise to 853 million by 2050, underscoring a rapidly growing global health challenge. Notably, there are significant regional variations in diabetes prevalence and projected surges: diabetes is expected to increase by 134% in Africa, 68% in South-East Asia, and 13% in Europe by 2050. In the United States, around 38

million people—approximately 11.3% of the population—are living with diabetes, and there are about 1.4 million new cases diagnosed annually. Australia reports nearly 1.3 million affected individuals, or about one in twenty citizens. China continues to have the world's highest diabetes burden, with 141 million diagnosed cases as of the latest estimates.

Alarmingly, approximately 252 million adults—over 40% of those with diabetes are unaware of their condition, greatly increasing the risk of complications and premature death due to delayed diagnosis. Globally, diabetes is responsible for more than 3.4 million deaths each year [37].

Pakistan ranks third in numbers of adults with diabetes, behind China and India, with 31.4% of its adult population—about 34.5 million individuals—affected as of 2024. This marks a dramatic rise, highlighting the urgent need for improved diabetes management, prevention strategies, and innovative therapies to prevent further escalation of this epidemic in Pakistan and worldwide [37].

## 2.5 Global Economic Burden Due to Diabetes

Diabetes was responsible for 3.4 million deaths in 2024, which equates to one death every nine seconds globally. The annual healthcare expenditure related to diabetes has surpassed USD 1 trillion, marking a 338% increase over 17 years. Over 81% of adults with diabetes live in low- and middle-income countries, where healthcare access and medication rates lag behind those in high-income nations. Diabetes is associated with severe complications including blindness, kidney failure, heart attacks, strokes, and lower limb amputations. In 2021, diabetes directly caused 1.6 million deaths, and an additional 530,000 kidney disease deaths were attributable to diabetes.

Furthermore, about 11% of cardiovascular deaths result from high blood glucose linked to diabetes [WHO]. The prevalence of diabetes is rising more rapidly in low- and middle-income countries, and more than half of people with diabetes globally are currently undiagnosed or untreated.

These facts emphasize diabetes as both a public health and a socioeconomic challenge, requiring urgent global action for prevention, early diagnosis, and comprehensive management [37].

TABLE 2.2: Prevalence of diabetes in different global regions along with Pakistan data based on the latest IDF Diabetes Atlas information for 2025

| **Region/Country** | **Diabetes Prevalence (%)** | **Number of Adults (millions)** | **Ref** |
|---|---|---|---|
| Global (all regions) | 11.1 | 0:00 | [37] |
| Western Pacific | 12.4 | 9:36 | [37] |
| Middle East & North Africa | 12.2 | 19:12 | [37] |
| South-East Asia | 10.6 | 12:00 | [37] |
| Europe | 10.2 | 9:36 | [37] |
| North America & Caribbean | 13 | 58.2 | [37] |
| South & Central America | 9.2 | 7:12 | [37] |
| Africa | 4.5 | 0:00 | [37] |
| Pakistan | 31.4 | 12:00 | [37] |

## 2.6 Glucose Metabolism in Body

Glucose metabolism is a complex process that is essential for the body's homeostasis and energy generation. It involves various pathways and organs that work together to ensure that glucose is efficiently utilized or stored according to the body's needs. The ratio of glucose entering the bloodstream to glucose leaving it is what determines blood glucose concentration [37].

When we eat food, carbohydrates are ingested and converted into monosaccharides by amylases. This leads to increased blood glucose levels in the bloodstream. By secreting two essential hormones, glucagon and insulin, the pancreas plays a major role in controlling blood sugar levels. The incretin effect stimulates $\beta$-cells in the

pancreas, driving insulin production and release. Insulin helps cells, especially muscle and fat cells, absorb glucose thereby lowering blood sugar levels. It also promotes the storage of glucose as glycogen in the liver and muscle tissues.

Additionally, blood glucose levels promote the synthesis of insulin, which is regulated by the hormones GLP-1 and glucose inhibitory polypeptide (GIP). Through diffusion, GLUT molecules move glucose from the blood into cells via cell membranes, removing extra glucose from the circulation and lowering its [38].

In contrast, glucagon is secreted when blood glucose levels drop e.g., during fasting. It stimulates the liver to convert stored glycogen back into glucose and release it into the bloodstream, thus raising blood sugar levels.

The liver is essential for the metabolism of glucose. It stores glucose as glycogen and engages in gluconeogenesis i.e. it produces glucose from non-carbohydrate sources like amino acids and glycerol during prolonged fasting.

This ability to switch between storing and producing glucose is essential for maintaining stable blood sugar levels. The kidneys are also integral to glucose regulation.

They filter glucose from the blood and reabsorb it, ensuring that glucose is not lost in urine. They also participate in gluconeogenesis and help clear insulin from the bloodstream, which is vital for maintaining insulin sensitivity and overall glucose homeostasis [39].

The body employs complex homeostatic mechanisms to regulate blood glucose levels. Negative feedback systems are crucial in this process, they detect changes in blood glucose levels and activate responses to restore balance. For instance, insulin production rises while glucagon secretion falls in reaction to high blood sugar levels and vice versa when blood glucose levels fall as shown in figure 2.2.

This dynamic interplay ensures that glucose levels remain within a normal range, typically between 70 to 110 mg/dL [40]. When the glucose regulatory system is disrupted, it can lead to metabolic disorders such as diabetes mellitus.

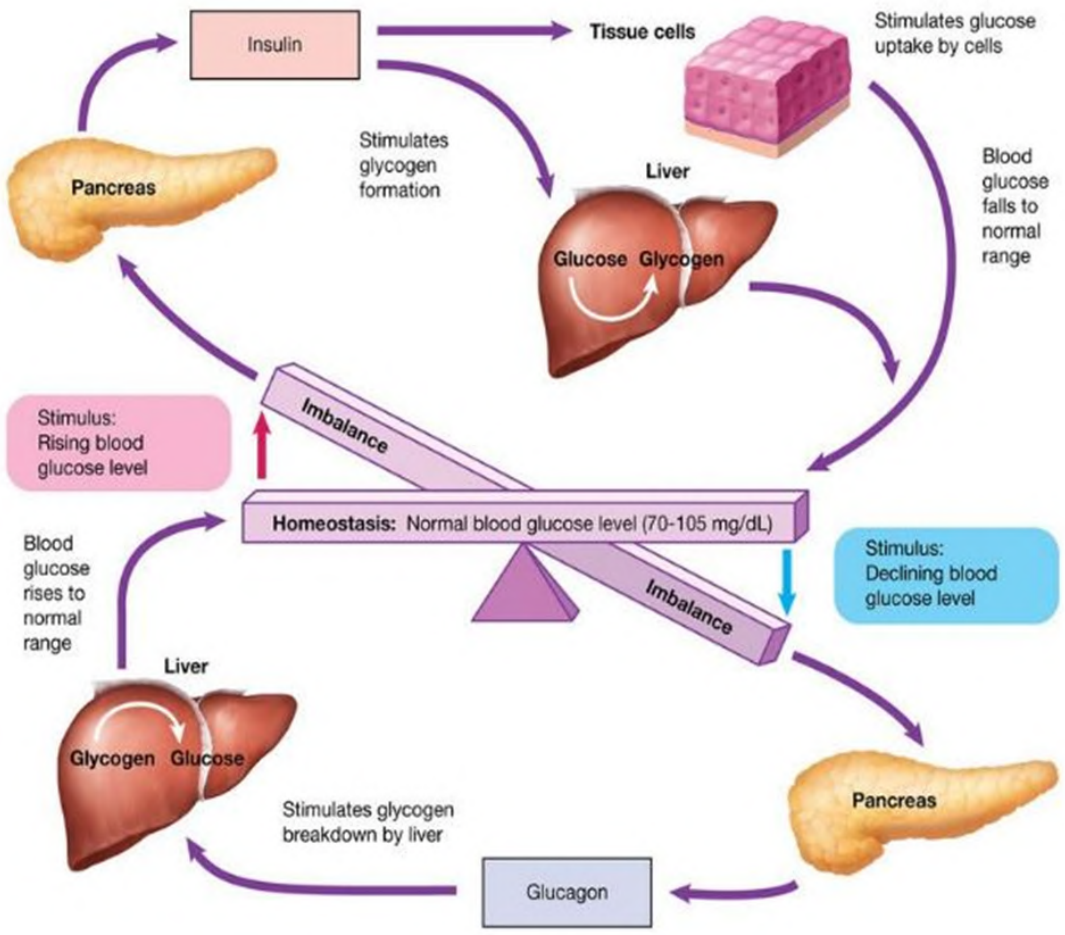


FIGURE 2.2: Glucose homeostasis in the human body [40]

## 2.7 Insulin Signaling Pathway

After a meal, tissue insulin sensitivity triggers the insulin release by $\beta$-cells in the pancreas to keep the body's glucose levels stable. There are several mechanisms in different organs involved in this homeostatic system including attenuating increased absorption of glucose by muscle and fat due to the liver's release of glucose, increasing lipid buildup in the liver and adipocytes, and inhibiting the release of free fatty acids from adipocytes [6].

A sophisticated signal transduction cascade that is insulin-dependent controls these metabolic activities. A complicated signal transduction cascade that is dependent on insulin controls these metabolic activities [41].

There are proximal and distal sections of the insulin signaling network. The insulin receptor, insulin receptor substrate proteins (IRS), phosphoinositide 3-kinase (PI3K), and Akt are all found in the proximal region.

These elements are included in a broader network that is dynamically controlled by inputs from combinatorial signaling. The distal segment includes the Akt substrates that are closely related to the many physiological roles of insulin and are frequently cell-type specific [42].

As seen in figure 2.2, distal elements bind proteins and are often phosphorylated on several sites that are seen in non-structured domains.

### 2.7.1 Proximal Insulin Signaling

The tetrameric structure of the insulin receptor is made up of two transmembrane $\beta$-subunits and two extracellular $\alpha$-subunits. The extracellular $\alpha$-subunit is bound by insulin, causing the receptor to become autophosphorylated at tyrosine residues (Y972, Y1158, Y1162, and Y1163) in the $\beta$-subunit. This phosphorylation activates the receptor's intrinsic tyrosine kinase activity. The insulin receptor (INSR) gene encodes this receptor, with two isoforms, IR-A and IR-B, differing in insulin binding affinities. Activated INSR recruits IRS proteins (IRS1-IRS4), which are phosphorylated at specific tyrosine residues, creating docking sites for SH2 domain-containing proteins. IRS1 has a major role in muscles of the skeleton and fatty tissue glucose uptake and the IRS2 is essential for $\beta$-cell function present in the pancreas and hepatic regulation of glucose while IRS3 and IRS4 have tissue-specific functions [43].

Phosphoinositide 3-kinase is recruited to IRS proteins via its SH2 domains. PI3K comprises a regulatory subunit (p85) and a catalytic subunit (p110). The activation of PI3K results in the conversion of phosphatidylinositol 4,5-bisphosphate (PIP2) to Phosphatidylinositol 3,4,5-trisphosphate (PIP3) on the plasma membrane. PIP3 serves as a docking site for phosphoinositide-dependent kinase-1 (PDK1) and Akt also known as protein kinase B (PKB). PDK1 phosphorylates

Akt at Thr308, and mTORC2 phosphorylates Akt at Ser473, leading to full activation. Akt has various isoforms, Akt1 regulates cell survival and growth, Akt2 is critical for glucose homeostasis and Akt3 is involved in brain development [44].

### 2.7.2 Distal Insulin Signaling

In muscle and adipose tissue, activated AKT phosphorylates AS160 (TBC1D4), an inhibitor of Rab proteins responsible for GLUT4 vesicle trafficking. This phosphorylation inactivates AS160, allowing the translocation of GLUT4 vesicles to the plasma membrane for the absorption of glucose. Akt also phosphorylates and deactivates glycogen synthase kinase-3 (GSK3) to sustain glycogen synthase activity and promote glycogen storage in the muscle and liver. It also suppresses lipolysis in adipose tissue by phosphorylating PDE3B, reducing cAMP levels and inhibiting hormone-sensitive lipase (HSL). Simultaneously, it activates lipogenesis via the mTORC1-SREBP1 pathway. mTORC1, activated by Akt, promotes anabolic processes, including protein synthesis and cell proliferation, through phosphorylation of S6 kinase (S6K) and 4E-BP1. In hepatocytes, Akt phosphorylates FOXO1, excluding it from the nucleus. This stops gluconeogenic genes like PEPCK and G6Pase from being transcriptionally active [45].

### 2.7.3 Insulin Signaling in Skeletal Muscle

The skeletal muscle plays a crucial role in maintaining glucose homeostasis, responsible for 80% of the human body's postprandial glucose elimination. 75% of all glucose elimination occurs in the muscle as a result of glucose's principal function of promoting glycolysis, or the synthesis of glycogen. When blood glucose levels rise, the pancreas releases insulin, and it binds to INSR to facilitate glucose absorption and glycogen storage. S6K, AKT, PKC, and PDK1 are among the kinases that mediate the cycle of phosphorylation and dephosphorylation that is brought on by INSR activation. These proteins regulate various muscle routes involved in the metabolism of glucose [46].

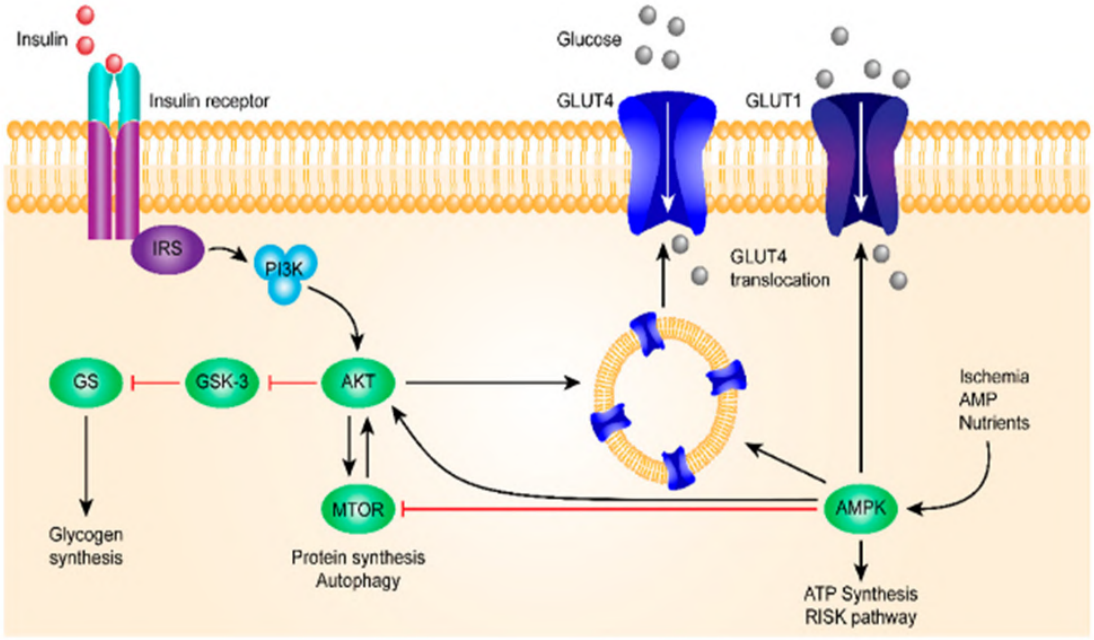


FIGURE 2.3: Insulin Signaling Pathway [6].

One signaling route is controlled by Akt2 and includes storage vesicles (GSVs) carrying GLUT4 moving to the plasma membrane. G6P rises as a result of other downstream actions, which also dephosphorylate glycogen metabolic proteins and promote glycogen production. Regular insulin-stimulated muscle glucose uptake necessitates IRS1/PI3K/AKT pathway maintenance.

While serine and threonine phosphorylation of IRS promotes the opposite effects, tyrosine phosphorylation of IRS increases PI3K recruitment and insulin-stimulated glucose uptake. Akt1 knockoffs develop and tolerate glucose normally but Akt2 knockouts exhibit severe glucose insensitivity, based on studies on mice. For insulin-stimulated glucose absorption, Akt2 is more crucial [47].

### 2.7.4 Insulin Signaling in Liver

Insulin signaling in the liver is initiated by INSR trans-autophosphorylation, activation, and recruitment of scaffold signaling proteins, such as IRS1 and IRS2. IRS1 might have had a more significant role in normal glucose homeostasis, and insulin activation of PI3K-Akt activity was significantly reduced upon deletion of both isoforms. Forkhead box 01 (FOXO1) a transcription factor, mTORC1,

and glycogen synthase kinase (GSK3) are substrates of Akt signaling, which is essential for the hepatocellular action of insulin [48].

Insulin suppresses transcriptional gluconeogenic genes in a fed state, particularly those regulated by FOXO. FOXO1 targets Akt having sites responsible for phosphorylation at Thr24, Ser256, and Ser319. Additionally, insulin controls the genes that convert the sugar to fat, by de novo lipogenesis (DNL) process. This mechanism is primarily regulated by the transcription factor protein-1c that binds to sterol regulatory elements (SREBP-1c). Although the insulin controls the activity of this protein, it can also be inhibited by PI3K-Akt-mTORC1 axis suppression. Insulin contributes to the metabolism of fats and carbohydrates by controlling the production of proteins in hepatocytes [49].

### 2.7.5 Insulin Signaling in Adipose Tissue

Adipose tissue plays a crucial role in affecting the metabolism of fats and carbohydrates by producing proinflammatory cytokines, adipokines, and free fatty acids. It is a tissue that responds to insulin, and insulin causes triglyceride accumulation by promoting preadipocyte development into adipocytes, preventing lipolysis, and enhancing the absorption of glucose and fatty acids. Insulin signaling in adipocytes is mediated by both IRS1 and IRS2 revealing how insulin has its physiologic effects through the signaling cascade IRS-PI3K-AKT2-GLUT4. Adipocytes also express Rab-GAP-TBC1D, which facilitates signaling of insulin via the trafficking of vesicles and translocation of GLUT4 to the membrane of the cell [50].

Insulin plays a key function in adipose tissue by promoting the inhibition of lipolysis, which is the process by which lipid triglycerides hydrolyze into fatty acids and glycerol for energy reserves during action or fasting. A signaling route for protein kinase A is crucial for controlling lipolysis. Insulin stimulates AKT2 in a fed state, which in turn triggers PDE3 and inhibits PKA, so reducing lipolysis. Conversely, the insulin resistance in adipose tissue causes Akt2 phosphorylation to decline, which prolongs lipolysis activation. Increased circulating fatty acids and non-esterified fatty acid synthesis result from this, and the liver and muscle

absorb these fatty acids, which helps cause ectopic lipid buildup in both organs [51].

## 2.8 PPAR-$\gamma$ Pathway

PPAR-$\gamma$ belongs to the class of ligand-activated transcription factors [52]. They are nuclear hormone receptors and participates in several physiological processes, most notably the control of glucose metabolism, fatty acid storage, inflammation, adipogenesis, and insulin sensitivity [53]. There are two isoforms of PPAR: PPAR$\gamma$1 and PPAR$\gamma$2. While the PPAR$\gamma$2 present in fat tissues, PPAR$\gamma$1 is present in a variety of organs, including phagocytes, fat tissue, and the smaller intestine. In mammals, besides PPAR-$\gamma$ there is also PPAR$\alpha$ and PPAR$\beta/\delta$. PPAR$\alpha$ is a key stimulator of oxidative fatty acid processes and is the intended target of hypolipidemic medications. It is found in the kidneys, liver, heart, muscles of the skeletal system, and the fat tissue [54].

Similar to PPAR$\alpha$, PPAR$\beta/\delta$ is widely expressed and plays a crucial part in fatty acid oxidation in the liver, heart, and skeletal muscle. PPARs are composed of three distinct functional domains: the N-terminal transactivation domain, the highly conserved DNA-binding domain (DBD), and the C-terminal ligand-binding domain (LBD). After the PPARs are anchored to their DNA template binding locations by the DBD, they obligately form combinations containing the RXR or retinoid X receptor, that attaches itself to certain areas of the target gene's DNA. PPAR response elements (PPREs) are the name given to these particular DNA regions [55**?** ].

Natural products including amorfrutins, polyacetylenes, alkamides, sesquiterpene lactones, diterpenoids, triterpenoids, flavonoids, stilbenes, and neolignans act as agonists of PPAR [56]. Insulin resistance is facilitated by proinflammatory cytokines secreted by adipose tissue that is chronically inflamed in type 2 diabetes. Through improved fatty acid oxidation and suppression of hepatic glucose synthesis, agonists of PPAR have been demonstrated to decrease proinflammatory

cytokines and raise plasma concentrations of the hormone adiponectin, which is favorably correlated with insulin sensitivity. For instance, it was discovered that administering a PPAR-$\gamma$ agonist increased the process of phosphorylation of tyrosine in the IRS-1, insulin receptor and activated Akt. Skeletal muscles showed increased Akt phosphorylation and increased PI3K function triggered by insulin [57].

In T2DM, Thiazolidinediones, the synthetic insulin-sensitizing drugs activate the PPAR-$\gamma$ pathway by promoting basal glucose absorption in muscle cells and adipocytes that is based on insulin by translocating GLUT4 and GLUT1 to the cell surface but they can cause serious side effects, such as an increase in whole-body adipocity, fluid retention, an increased risk of heart failure, and bone fractures, which led to their removal from the market. It can be challenging to find ligands with the perfect pharmacological profile, or those that draw coactivators and have antidiabetic benefits with little to no adverse effects. Coactivator placement that increases energy consumption and glucose utilization without causing fat accumulation should be the outcome of a desirable PPAR agonist profile [58].

Because plant extracts include typical PPAR activators including polyunsaturated fatty acids, they have high response rates when evaluated for PPAR activity [59].

## 2.9 Pathophysiology Insulin Resistance

Various mechanisms contribute in the pathophysiology of T2DM such as decreased secretion of insulin from the beta cells, increased glucagon secretion from the $\alpha$ cells of the islets of Langerhans, increased liver glucose production, neurotransmitter dysfunction and insulin resistance in the brain, increased lipolysis, increased kidney reabsorption of glucose, diminished small intestine incretin effect, and impaired or decreased glucose uptake by peripheral tissues. The resistance of insulin and $\beta$-cell depletion result from this [60].

People with insulin resistance exhibit both poor insulin regulation of hepatic glucose production and impaired insulin-stimulated glucose absorption into muscle


FIGURE 2.4: Pathophysiology of Insulin resistance [61].

and adipocytes. The characteristic of this sickness is hyperinsulinemia, a condition in which blood insulin levels are higher than normal compared to glucose levels after both fasting and feeding. To restore normal blood glucose levels, this hyperinsulinemia makes up for the insulin resistance (IR) in peripheral tissues. Hyperglycemia and glucose intolerance, the hallmarks of type 2 diabetes, are caused by a significant disruption in whole-body glucose homeostasis in people with insulin resistance, which occurs when the pancreas is unable to produce enough insulin. Relative hyperinsulinemia is often maintained by people with type 2 diabetes until the condition is advanced [62].

Insulin's capacity to initiate glucose transfer into these tissues is compromised in insulin resistance because the GLUT4 glucose transport mechanism in muscle and adipose cells is malfunctioning [63]. The inability to reduce hepatic glucose

synthesis, which is mostly brought on by a sustained increase in gluconeogenesis, is what defines IR, as seen in Figure 2.4. Insulin levels must now be measured in order to diagnose insulin resistance in humans, which is not frequently done in clinical practice because many individuals with the condition do not have high blood glucose levels. As a result, IR is not commonly identified or treated in humans. There are no ways to detect this predisposed subpopulation, and the majority of people with IR acquire type 2 diabetes, which probably needs extra susceptibility to $\beta$-cell failure [64].

Various extrinsic and intrinsic factors are responsible for developing insulin resistance in T2DM. Cell-extrinsic factors are circulating or paracrine molecules released from cells or tissues outside either taken up by the intestinal tract or the target cell. They are metabolites, such as hormones, cytokines, lipids, and metabolites. Cell-intrinsic factors persist after extrinsic factors are removed or normalized, often due to genetic or epigenetic effects. These factors can affect insulin receptor- or kinase-mediated signaling, causing type 2 diabetes to develop insulin resistance [52].

## 2.10 Extrinsic Factors

Insulin resistance in type 2 diabetes is primarily due to extrinsic factors such as the gut microbiota, circulating metabolites, inflammatory signals, and adipose tissue, as seen in figure 2.4. Overnutrition-induced elevation of circulating fatty acid levels and ectopic lipid accumulation in the liver and muscle cause the emission of intermediary metabolites, including ceramides and diacylglycerols (DAG), which exacerbate insulin resistance. Members of the new PKC family are activated by these intermediate metabolites causing a decrease in the tyrosine and an increase in serine/threonine phosphorylation of insulin receptor proteins [65].

Additionally, insulin receptor substrate 2 signaling is impacted by serine/threonine phosphorylation even though IRS1 is the most researched substrate in relation to insulin resistance. Furthermore to increasing Ser/Thr phosphorylation of IRS1,

fatty acid molecules also cause toll-like receptor 4 to become active, which in turn promotes c-Jun N-terminal kinase (JNK) inhibitor of B kinase (IKK) actions. This decreases the effect of insulin [66].

Ceramide buildup can also inhibit Akt2 via activating PKC and protein phosphatase 2A. Increased adipose tissue inflammation and hypoxia are also linked to adipose tissue expansion. These factors encourage the recruitment of proinflammatory macrophages, which release cytokines like TNF-$\alpha$ and IL-6. These cytokine receptors, including the TNF-$\alpha$ receptor (TNFR), exacerbate insulin resistance [67].

The production of cytokine signaling suppressor (SOCS) proteins, including SOCS1 and SOCS3 is induced by cytokine signaling. These proteins bind directly via SH2 domains to the insulin receptor, limiting the tyrosine phosphorylation of IRS1/2 and encouraging their ubiquitination and proteasomal breakdown.

In insulin-resistant conditions, target tissues also experience rises in endoplasmic reticulum stress and the development of the reactive oxygen species, which triggers induction of additional serine/threonine kinases, IKK isoforms, and JNK [68].

Insulin resistance is also linked to amino acids which are branched and aromatic in the bloodstream at least in mice, reducing these amino acid levels can increase insulin sensitivity. Systemic insulin sensitivity may be affected by the gut microbiota's control over the synthesis of several metabolites, including short-chain fatty acids as well as the supply of branch chain amino acids (BCAAs) [69].

Figure 2.4: Extrinsic factors contributing to insulin resistance. Numerous environmental variables can cause systemic alterations that impact various tissues and impede insulin signaling. Adipose tissue growth and compromised insulin signaling are caused by obesity.

In insulin-sensitive tissues, this can result in lipid buildup, mitochondrial malfunction, the production of reactive oxygen species, and endoplasmic reticulum stress. Overnutrition can also alter exosomal miRNA release, impacting systemic metabolism [52].

## 2.11 Intrinsic Factors

In vitro approaches to studying insulin resistance in type 2 diabetes have shown that cells cultured under controlled conditions can minimize separate cell - autonomous determinants and the impact of external stimuli.

Insulin resistance and a number of metabolic abnormalities, such as defective signaling of insulin at the level of reduced glucose uptake, production of glycogen rates, and Skeletal muscle biopsy procedures from individuals with type 2 diabetes and cultured myoblasts both exhibit PI3K activity and AKT/GSK3 phosphorylation associated with IRS-1 [70].

The restricted expandability and screening capabilities of primary cell models utilizing RNA interference (RNAi), chemical genetics, or CRISPR make them unsuitable for identifying the molecular pathways underlying insulin resistance.

A step in this direction is represented by induced stem cells with pluripotency (iPSCs), which can proliferate and distinguish themselves into a range of lineages, enabling the use of patient cells for gene-editing, mechanistic research, and extensive omics [71].

Researchers have recently used iPSC technology to investigate the signaling abnormalities that underpin type 2 diabetes-related resistance of insulin in muscles of skeleton.

Similar to these abnormalities seen in diabetic muscle, iPSC-derived myoblasts (iMyos) from people with the disease exhibit impairments in the process of insulin signaling where Akt/GSK3/FOXO1 phosphorylation is present as well as decreased glucose absorption triggered by insulin and mitochondrial respiration.

These abnormalities are a component of a broad multi-dimensional network of signaling alterations encompassing over 725 proteins with 1200 serine/threonine sites for phosphorylation, according to global phosphoproteomics utilizing LC-MS/MS [72].

The identification of the molecular defects that cause these signaling alterations will be a significant task in the future. Potential causes include different co-activators of kinase and phosphatases, ionic milieu, scaffolding proteins, redox balance, and other elements.

Understanding the fundamental problem is still a significant difficulty, even though genetic reprogramming of iPSCs is known to remove the majority of epigenetic markers [73].

With the development of profiling technologies, the potential contribution of long non-coding RNAs and miRNAs to controlling the metabolism of cells has become more well recognized.

Figure 2.5 illustrates how research employing in vitro models, tissues derived from rat models, as well as humans having type 2 diabetes and obesity has identified a system of changed micro RNAs that target the IRS/PI3K/Akt cascade and the receptor of insulin, hence causing problems related to metabolism [74].

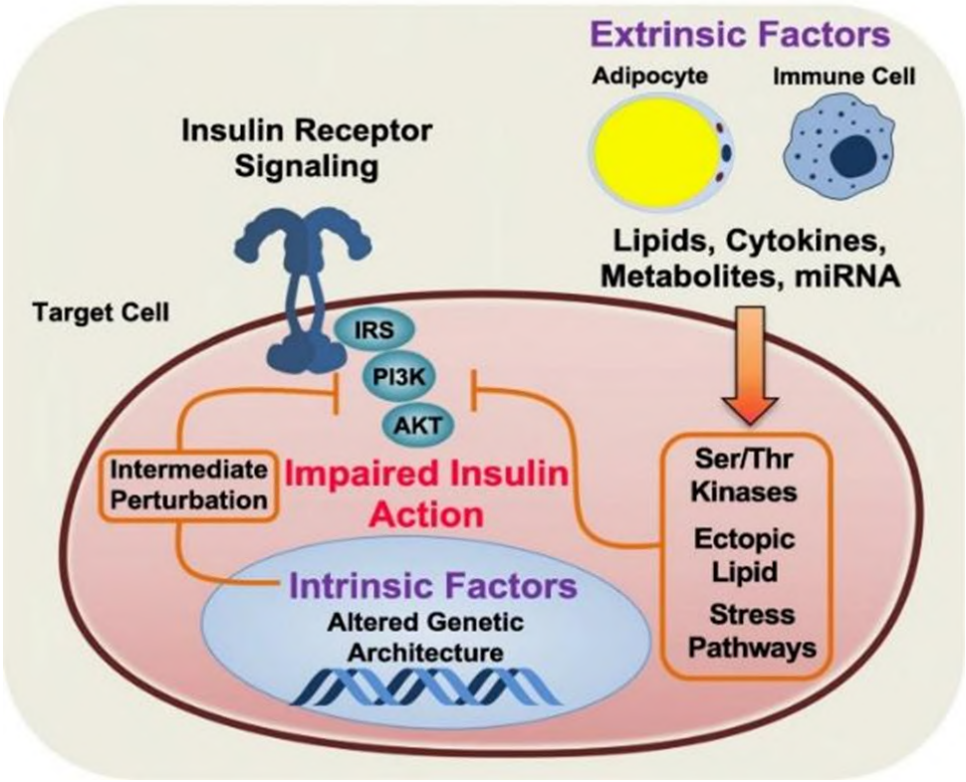


FIGURE 2.5: Extrinsic and Intrinsic factors contributing to insulin resistance [72]

## 2.12 T2DM Associated Health Complications

Diabetes can cause serious complications, which can go into one of two categories: macrovascular or microvascular. Damage to the neurological system, kidneys, and eyes are examples of microvascular problems; as seen in figure 2.5, while macrovascular problems include peripheral vascular disease, stroke, and cardiovascular disease. Paralysis, gangrene, and lesions all are consequences of peripheral blood vessel diseases. The regularity of occurrence of microvascular complications is higher than macrovascular complications, such as stroke, congestive heart failure, coronary heart disease, chest discomfort, and heart attacks. Both progressive and episodic complications are possible resulting in further damage to the organ and irreversible functionality. Other complications include dental disease, reduced resistance to infections, and macrosomia in pregnant women with diabetes [10].

### 2.12.1 Cardiovascular Diseases

One major cause of mortality for diabetics is cardiovascular disease accounting for up to 65% of all deaths. Ischemic heart disease and stroke are the most common morbidity associated with diabetes, with diabetes patients having death rates that are two to four times greater than those of people without the disease. Additionally, diabetes patients have a twice as much higher risk of stroke. Over 70 percent of diabetics either have high blood pressure or are on medication for it. Cardiovascular disease risk factors include hypertension, hypercholesterolemia, and smoking [75].

### 2.12.2 Peripheral Arterial Disease

It is characterized by the narrowing of blood vessels that transport blood to the arms, legs, stomach, and kidneys. Risk increases in diabetes patients due to age, diabetes duration, and neuropathy. The risk is also increased by other cardiovascular disease risk factors, such as homocysteine and C-reactive protein levels. It is

differentiated by intermittent claudication and resting discomfort brought on by perfusion in the injured limbs [76].

### 2.12.3 Retinopathy

It is a common microvascular complication in diabetes patients, causing over 10,000 blindness cases annually. It is linked to prolonged hyperglycemia and may appear up to seven years before type 2 diabetes is diagnosed. As people age, the prevalence rises, 27% of those whose age is seventy or more reported vision deterioration, in comparison to 15% of those between the ages of 18 and 44. Diabetes-afflicted women were more inclined to have visual impairment than men. Early detection and the treatment can prevent up to 90% of retinopathy-related blindness. Every diabetic patient should get a dilated eye exam every year [77].

### 2.12.4 Nephropathy

Patients with chronic proteinuria who do not have urinary tract infections or other illnesses are said to have diabetic nephropathy Diabetic proteinuria may be evident upon diagnosis, but clinical nephropathy occurs rather late in type 1 diabetes. Diabetic nephropathy is uncommon in the first 10 to 15 years of diabetes, then rises quickly to a peak at around 18 years, after which it starts to diminish. It was responsible for 44% of newly diagnosed chronic renal failure in 2002. Several risk factors are involved in diabetic nephropathy, including metabolic regulation, blood pressure, hypertension, inheritance, weight gain, hemorrhage and tobacco use [78].

### 2.12.5 Peripheral Neuropathy

It is a frequently occurring issue affecting 30% to 50% of individuals with diabetes, with hyperglycemia being the primary risk factor. Age, length of illness, cigarette

smoking, high blood pressure, raised triglycerides, a higher body mass index, drinking alcohol, and being taller are additional risk factors.

The most common kind of sensorimotor polyneuropthy is prevalent kind of the diabetic neuropathy, which could cause discomfort, muscular weakness, and sensory loss. Years may pass before sensory impairment symptoms, such as burning and numbness in the feet, are noticed.

Neuropathic pain may be severe, but only 11% to 32% of individuals with polyneuropathy experience it. It leads to impairments and functional limitations, including an increased risk of lower-extremity amputation and ulcerated feet [79].

### 2.12.6 Periodontal Diseases

Oral health issues, including periodontal disease, can arise as a consequence of diabetes. Diabetes has the potential to impact oral health by altering the composition of saliva, the essential fluid responsible for maintaining mouth moisture. Through its ability to wash away food particles, stop bacterial development, and neutralise the acid produced by bacteria, saliva plays a critical role in preventing tooth decay.

Saliva also contains minerals, which protect oral tissues and help to prevent tooth decay. Both diabetes itself and certain medications used for its management can lead to reduced saliva production by the salivary glands in the mouth. A decrease in saliva flow elevates the risk of dental cavities, gum disease, and other oral complications.

Furthermore, diabetes can elevate the glucose levels in saliva. In cases of diabetes, where blood glucose levels are excessively high, this surplus glucose can also accumulate in saliva. The presence of glucose in saliva can serve as a nutrient source for harmful bacteria, which, in combination with food particles, forms a soft, adhesive film known as plaque. Failure to remove plaque can lead to its hardening near the gum line, forming a deposit referred as tartar, which can provoke gum disease [80].

### 2.12.7 Lower-Extremity Amputations

These are faced by 15% of diabetic patients which is a serious consequence of the disease. Lower extremity amputations are 10-20 [81].

## 2.13 Management and Treatment for T2DM Complications

Diabetes mellitus is a chronic disease with no approved cure, requiring management and treatment. Exercise, medication, and dietary therapy are all part of the treatment [82]. Maintaining appropriate blood glucose levels is the key objective in order to avoid problems. To maintain a healthy body weight, control blood pressure, drop blood cholesterol, and lower blood glucose, regular aerobic activity is recommended. The kind of DM that is diagnosed determines the pharmacotherapy treatment. T2DM can be managed with a variety of oral medicines, and doctors use clinical judgment to choose the best treatment combination [83]. The currently available treatments for diabetic control are discussed below.

### 2.13.1 Blood Sugar Monitoring

Blood sugar monitoring is essential for determining how well the current treatment plan is working. It offers information about managing diabetes on a daily and sometimes even hourly basis. The FreeStyle Libre is a flash glucose monitor that lasts for 14 days. It stores glucose readings for eight hours using a tiny, round sensor with a thin fiber within [84]. Continuous glucose monitors (CGMs) offer real-time data and notifications without physical sensor scanning, making their use in type 2 diabetes more widespread. Eversense, the first implantable CGM, provides glucose data for a maximum of 180 days when used in conjunction with a portable transceiver and smartphone app. Three studies involving T2DM patients assessed its safety and accuracy, showing it provides accurate readings and has

superior safety record compared to traditional transcutaneous CGMs. It is suitable for patients with comorbidities, longer sensor life, and on-body alerts [85].

### 2.13.2 Insulin

People with type 1 diabetes need to inject synthetic insulin to stay alive and manage their condition. Some people with type 2 diabetes also require insulin. Different types of artificial insulin exist.

They all start off at various rates and remain in the body for varied lengths of time. Rapid-acting inhaled insulin, insulin pens, insulin pumps, and syringe-based injectable insulin are the four main methods of administering insulin [86].

Insulin pens for T2D patients have evolved with memory functions, caps, and attachments to improve monitoring and dosing adherence. Insulin pumps are a convenient and portable method for pediatric T1D patients and have been used since the 1970s, but their use is discouraged by NICE guidelines.

In type 2 diabetes, glucose-responsive insulin delivery systems also referred to as artificial pancreas systems, direct insulin pump delivery based on real-time glucose readings via a CGM monitor [87].

### 2.13.3 Healthy Lifestyle

While pharmacological treatments provide therapeutic options, lifestyle modifications are crucial for managing diabetes mellitus. Adopting a healthier diet and engaging in regular physical activity are essential to achieving optimal outcomes alongside medical interventions.

Blood pressure, weight control, and blood glucose levels are all greatly influenced by diet. There are several advantages to physical activity, including increased tissue sensitivity to insulin, better glycemic management, favorable effects on blood pressure and lipid profiles, encouragement of weight reduction, and cardiovascular benefits [88].

### 2.13.4 Insulin Sensitizers

The two types of drugs that fall within the category of insulin sensitizers are thiazolidinediones (rosiglitazone and pioglitazone) and biguanides (metformin) [89].

### 2.13.5 Biguanides

Patients with type 2 diabetes who are obese are frequently treated with biguanides; metformin is frequently used in conjunction with insulin or other oral antidiabetic medications. Metformin's main function is to reduce hepatic glucose production by reducing glyconeogenesis and glycogenolysis, improving peripheral insulin sensitivity, and ameliorating hyperglycemia. This increases hepatic insulin sensitivity, contributing to basal plasma glucose lowering effects.

Additionally, AMPK, controls the metabolism of fats and glucose, is activated by metformin. By inhibiting the expression of two crucial hepatic gluconeogenic genes, PEPCK and G6Pase, AMPK increases fatty acid oxidation and lipolysis while suppressing gluconeogenesis and lipogenesis once it is activated. Increased glucose metabolism in the splanchnic bed results from this, along with other metabolic benefits including triglyceride reduction and fatty acid oxidation suppression [89].

### 2.13.6 Thiazolidinediones

The FDA has authorized two thiazolidinedione medications for type 2 diabetes treatment: pioglitazone and the rosiglitazone. Thiazolidinediones function by binding to the PPAR-$\gamma$ receptor, primarily found in adipocytes, it causes gene transcription by mediating binding to the retinoic-X receptor.

A nuclear response element attaches to this heterodimer, affecting carbohydrate and lipid metabolism. TZDs also suppress TNF-$\alpha$ expression in adipocytes, highlighting their role in cellular metabolism [90].

### 2.13.7 Insulin Secretagogues

Insulin secretagogues i.e. sulfonylureas and meglitinides reduce blood glucose levels by promoting the release of insulin [90].

### 2.13.8 Sulfonylureas

Sulfonylureas, such as glibenclamide, gliclazide, glipizide, and glimepiride, enhance the beta-cell's sensitivity to glucose by closing potassium-sensitive ATP channels on the cell membrane.

This reduces potassium cellular efflux and promotes calcium influx through voltage-dependent $Ca^{2+}$ channels, releasing pre-formed insulin granules. This increases beta cells responsiveness to both glucose and non-glucose secretagogues, leading to more insulin release at all blood glucose concentrations [91].

### 2.13.9 Meglitinides

Type 2 diabetes can be curable with meglitinide analogs nateglinide and repaglinide. By affecting potassium efflux through potassium channels, these drugs regulate the release of insulin from beta cells.

Meglitinides share molecular binding sites with sulfonylureas, with two sites in common and one distinct site. However, unlike sulfonylureas, meglitinides do not directly affect insulin exocytosis [92].

### 2.13.10 Incretin-Based Therapies

Incretin-based therapies are a class of medications used to manage T2DM by leveraging the physiological effects of incretin hormones, primarily glucagon-like peptide-1 (GLP-1) and glucose-dependent insulinotropic polypeptide (GIP). This includes GLP-1 mimetics and dipeptidyl peptidase 4 inhibitors [93].

### 2.13.11 Glucagon-Like Peptide 1 Agonists

GLP-1, a natural peptide in the small intestine, is directly related to delaying stomach emptying and promoting fullness, and it is implicated in glucose homeostasis. By encouraging glucose-dependent insulin production, GLP-1 dramatically reduces HbA1c levels without rendering hypoglycemia more likely.

They also encourage weight reduction and improvements in blood pressure and cholesterol. Compared to existing medications, oral semaglutide, a new GLP-1 agonist that is 94% identical to human GLP-1, has shown better results on decreasing blood sugar and weight. It has been shown to play a part in all stages of diabetes and has a minimum bioavailability of 0.01% when taken orally [93].

### 2.13.12 Dipeptidyl peptidase 4 Inhibitors

DPP-IV inhibitors stimulate insulin secretion in a glucose-dependent manner, minimizing hypoglycemic side effects. These medications can be taken either alone or in conjunction with metformin, sulfonylurease, TZDs, or insulin if the existing regimen is insufficient.

Sitagliptin, saxagliptin, linagliptin, and vildagliptin can reduce HbA1C levels by 0.6-1%, with DPP-4 inhibitors decreasing HbA1c up to 3% if the basal level of HbA1c is high enough [94].

### 2.13.13 $\alpha$-Glucosidase Inhibitors

Adults with type 2 diabetes can be treated with the $\alpha$-glucosidase inhibitors acarbose, miglitol, and voglibose. The glycosidase enzymes found in the intestinal villi's brush border of enterocytes are inhibited by acarbose.

A net reduction in intestinal absorption of carbohydrates is achieved by preventing the cleavage of disaccharides and oligosaccharides. Overall, by reducing the rise

in postprandial glucose levels, $\alpha$-glycosidase inhibitors lower postprandial insulin concentrations [95].

### 2.13.14 Sodium-Glucose Cotransporter-2 Inhibitors

A novel family of antidiabetic medications called sodium-glucose transporter 2 (SGLT2) inhibitors reduces blood sugar levels by affecting the kidneys' ability to handle glucose. Invokana, the first SGLT2 inhibitor, has received FDA approval for treating T2DM.

For moderate impairment, dosage modification is recommended, and usage is contraindicated in cases of severe liver disease or renal impairment. Sergliflozin has been proven in clinical studies and animal research to exhibit dose-dependent urine glucose excretion. Although it has been shown to cause modest side effects including headache, sore throat, and dyspepsia in diabetic individuals, it dramatically decreased weight in healthy obese people [96].

### 2.13.15 Amylin Analogues

Patients with T1DM and T2DM who are currently receiving prandial insulin may benefit from the supplementary use of pramlintide. Due to the higher risk of hypoglycemia, it is not recommended for individuals who have been diagnosed with both gastroparesis and hypoglycemia unawareness. To lower the risk of hypoglycemia, dose titration is advised and prandial insulin dosages should be lowered by 50% at the start of treatment [97].

## 2.14 Side Effects of Diabetic Treatments

Oral hypoglycemic agents and insulin are central to diabetes treatment, effectively managing hyperglycemia. However, these drugs may have unfavorable side effects and frequently fall short of fully controlling the illness.

### 2.14.1 Hypoglycemia

Hypoglycemia can occur when insulin or insulin secretagogues like sulfonylureas and meglitinides are used, especially if meals are skipped or if there is excessive physical activity. By attaching to sulfonylurea receptors and blocking ATP-sensitive potassium channels, these drugs cause depolarization and calcium influx, which in turn causes the release of insulin from the pancreas. Its symptoms include dizziness, sweating, palpitations, confusion, and in severe cases, loss of consciousness [98].

### 2.14.2 Weight Gain and Weight Loss

Thiazolidinediones and insulin therapy are associated with weight gain. They increase insulin sensitivity and promote adipogenesis, leading to fat accumulation. Insulin can also stimulate appetite and increase fat storage. Weight gain can complicate diabetes management and increase cardiovascular risks. TZDs may affect bone metabolism, increasing osteoclast activity and reducing bone density. Weight loss is often seen with GLP-1 receptor agonists and SGLT2 inhibitors. These medications suppress appetite and increase glucose excretion, leading to weight loss. It can be beneficial for overweight patients but may be undesirable for others [99].

### 2.14.3 Gastrointestinal Issues

Gastrointestinal issues commonly arise with biguanides e.g., metformin and GLP-1 receptor agonists. They can alter gut microbiota and slow gastric emptying, resulting in abdominal pain and diarrhea. GLP-1 agonists stimulate the central nervous system, causing nausea and vomiting. GLP-1 receptor agonists and DPP-4 inhibitors also cause pancreatitis by triggering an inflammatory response in the pancreas in case of increased insulin secretion or alterations in pancreatic enzyme activity [100].

### 2.14.4 Lactic Acidosis

Lactic acidosis is a medical emergency and occurs particularly in patients with renal impairment.

Metformin inhibits gluconeogenesis and can lead to lactate accumulation, especially if kidney function is compromised. Its symptoms include muscle pain, difficulty in breathing, abdominal discomfort, and malaise [101].

### 2.14.5 Cardiovascular Diseases

Some sulfonylureas are linked to cardiovascular diseases. There may be increased insulin and glucose levels, leading to vascular changes and endothelial dysfunction.

These heart-related issues lead to increased morbidity and mortality [102].

### 2.14.6 Urinary Tract Infections

SGLT2 inhibitor drugs promote glucose excretion in urine, creating an environment conducive to bacterial growth which results in frequent urination, a burning sensation during urination, fever, and back pain. These medications can lead to dehydration and reduced renal perfusion, potentially causing acute kidney injury [103].

### 2.14.7 Hepatotoxicity

Hepatotoxicity is observed with thiazolidinediones. They may cause liver enzyme elevation, potentially leading to liver damage resulting in jaundice, dark urine, abdominal discomfort, and fatigue [104].

### 2.14.8 Vision Changes and Allergic Reactions

Vision changes are associated with rapid changes in blood glucose levels, particularly with insulin. Fluctuations in glucose can cause swelling of the eye's lens, leading to blurred vision [105].

Allergic reactions can occur with any medication but most common with DPP-4 inhibitors and SGLT2 inhibitors. Hypersensitivity and dermatological reactions occur when the immune system reacts to drug components resulting in rash, blisters and itching. Some diabetes medications may increase sensitivity to sunlight, leading to skin reactions [106].

### 2.14.9 Fluid Retention and Gout

Thiazolidinediones can cause sodium retention, leading to edema and increased fluid volume resulting in swelling in the legs, ankles, or feet. SGLT2 inhibitors increase uric acid excretion, leading to an acute gout attack in predisposed individuals resulting in severe pain in the joints, often the big toe [107].

TABLE 2.3: Current antidiabetic medications including drug class, drug name, molecular targets and unfavorable side effects.

| **Drug Class** | **Drug Name(s)** | **Molecular Targets** | **Unfavorable Side Effect** | **Ref** |
|---|---|---|---|---|
| Sulfonylureas | Glimepiride, Glipizide, Glyburide | Pancreatic $\beta$-cell $K_{ATP}$ channels (stimulate insulin release) | Hypoglycemia, weight gain, nausea, headache, hypersensitivity | [45] |
| Biguanides | Metformin | Inhibition of hepatic gluconeogenesis, activation of AMPK | Gastrointestinal upset (nausea, diarrhea), lactic acidosis (rare) | [45] |
| Thiazolidinediones (TZDs) | Pioglitazone, Rosiglitazone | PPAR-$\gamma$ nuclear receptors (enhance insulin sensitivity) | Weight gain, fluid retention, risk of heart failure, bone fractures | [45] |

**Table 2.3 – continued from previous page**

| Drug Class | Drug Name(s) | Molecular Targets | Unfavorable Side Effect | Ref |
|---|---|---|---|---|
| DPP-4 Inhibitors | Sitagliptin, Linagliptin, Saxagliptin | DPP-4 enzyme (prolong incretin activity) | Nasopharyngitis, pancreatitis, joint pain | [45] |
| SGLT2 Inhibitors | Canagliflozin, Dapagliflozin, Empagliflozin | SGLT2 in proximal renal tubules (reduce glucose reabsorption) | Genital infections, urinary tract infections, dehydration | [45] |
| Meglitinides | Repaglinide, Nateglinide | Pancreatic $\beta$-cell SUR (stimulate insulin secretion) | Hypoglycemia (less than sulfonylureas), weight gain | [45] |
| GLP-1 Receptor Agonists | Exenatide, Liraglutide | GLP-1 receptor (enhance insulin secretion, suppress glucagon) | Nausea, vomiting, pancreatitis risk | [45] |
| Amylin Analogues | Pramlintide | Amylin receptor (slow gastric emptying, suppress glucagon) | Nausea, vomiting, headache, hypoglycemia (with insulin) | [45] |

## 2.15 Medicinal Plants as an Alternative to Antidiabetic Drugs

Traditional antidiabetic drugs have limitations due to their adverse consequences and cost ineffectiveness. Because of their accessibility, affordability, and lack of side effects, plants with antidiabetic properties have emerged as a substitute for traditional treatments. In scientific study, they are also becoming more and more prominent as a source for finding novel medication templates. It has been established that over 410 medicinal herbs contain anti-diabetic effects [108]. By controlling the absorption of glucose and the release of insulin, the phytochemicals found in these plants such as tannins, alkaloids, flavonoids, and phenolics are crucial for enhancing the efficiency of pancreatic tissues. Antioxidants included

in holy basil, betel leaf, neem, and aloe vera aid in controlling blood sugar and body weight [109]. Berries, stone fruits, and citrus fruits lower oxidative stress and increase satiety. Special phytochemicals found in olives and amla improve insulin sensitivity. Essential fatty acids and micronutrients are found in seeds such as tamarind, cashew nut, almond, walnut, cumin, cashew nut, cocoa, and coconut. Grains high in fiber, such as quinoa, maize, and oats, aid in controlling obesity and blood sugar levels [110, 111].

Some vegetables that are great for their rich nutritional profiles and low-calorie content include bitter gourds, snake gourds, ridge gourds, bottle gourds, sweet potatoes, centella twigs, fungi, potatoes, cauliflower, kale, radish root, carrots, tomatoes, cucumbers, spinach, lettuce, okra, the asparagus plant, eggplants, beetroot, and moringa leaves. The following herbs and spices have antidiabetic properties and increase metabolic rate, curry and bay leaves, cloves, saffrons, cinnamon bark, peppers, turmeric root, ginger and garlic, mint extract, the herb parsley, celery stalks, rosemary oil, and thyme. Other foods that help with weight control and glucose metabolism include grapevines, chinese rose, coffee beans, and the onion. By improving insulin sensitivity, encouraging improved glycemic control, and promoting weight loss, incorporating these foods into a balanced diet can help manage type 2 diabetes and obesity [112].

## 2.16 Phytochemicals Significance in the Management and Treatment of Complications from Diabetes

Phytochemicals are naturally occurring chemical compounds present in cereal grains, fruits, vegetables, and plant-based liquids. They are present in different plant parts and categorized as primary and secondary metabolites. As seen in figure 2.6, anti-inflammatory, antigenotoxic, antibacterial and other beneficial qualities offer defensive mechanisms against detrimental disorders. Plant-based

diets contain classes of phytocompounds such as tannin, polyphenol, carotenoid, anthocyanin, flavonoid, and saponin which are essential for diabetes management.

By a number of methods, such as increasing insulin sensitivity, blocking the enzymes involved in breaking down carbohydrates, and lowering the liver's synthesis of glucose, these substances aid in blood sugar regulation.

They also help prevent diabetes and enhance overall metabolic function by reducing inflammation, reducing oxidative stress, promoting the production of glucoregulatory or satiating gut hormones, and improving gut health [113].

Studies have shown that antidiabetic parameters can be modulated in phytochemical-based diets. Flavonoid-rich okra can block enzymes that break down carbohydrates and promote GLUT-4 translocation, whereas polyphenols found in pineapple have anti-inflammatory properties.

Moreover, tea's high tannin content may have anti-inflammatory and insulin-sensitizing effects.

Rich in saponin, oats can help with insulin resistance and lipid profiles. The powerful antidiabetic effects of saffron, which is enhanced by advantageous phytochemicals, include lowering mitochondrial malfunction, cytokines associated with inflammation, and triglyceride levels.

Fruit polyphenols can inhibit carbohydrate disintegration, and increase the absorption of glucose hence improving insulin sensitivity. The anthocyanins found in berries can improve the sensitivity to insulin, protect $\beta$-cells, and inhibit carbohydrate - digesting enzymes [114].

Phytochemicals antidiabetic properties in the treatment of diabetes. Plant-based diets high in phytochemicals, such as flavonoids, anthocyanins, carotenoids, saponins, tannins, and polyphenols, are essential for managing diabetes because they improve insulin sensitivity, improve beta-cell activity, block enzymes that break down carbohydrates, and lower the generation of glucose in the liver, improve gut health, and reduce inflammation [115].

## 2.17 *Astragalus membranaceus*

*Astragalus membranaceus* sometimes referred to as *Astragalus propinquus* is a member of the legume family Fabaceae and sub-family Faboideae) [116]. It typically grows to a height of 60-150 cm with villous (hairy) stems. The leaves are pinnately compound with 8 to 12 pairs of ovate-lanceolate leaflets measuring 21-31 mm each. The plant produces flowers rich in nectar, attractive to pollinators like bees and butterflies. Its roots are cylindrical, 30-90 cm long with a tough yellowish-brown outer skin and a sweet white inner pulp, harvested at 4 to 5 years for medicinal use. The plant prefers dry, well-drained sandy or slightly alkaline soils in sunny positions and is hardy to temperatures as low as -15°C. It engages in nitrogen fixation via symbiotic soil bacteria forming nodules on the roots, benefiting soil fertility. The root is the principal medicinal part, containing polysaccharides, triterpenoid saponins (astragalosides), and flavonoids, which contribute to its traditional uses as an immune stimulant, tonic, antioxidant, and anti-inflammatory agent [117].

FIGURE 2.6: *Astragalus membranaceus* [116]

### 2.17.1 Geographic Distribution and Cultivation

The plant is indigenous to northern China and neighboring areas, such as Inner Mongolia, Gansu, Hebei, Shanxi, and Ningxia, where it thrives on arid, sunlit,

sandy-loam or gravelly soils, frequently at elevated altitudes. In the TCM pharmacopeia, two often cited variations are *A. membranous* and *A. mongholicus*, both referred to as huáng qí [50]. Due to significant demand, widespread cultivation has taken place in China, rendering it one of the most often utilized therapeutic herbs in the Chinese herbal tradition [117].

## 2.17.2 Therapeutic attributes of *A. membranaceus*

### 2.17.2.1 Principal Phytochemical Components

The origin of *A. Membranaceus* comprises many bioactive ingredients, including polysaccharides (*Astragalus polysaccharides*, APS), flavonoids (such as formononetin and calycosin), triterpenoid saponins (notably astragalosides, including astragaloside IV), and isoflavones [45]. It has recognized polysaccharides, flavonoids, and saponins as primary groups [47]. It also possess isoflavone compounds which has potential pharmacological properties [118].

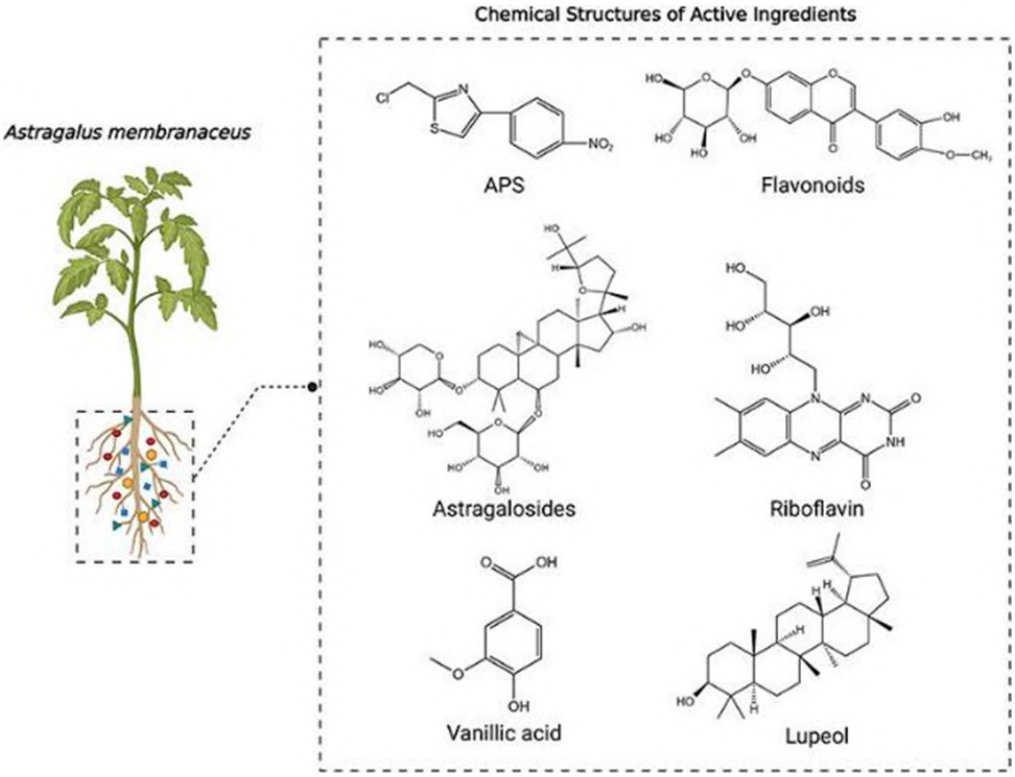


FIGURE 2.7: Chemical structures of key active ingredients in *Astragalus membranaceus* [118]

#### 2.17.2.2 Immunomodulatory and Immune-Enhancing Activities

*Astragalus polysaccharides* (APS) have demonstrated the capacity to enhance immune organ indices, such as the spleen and thymus.

It stimulate the proliferation and differentiation of immune cells including B and T lymphocytes, NK cells, and macrophages, facilitate dendritic cell maturation and antigen presentation, and modulate cytokine secretion by increasing beneficial cytokines and regulating pro-inflammatory cytokines across various experimental systems.

For example, APS modulate immune function by augmenting immune organ indices, facilitating immune cell proliferation, boosting cytokine secretion, and influencing immunoglobulin production [119]. Astragalus improved immune responses and decreased proinflammatory cytokine levels [120].

#### 2.17.2.3 Antioxidant, Anti-inflammatory, and Organ-protective Actions

Extracts from *A. Membranaceus* possesses antioxidant qualities by scavenging reactive oxygen species and upregulating Nrf2/antioxidant pathways, exhibits anti-inflammatory effects through the suppression of NF-$\kappa$B and downregulation of iNOS, COX-2, TNF-$\alpha$, and IL-6, and may safeguard organs such as the heart, liver, kidneys, and brain from injury. These extracts can enhance telomerase activity and exhibit vascular-protective and neuroprotective properties [121].

#### 2.17.2.4 Metabolic Effects: Hypoglycemic, Hypolipidemic, Anti - Fibrotic

*A. Membranaceus* may enhance glucose metabolism (decrease fasting blood sugar, increase insulin sensitivity), lower lipid levels, and alleviate organ fibrosis (renal and hepatic) in expert [46]. APS enhance insulin sensitivity and lower blood glucose levels [121].

#### 2.17.2.5 Antineoplastic and Adjunctive Effects in Oncology

*Astragalus membranaceus* has shown the anti-cancer potential through immunological augmentation, direct pro-apoptotic and anti-proliferative actions on tumor cells (e.g., via astragaloside IV), prevention of metastasis, and reduction of angiogenesis. *A. membranous* actions encompass cell cycle arrest, induction of apoptosis, and suppression of proliferation in NSCLC [121].

#### 2.17.2.6 Anti-fatigue and Ergogenic Characteristics

*A. Membranaceus* enhances exercise performance, diminishes exhaustion indicators (blood lactate, ammonia), and augments glycogen storage in the liver and muscle. This indicates a potential adaptogenic or tonic impact that improves endurance and resilience [122].

#### 2.17.2.7 Cardiovascular Disorders and Cardiac Insufficiency

*A. membranaceus* may enhance cardiac function, especially as an additional treatment for heart failure. A meta-analysis conducted in 2024 revealed that the combined medication of *A. Membranaceus* therapy in HFrEF enhanced left-ventricular ejection fraction, decreased left-ventricular end-diastolic diameter, lowered inflammatory markers (TNF-$\alpha$, IL-6, hs-CRP), and increased 6-minute walk distance, all without elevating side effects [5]. Mechanisms encompass anti-inflammatory and antioxidant actions, accelerated cardiac remodeling, better ejection fraction through augmented cardiomyocyte activity, and decreased fibrosis [120].

## 2.18 Diabetes, Diabetic Complications and Metabolic Disorders

Astragalus has been assessed for glycemic regulation, renal protection in diabetic nephropathy, and enhancement of insulin sensitivity. The NCCIH indicates a 2024

evaluation of 20 trials involving 953 individuals, which found that the addition of astragalus to metformin resulted in greater reductions in fasting blood glucose and HbA1c compared to metformin alone, while the quality of evidence was low [3].

Additional evaluations indicate that APS enhances insulin sensitivity, reduces blood glucose levels, and facilitates neuro-metabolic control [6].

Mechanisms encompass enhanced insulin sensitivity, regulation of glucose metabolic signaling, attenuation of oxidative stress in pancreatic cells, safeguarding renal cells from hyperglycemic injury, and anti-fibrotic actions on the kidneys [122].

### 2.18.1 Renal Pathology and Nephroprotection

Utilization of *A. Membranaceus* in membranous nephropathy in chronic kidney disease (CKD) and diabetic nephropathy has been investigated. The NCCIH evaluations indicate that supplementary usage enhances some kidney indicators [3].

It decrease in albuminuria/proteinuria and blood creatinine levels with astragalus formulations [123].

Mechanisms encompass anti-inflammatory, anti-fibrotic, and antioxidant effects; enhancement of renal microcirculation; and modification of signaling pathways that mitigate glomerular injury [120].

### 2.18.2 Applications in Anti-aging, Longevity, and Tonic Formulations

*A. membranaceus* has heightened telomerase activity, enhanced immune-aging indicators, and vascular protection.

Mechanisms encompass telomerase activation, decreased vascular oxidative damage, enhanced mitochondrial resilience, and mitigation of micro-inflammation [123].

## 2.19 Toxic impacts of *A. Membranaceus*

### 2.19.1 Adverse Effects

Most common side effects are typically modest, including gastrointestinal discomfort (e.g., nausea, diarrhea) and infrequent allergic responses; certain studies also indicate possible decreases in blood glucose or blood pressure [121].

### 2.19.2 Pharmacological Interactions

Due to *A. Membranaceus* can enhance immune function and may mitigate the effects of immunosuppressive medications, such as those used in organ transplantation or autoimmune patients.

It may potentially interfere with anti-diabetic or anti-hypertensive medications due to its hypoglycemic and hypotensive properties [119].

Insufficient safety data exist regarding pregnancy and lactation, and usage is not advised without expert oversight.

Some Astragalus species, not just *A. Membranaceus*, have the capacity to accumulate selenium or synthesize swainsonine, a neurotoxic alkaloid; hence, accurate species identification and product quality are imperative [120].

### 2.19.3 Contraindications and Precautions

Utilization should be circumvented or closely overseen in autoimmune disorders except under expert supervision, owing to immune-stimulatory effects [115].

Patients with uncontrolled diabetes or hypertension, as well as pregnant or nursing women, should exercise caution.

Healthcare professionals must be apprised of any Astragalus consumption to prevent drug-herb interactions [115].

TABLE 2.4: Major phytoactive compounds present in *Astragalus membranaceus* with compound name, molecular weight, medicinal properties/uses

| **Compound Name** | **Mol. Weight (g/mol)** | **Medicinal Properties/Uses** | **Ref** |
|---|---|---|---|
| Astragaloside IV | ∼784.94 | Immunomodulatory, anti-inflammatory, anti-cancer, antioxidant | [123] |
| Calycosin (Isoflavone) | ∼284.26 | Antioxidant, anti-inflammatory, neuroprotective | [123] |
| Formononetin (Isoflavone) | ∼268.26 | Anti-inflammatory, cardiovascular protection | [123] |
| Astragalans I (Polysaccharide) | ∼36,000 (varies) | Immune-enhancing, anti-tumor | [123] |
| Astragalans II & III (Polysaccharides) | 12,000 & 34,000 | Immunomodulatory | [123] |
| Cycloastragenol | ∼490.7 | Anti-aging, telomerase activation, anti-inflammatory | [123] |
| Isoflavonoid CG | ∼302.3 | Antioxidant, anti-inflammatory, neuroprotective component | [123] |

# Chapter 3

# Materials and Methods

## 3.1 Collection, Drying and Extract Preparation

The leaves of Astragalus membranaceous were obtained from the local market and thoroughly washed with tap water. The leaves were cleaned and then allowed to dry for 15–17 days at room temperature. To get a uniformly coloured powder, dried leaves were pulverised using a grinder. For extract preparation, the 5:1 ratio of methanol and dry powder was taken in reagent bottles and shaken for a whole day. The solution was then centrifuged, followed by filtration, and poured into petri dishes until it had evaporated. The final yield of the dried extract was calculated and it was stored at 4°C [124].

## 3.2 Phytochemical Screening

The phytochemical screening provides valuable information about the bioactive compounds present in A. membranaceous. For identification, thin-layer chromatography (TLC) analysis was performed on silica gel plates. For fractionation, column chromatography was performed on silica gel and Diaion HP-20. The fractions obtained were mixed to super-fractions based upon TLC analysis and checked for their phenolic count and antioxidant potential by performing total

phenolic content and radical scavenging assay. Moreover, their anti-diabetic effectiveness was assessed by performing alpha-glucosidase and alpha-amylase assays. The liquid chromatography-mass spectrometry (LC-MS) was performed for quantification of these super-fractions to ensure the phytochemicals present in them. All the organic solvents for the chromatographic separations and extractions were distilled before use and performed following the standard protocol with slight modifications [125].

### 3.2.1 Thin Layer Chromatography

Thin-layer chromatography is a widely used technique for separating and analyzing compounds in a mixture. The procedure began with the preparation of a TLC plate coated with silica gel. A small amount of the sample solution, i.e., methanolic extract of *A. membranaceous* was applied as a spot near the bottom of the plate using a capillary tube.

Care was taken to ensure that the spot is small and concentrated. Once the sample is applied, the plate is placed upright in a developing chamber containing a shallow layer of solvent or mobile phase that is appropriate for the compounds being analyzed [126].

Different solvent systems were tried to check whether the compounds show polar or non-polar behaviour. One of them is n-hexane: ethyl acetate. In this solvent system, n-Hexane is non-polar, and ethyl acetate is moderately polar.

This mixture is used to achieve a balance between non-polar and moderately polar compounds. It helps in separating compounds that range in polarity, allowing for effective resolution of mixtures containing both polar and non-polar substances. Different ratios were tried to fine-tune the separation [127].

Dichloromethane: Methanol was also used as a solvent system. Dichloromethane is moderately polar and effective for separating a range of compounds, particularly non-polar to moderately polar substances, while methanol is highly polar, which enhances the separation of polar compounds [128].

In n-hexane: chloroform, n-hexane is a non-polar solvent, effective for separating non-polar compounds. It has low interaction with polar stationary phases, while chloroform is moderately polar, which helps in separating compounds that exhibit some polarity [129].

In chloroform: methanol, chloroform is moderately polar, and methanol is highly polar. This combination is particularly effective for separating polar compounds. The increasing polarity of methanol enhances the movement of polar analytes, while chloroform aids in moderating interactions with the stationary phase. This mixture is useful for compounds that exhibit strong polar characteristics [130]. The selected solvent systems for TLC of A. membranaceous, along with ratios and usefulness based upon separation of polar, moderate or non-polar substances, are shown in table 3.1.

TABLE 3.1: Solvent Systems and Their Usefulness

| S.No | Solvent Systems Used | Ratios | Usefulness of the selected ratios |
|---|---|---|---|
| 1 | n-hexane: ethyl acetate | 5:05 | A balanced polarity that can separate moderately polar compounds |
| | n-hexane: ethyl acetate | 1:10 | More polar, suitable for separating polar compounds that require a stronger solvent to move |
| | n-hexane: ethyl acetate | 10:01 | Less polar, ideal for non-polar compounds |
| 2 | Dichloromethane: Methanol | 5:05 | This ratio creates a solvent system that is neither too polar nor too non-polar, providing a balanced environment for the separation of a wide variety of compounds |
| 3 | n-hexane: Chloroform | 9:01 | The 9:1 ratio favors n-hexane, making the solvent system predominantly non-polar. This is beneficial for separating non-polar compounds |
| 4 | Chloroform: Methanol | 100% M | Methanol is highly polar, making it excellent for separating very polar compounds |
| 5 | Chloroform: Methanol | 1:01 | This ratio allows both polar and non-polar compounds to be separated. It's useful for compounds that have intermediate polarity |
| 6 | Chloroform: Methanol | 5:01 | This ratio leans towards non-polarity while still allowing some interaction with polar compounds. It is effective for moderately polar substances |

**Table 3.1 – continued from previous page**

| S.No | Solvent Systems Used | Ratios | Usefulness of the selected ratios |
|---|---|---|---|
| 7 | Chloroform: Methanol | 9:01 | It provides a slight preference towards non-polarity, useful for separating a range of moderately polar to non-polar compounds |
| 8 | Chloroform: Methanol | 10:01 | This ratio can effectively resolve a wide range of polarities, facilitating better resolution of polar compounds |
| 9 | Chloroform: Methanol | 15:01 | It is useful for separating compounds with higher polar interactions |
| 10 | Chloroform: Methanol | 20:01 | It is suitable for compounds with low to moderate polarity. It allows for slower movement, which can help achieve better separation of compounds |
| 11 | Chloroform: Methanol | 30:01:00 | Very non-polar, useful for separating non-polar compounds or those with minimal polarity |
| 12 | Chloroform: Methanol | 1:05 | This ratio favors polar interactions, effectively separating polar compounds while reducing the mobility of non-polar substances |
| 13 | Chloroform: Methanol | 1:10 | This ratio enhances the separation of polar analytes, making it ideal for compounds with strong polar characteristics |
| 14 | Chloroform: Methanol | 1:20 | This is best for very polar compounds. The high proportion of methanol ensures that polar analytes are effectively mobilized |
| 15 | Chloroform: Methanol | 100% C | Chloroform is moderately polar, using it in 100% allows for the separation of non-polar compounds |

These solvents gradually ascended the plate through capillary action, carrying the sample with them. As the solvent moved, the different components of the sample separated based on their affinities for the stationary phase (the silica gel) and the mobile phase (the solvent). Once the solvent front reached a predetermined height, the plate was removed and allowed to dry. Visualization of the separated compounds was achieved using UV light and by applying Wagner's and Dragendorff staining reagents. The positions of the compounds were marked, and the

retention factor (Rf value) was calculated by measuring the distance traveled by each compound relative to the solvent front [131].

### 3.2.2 Column Chromatography

Column chromatography was performed by preparing the column by cleaning it thoroughly and adding a small amount of the mobile phase to the bottom to prevent the stationary phase from drying out. Next, the column was packed with the stationary phase, such as silica gel, by using a funnel to ensure a uniform layer formation. The mobile phase was added continuously to saturate the stationary phase and to eliminate air bubbles. The sample was prepared by dissolving it in a small amount of the mobile phase and filtering it to remove insoluble particles. Carefully sample was loaded onto the stationary phase and adsorbed for a few minutes. Elution began by adding the mobile phase at a steady flow rate, collecting the eluent in fractions using test tubes. Separation was monitored with TLC to track the progress and identify distinct components. Fractions were collected and combined to make super-fractions based on TLC analysis [132].

#### 3.2.2.1 Bioactivity Assays

**i. Radical Scavenging Assay**

The antioxidant activity of column chromatography super-fractions of A. membranaceous was evaluated using the DPPH free radical scavenging assay [133]. The experiment was conducted by using 0.004% (w/v) DPPH solution prepared in methanol. For this purpose, 1mg/1ml dilution of each super-fraction was prepared by taking 1mg of dried fraction in 1ml of methanol. 100uL of each dilution was mixed with 3ml DPPH. The methanolic leaf extract of A. membranaceous was gradually added to the DPPH solution, resulting in gradual shift in the solution's color from deep violet to pale yellow. The reduction of DPPH's purple color in test samples indicates the antioxidant action. The DPPH solution was left undisturbed for thirty minutes in order to verify its stability. Throughout

the experiment, the solution's color remained unchanged, indicating that DPPH's maximal stability had occurred. The absorption intensity of the solution was measured using a spectrophotometer at 517 nm. The antioxidant activity percentage was calculated using the following formula.

$$Scavenging\ percentage\ = \frac{(Acontrol\ -\ Asample\ )}{Acontrol} \times 100$$

$A_{sample}$ is the treatment with plant fraction absorbance is at 517 nm. $A_{control}$ is the sample's absorbance at 517 nm without plant fraction.

### ii. Total Phenolic Assay

Phenolic compounds are family of antioxidant agents that may both adsorb and neutralize free radicals. The FC method was utilized to observe the total phenolic content of the A. membranaceous super-fractions [134]. Gallic acid was used as standard. 10% FC reagent was mixed with 7.5% $Na_2CO_3$. It was further mixed with gallic acid (0-12 ppm) and incubated at 45°C for 45 minutes in incubator. It was followed by measuring absorbance at 765 nm. A calibration curve was created using gallic acid. The standard curve was used to create a regression equation, which was then used to quantify the amount of gallic acid in the A. membranaceous super-fractions. Phenolic concentrations were measured by mixing 270 $\mu$L of each super-fraction dilution with 10% FC reagent and 7.5% $Na_2CO_3$. The absorbance was again measured at 765 nm.

### iii. Inhibition of Alpha-amylase

Alpha-amylase is involved in starch digestion, and its inhibition can have significant implications for diabetes management and food processing. Here we investigated the inhibitory effects of super-fractions of A. membranaceous against alpha amylase activity by mixing 125 $\mu$L phosphate buffer (pH 6.9), 250 $\mu$L super-fraction dilution and 250 $\mu$L alpha-amylase enzyme (0.5 mg/mL). It was pre-incubated at 25°C for 10 minutes. Then 250 $\mu$L of 1% starch in 0.02 M sodium phosphate buffer (pH 6.9) was added and incubated again at 25°C for 10 minutes. Reaction was stopped by adding 0.5ml DNSA reagent, then it was incubated in a

boiling water bath for 5 minutes and cooled to room temperature. The reaction mixture was then diluted after adding 5 ml of distilled water. Acarbose was used as the positive control [135]. Absorbance was measured at 540 nm and percentage of inhibition was calculated using the following formula.

$$Alpha - amylase\ inhibition\ percentage = \frac{(A_{control} - A_{sample})}{A_{control}} \times 100$$

$A_{sample}$ is the treatment with plant fraction absorbance is at 540 nm. $A_{control}$ is the sample's absorbance at 540 nm without plant fraction.

**iv. Inhibition of Alpha-glucosidase**

To perform alpha-glucosidase assay, a mixture of 50 $\mu$l of each A. membranaceous super-fraction and 100 $\mu$L of 0.1 M phosphate buffer (pH 6.9) containing 50 $\mu$L $\alpha$-glucosidase solution was taken in a cuvette and incubated at 25°C for 10 min. After preincubation, 50 $\mu$L of 5 Mm PNPG solution in 0.1 M phosphate buffer (pH 6.9) was added to each cuvette. The reaction mixtures were incubated at 25°C for 5 min. Before and after incubation, absorbance was recorded at 405 nm by a spectrophotometer. Acarbose was used as the positive control [136]. The percentage of inhibition was calculated using the following formula.

$$Alpha - glucosidase\ inhibition\ percentage = \frac{(A_{control} - A_{sample})}{A_{control}} \times 100$$

$A_{sample}$ is the treatment with plant fraction absorbance is at 405 nm. $A_{control}$ is the sample's absorbance at 405 nm without plant fraction.

### 3.2.3 Liquid Chromatography-Mass Spectrometry

The apparatus used for LCMS analysis was a Triple Quadrupole Mass Spectrometer, model: TSQ Quantis (Thermo Electron Scientific, USA) equipped with a heated electrospray ionization (H-ESI) source. In this method, methanol was employed as the solvent for sample preparation, and samples were introduced through a direct insertion technique. The capillary voltage was set to 80 kV to optimize ion

generation. The sheath gas flow rate was configured at 15 units, complemented by an auxiliary gas flow rate of 5 units. Scanning occurred at a rate of 30 to 1500 m/z, and the capillary temperature is held at 275 °C.

Ionization was achieved using heated electro spray ionization, which effectively converts the samples into ions for detection. During the fragmentation phase of the MS/MS operation, multiple peaks were selected for analysis, with collision energies varying between 10 to 40 V. Xcalibur software was used for data collection. Samples were prepared with meticulous care, and the instrument was calibrated beforehand to ensure both accuracy and repeatability in the results. Data analysis was performed by carefully observing relative abundances and verifying fragmentation patterns of both positive and negative modes of MS/MS spectra for each super-fraction by using ChemDraw Ultra 12.0 software [137].

## 3.3 In silico Evaluation of *A. membranaceous* Phytocompounds

### 3.3.1 Selection of Target Proteins

The peroxisome proliferator-activated receptor-$\gamma$ (PPAR-$\gamma$), pancreatic and duodenal homeobox 1 (PDX-1), insulin receptor substrate-2 (IRS-2), phosphatidylinositol 3-kinase alpha (PI3K-$\alpha$), and protein kinase B (Akt2) were selected as target proteins for their potential roles in the development of Type 2 Diabetes.

### 3.3.2 Proteins 3D Structure Prediction and Refinement

The 3D structures of target proteins were predicted through PDB www.rcsb.org. The FASTA sequences were also retrieved using the same database [138]. PyMOL https://pymol.org/ is an open-source molecular graphics application widely used worldwide to examine and portray various proteins, small molecules, nucleic acids, electron densities, and varying surfaces, as well as trajectories. It is also used for

editing the molecules, tracing the ray, and also to make animations and movies. This is software that is based on Python and also contains many plugin tools to enhance its use and facilitate drug targeting and designing by the use of PyMol software. The excess components linked to the protein must be deleted after downloading the protein's structure which was done by the use of an open-source system PyMol [139].

### 3.3.3 Analysis of Physicochemical Properties of Target Proteins

The function of the proteins is significantly influenced by their physicochemical characteristics. ProtParam expasy tool https://web.expasy.org/protparam/ was used for the prediction of these features of target proteins. ProtParam was used to calculate the number of negatively charged residues (Asp+ Glu) and positively charged residues (Arg+ Lys), theoretical pI, molecular weight, aliphatic index, grand average of hydrophobicity, instability index, Ext coefficient (with Cys) and Ext coefficient (excluding Cys) [140].

### 3.3.4 Active Site Identification

The area in which the target protein's active site is located is where the ligand exhibits the greatest or maximal interaction with the protein. Amino acids have a major role in the ligand-protein complex building process. Dogsitescorer https://proteins.plus/help/dogsite software was used for the detection of protein binding pockets [141].

### 3.3.5 Selection of Active Metabolic Ligands

After an extensive literature review and examining LCMS results, those phytocompounds from *Astragalus membranaceus* were selected that have previously shown some potential medicinal properties. These include aristolone, medicarpin,

riboflavin and vasicine These compounds exhibit strong antioxidant, antidiabetic, anti-inflammatory, and anti-oxidative activities, which are crucial in mitigating Type 2 diabetes pathophysiology.

### 3.3.6 Retrieval of Chemical Structure of Ligands and Energy Minimization

PubChem https://pubchem.ncbi.nlm.nih.gov/ is the world's largest repository of easily accessible chemical information databases. So the chemical compounds that were selected as potential ligands were taken from the PubChem database in SDF format. If the selected ligand structure is not available, then our next attempt would be to download the canonical smiles from PubChem and then insert them in the software ChemDraw to obtain the 3D structure [142].

Ligand's energy was minimized by using Chem3D Pro. It is a necessary step to refine the ligands before performing docking; otherwise, there will be unreliable docking scores [143].

### 3.3.7 Virtual Screening and ADMET Analysis of Ligands

An essential criterion for determining whether ligands are likely to be drugs is the Lipinski rule. Certain chemicals are likely to be utilized as active pharmaceuticals in humans if they adhere to the lipinski rule of five. pkCSM omictools.com is an online tool that helps to check whether ligands obey lipinski rule or not. According to these rules, the log P value, rotatable bond and hydrogen bond donors should be in the range of five. While the hydrogen bond acceptors should be limited to ten, and the molecular weight should be below five hundred grams [144].

After filtering the ligands by applying the lipinski rule, the next step of the study was the prediction of pharmacokinetic and toxicity properties. The weak candidates of the drug would be eliminated during ADMET analysis [145]. The remaining candidates can be selected as potential drugs against the disease.

### 3.3.8 Molecular Docking and Analysis of Docked Complexes

For performing the molecular docking between the protein and the ligand, CB-dock (Cavity detection guided blind docking) was used. CB-dock clab.labshare.cn finds the sites of docking automatically. CB-Dock is a method of protein and ligand docking that indicates the sites of bonding, the size, and the center calculated [146].

The box size is adjusted according to the ligand and then docking is performed. The docking is performed through AutoDock Vina. Its accuracy ratio is greater because the docking process is more focused on cavity binding. We uploaded the proteins to do docking, using the 3D structure in pdb format and the ligand's 3D structure in SDF format. After this, docking is performed, the result would be 5 different poses of interaction.

To select the best pose, we would look at the lowest docking score which is given in KJ/m-1 CB- Dock will provide an interactive 3D visualization of results in 5 different poses. Based on the lowest vina score expressed in (kJ/m1), the optimal position was chosen [147].

To interpret docking findings, the interaction between the ligand and the protein's active pockets was calculated. Different types of interactions were examined including hydrophobic and hydrogen bonding. Discovery studio 2025 Client was used to analyze the protein-ligand interactions. The protein-ligand interactions for the designated ligands in the PDB file are automatically schematically diagrammed by this application [148].

### 3.3.9 Lead Compound Identification

The most active inhibitor was found after a thorough examination of docking scores, pharmacokinetic studies, toxicity features, and protein and ligand interactions. Our lead compound was the one that followed all these parameters.

### 3.3.10 Reference Drug Selection

The purpose of this step is to identify the commercial drug that are already in use for type 2 diabetes therapy. The Drug Bank https://go.drugbank.com/ database was used for this purpose because it provides details about drugs and their pathways [149].

### 3.3.11 Comparison between Lead Compound and Reference Drug

Docking values, molecular interactions, and pharmacokinetic features were compared between the reference drug and the suggested lead molecule.

# Chapter 4

# Results

## 4.1 Collection and Drying of *A. membranaceous*

The leaves of *A. membranaceous* were obtained from the local market and thoroughly washed with tap water. The leaves were cleaned and then allowed to dry for 15–17 days at room temperature. To obtain a uniformly colored powder, the dried leaves were pulverized using a grinder. The weight of dried powder was 1780 grams.

## 4.2 Extract Preparation

The effect of three extraction process factors: the methanol concentration, powder concentration and extraction time was evaluated. The protocol criteria were taken into consideration when selecting the factorial levels. In multiple reagent bottles, methanol and plant powders were mixed in a 5:1 ratio, and these bottles were placed on a shaker for 24 hours, respectively. Then the solutions were filled in 50 mg falcon tubes and centrifugation was done at 4000 rpm for 10 minutes. The supernatants (extracts) were separated from the pellet through filtration. The filtered extracts of *A. membranaceous* were taken in large petri dishes and placed at room temperature for the given period of time. It took 5-7 days to evaporate the

solvent at room temperature and a greenish-brown dry extract was obtained. The percentage yield of total extract is 36.5 grams. Then up to the time of additional testing, these extracts were stored at 4°C. Figure 4.1(a-f) represents all steps of extract preparation.

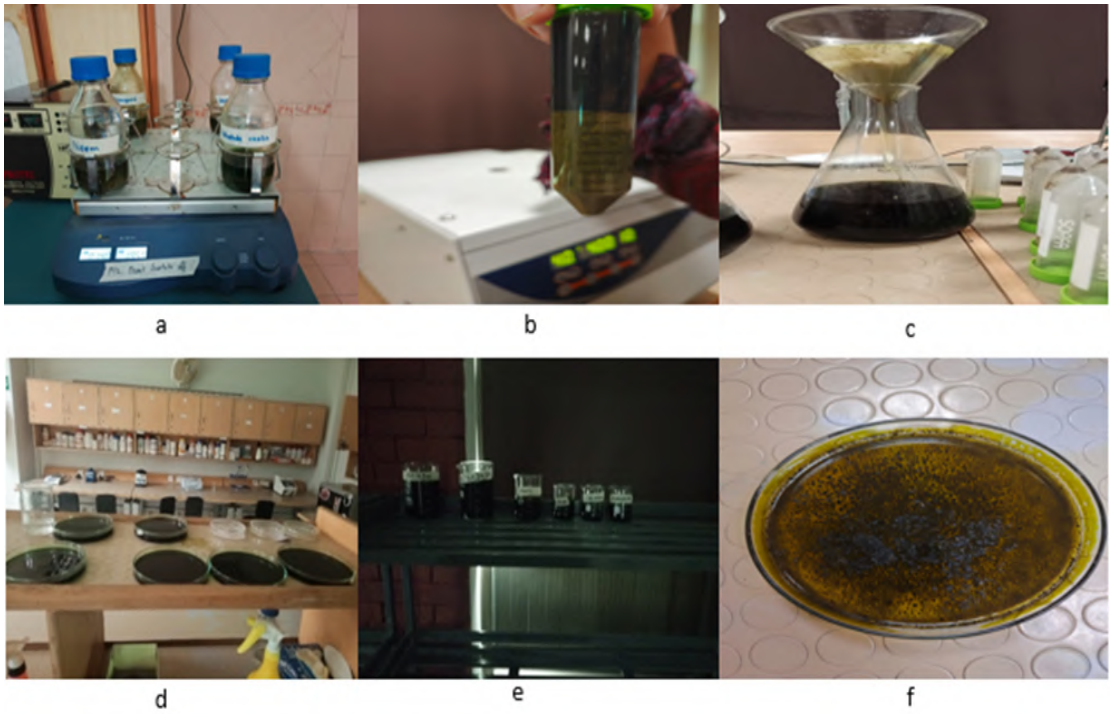


FIGURE 4.1: Extract preparation (a) Shaking (b) centrifugation (c) filtration (d) evaporation (e) greenish-brown extract (f) concentrated extract for use in experiments

## 4.3 Phytochemical Screening

For phytochemical screening of *A. membranaceous*, thin layer chromatography, column chromatography, and LCMS were performed.

### 4.3.1 Thin Layer Chromatography

Thin-layer chromatography of *A. membranaceous* was performed by taking different concentrations of the solvent systems, i.e., chloroform/methanol, n-hexane / chloroform, dichloromethane / methanol and n-hexane/ethyl acetate. The plant's response to these varying solvents was observed in visible light, UV366nm, UV

254 nm and staining reagent. TLC bands detection after dye treatment was also analyzed. Compounds having Rf values between 0.01-0.2 are highly polar while 0.3-0.6 are moderately polar. Compounds having Rf values between 0.7 and 0.8 are considered less polar, while Rf values above 0.8 are non-polar compounds. The chromatograms with all these observations are shown in the figures below.

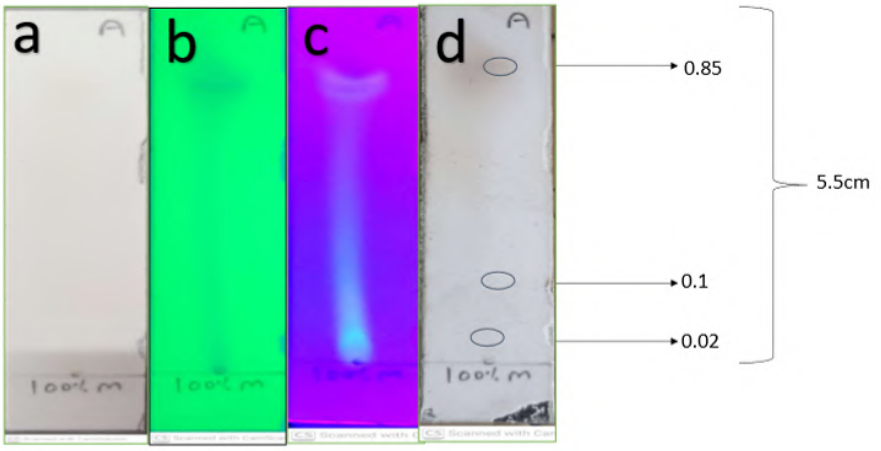


FIGURE 4.2: TLC chromatogram of *A. membranaceous* in 100% methanol (a) visible light (b) UV 360 nm (c) UV 254 nm (d) detection of bands with Rf value

Representative silica TLC separations of *A. membranaceous* extract are shown in figure 4.2. Separation of the extract in 100% methanol over 5.5 cm resulted in three bands with Rf values of 0.02, 0.2 and 0.85, indicating the presence of highly polar to non-polar compounds.

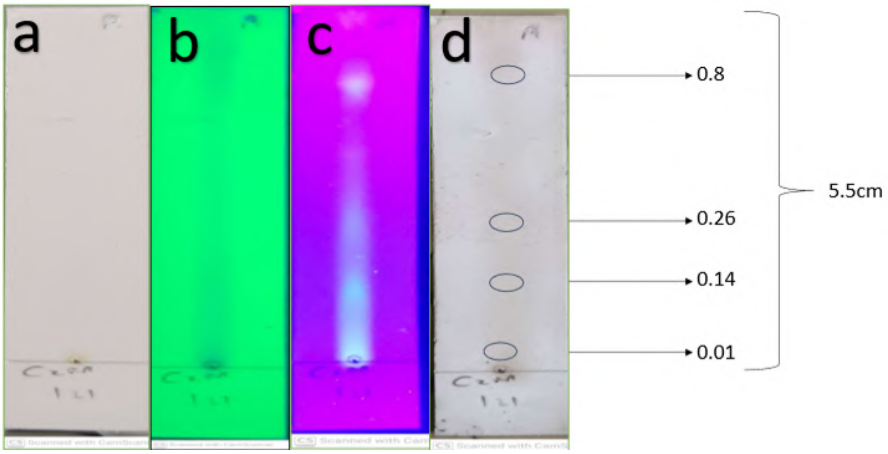


FIGURE 4.3: TLC chromatogram of *A. membranaceous* with chloroform:methanol of ratio 1:1 (a) visible light (b) UV 360 nm (c) UV 254 nm (d) detection of bands with Rf value

Figure 4.3 shows that separation of the extract in chloroform:methanol 1:1 over 5.5 cm resulted in four bands with Rf value 0.01, 0.14, 0.26 and 0.8, indicating the presence of highly polar to less polar compounds.

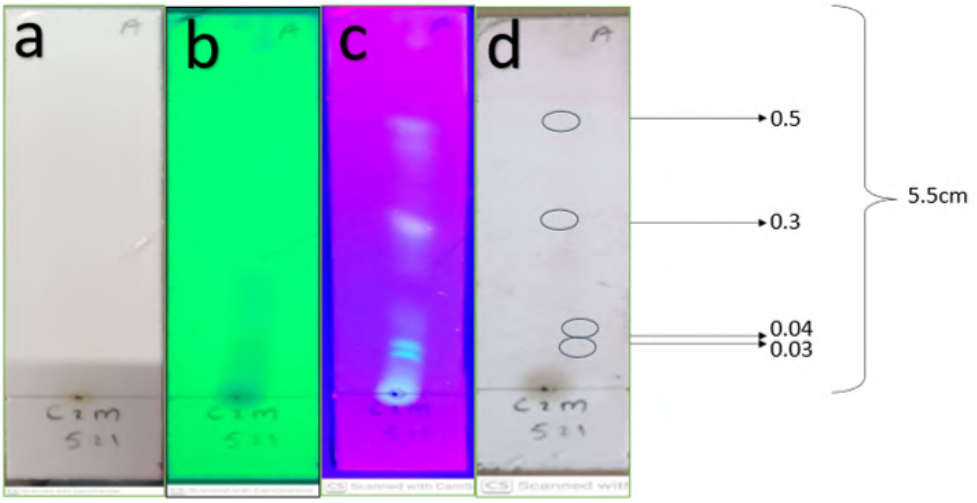


FIGURE 4.4: TLC chromatogram of *A. membranaceous* with chloroform:methanol of ratio 5:1 (a) visible light (b) UV 360nm (c) UV 254nm (d) detection of bands with Rf value

Figure 4.4 shows that separation of the extract in chloroform:methanol 5:1 over 5.5 cm resulted in four bands with Rf values 0.03, 0.04, 0.3 and 0.5, indicating the presence of highly polar to moderately polar compounds.

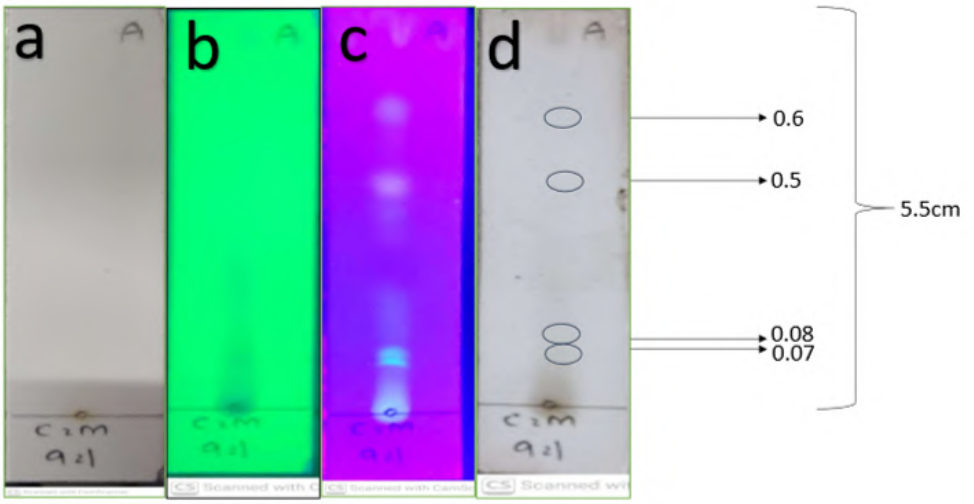


FIGURE 4.5: TLC chromatogram of *A. membranaceous* with chloroform:methanol of ratio 5:1 (a) visible light (b) UV 360 nm (c) UV 254 nm (d) detection of bands with Rf value

Figure 4.5 shows that separation of the extract in chloroform:methanol 9:1 over 5.5 cm resulted in four bands with Rf values 0.07, 0.08, 0.5 and 0.6, indicating the presence of highly polar to moderately polar compounds.

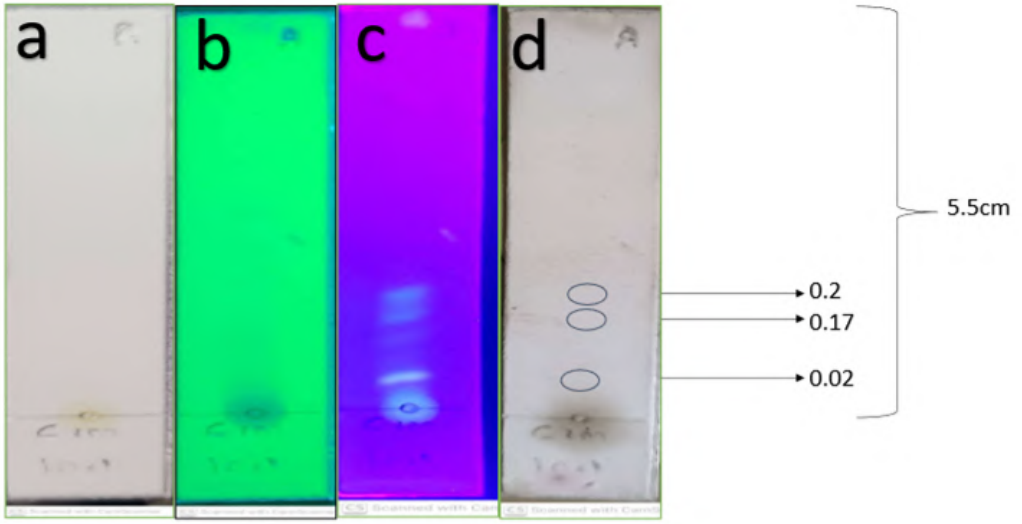


FIGURE 4.6: TLC chromatogram of *A. membranaceous* with chloroform:methanol of ratio 10:1 (a) visible light (b) UV 360nm (c) UV 254nm (d) detection of bands with Rf value

Figure 4.6 shows that separation of the extract in chloroform:methanol 10:1 over 5.5 cm resulted in three bands with Rf values 0.02, 0.17 and 0.2, indicating the presence of highly polar compounds.

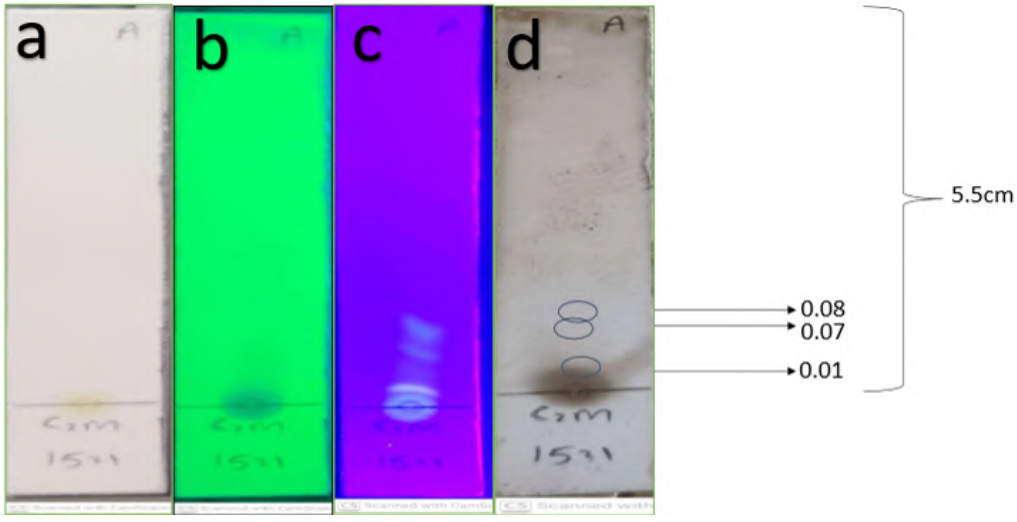


FIGURE 4.7: TLC chromatogram of *A. membranaceous* with chloroform:methanol of ratio 15:1 (a) visible light (b) UV 360nm (c) UV 254nm (d) detection of bands with Rf value

Figure 4.7 shows that separation of the extract in chloroform:methanol 15:1 over 5.5 cm resulted in three bands with Rf values 0.01, 0.07 and 0.08, indicating the presence of highly polar compounds.

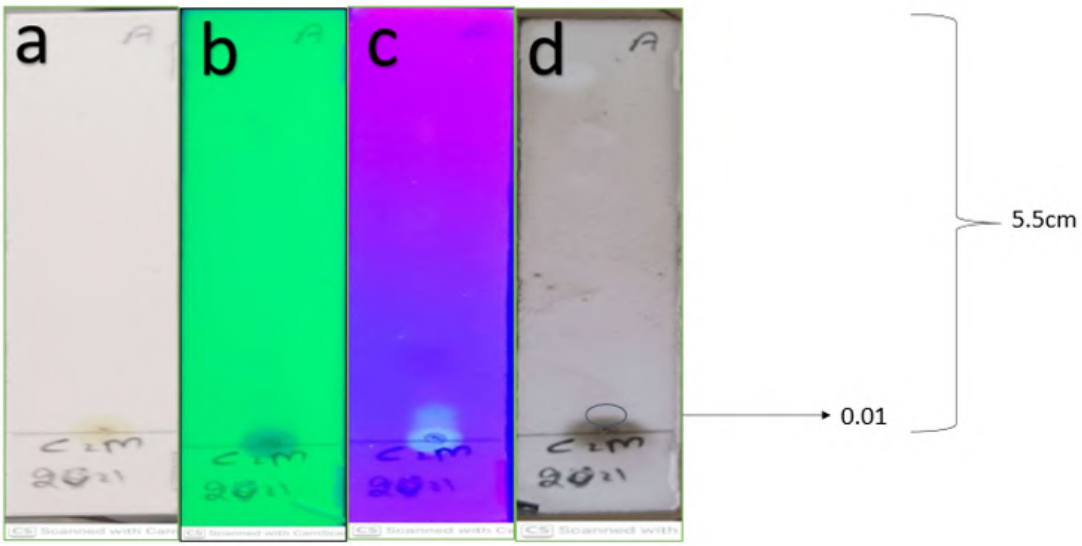


FIGURE 4.8: TLC chromatogram of *A. membranaceous* with chloroform:methanol of ratio 20:1 (a) visible light (b) UV 360nm (c) UV 254nm (d) detection of bands with Rf value

Figure 4.8 shows that separation of the extract in chloroform:methanol 20:1 over 5.5 cm resulted in one band with Rf value 0.01, indicating the presence of highly polar compounds.

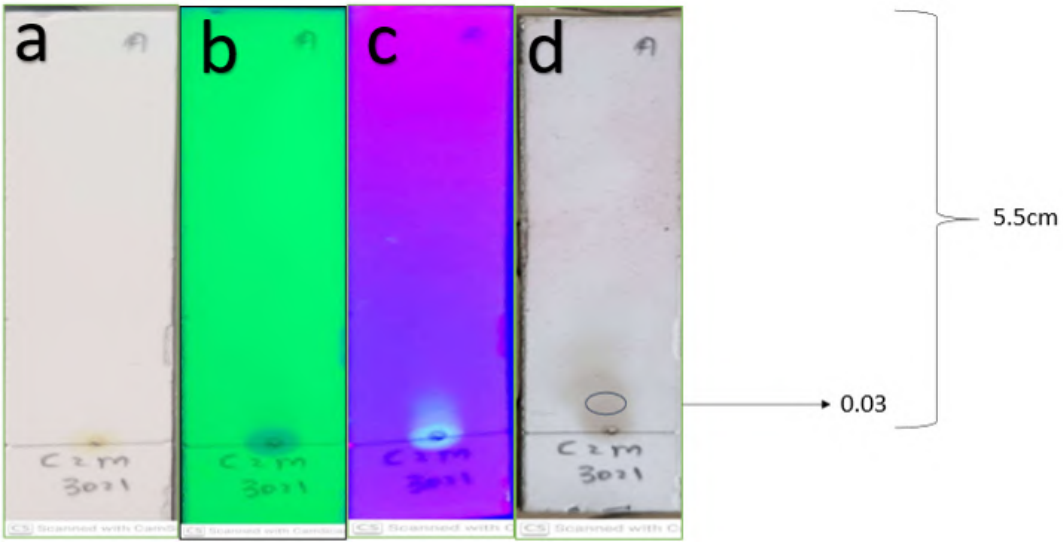


FIGURE 4.9: TLC chromatogram of *A. membranaceous* with chloroform:methanol of ratio 30:1 (a) visible light (b) UV 360nm (c) UV 254nm (d) detection of bands with Rf value

Figure 4.9 shows that separation of the extract in chloroform:methanol 30:1 over 5.5 cm resulted in one band with Rf value 0.03, indicating the presence of highly polar compounds.

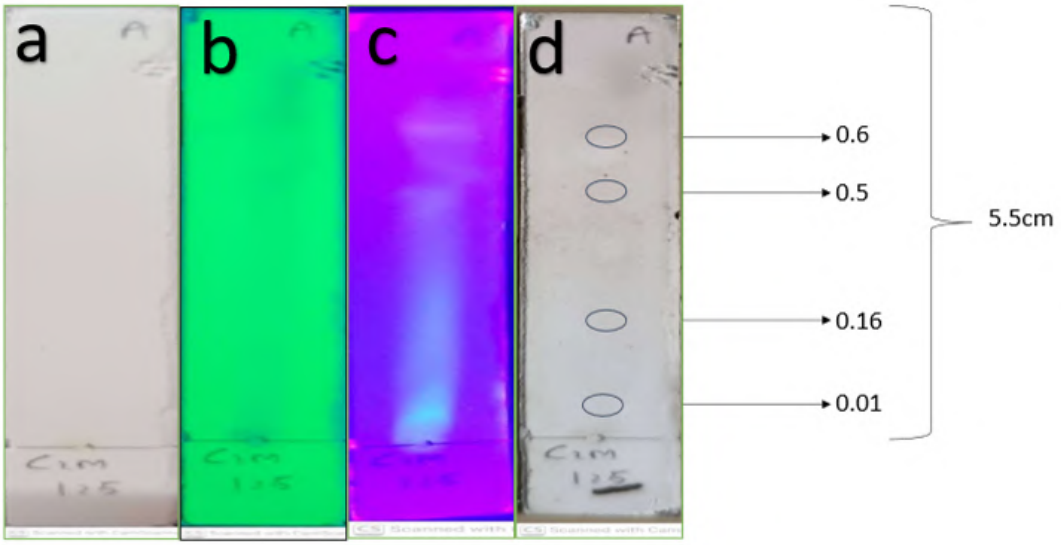


FIGURE 4.10: TLC chromatogram of *A. membranaceous* with chloroform:methanol of ratio 1:5 (a) visible light (b) UV 360 nm (c) UV 254 nm (d) detection of bands with Rf value

Figure 4.10 shows that separation of the extract in chloroform:methanol 1:5 over 5.5 cm resulted in four bands with Rf values 0.01, 0.16, 0.5 and 0.6, indicating the presence of highly polar to moderately polar compounds.

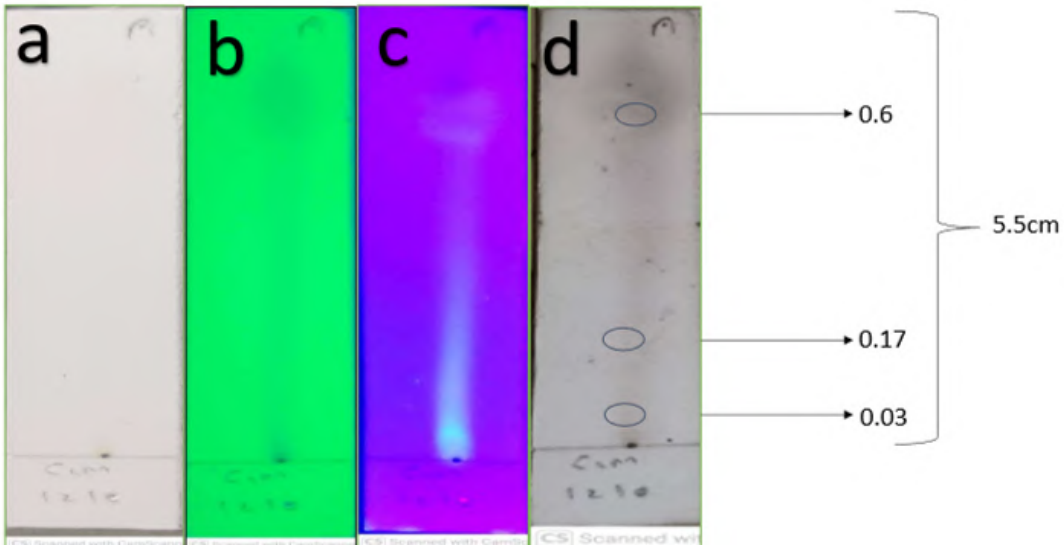


FIGURE 4.11: TLC chromatogram of *A. membranaceous* with chloroform:methanol of ratio 1:10 (a) visible light (b) UV 360nm (c) UV 254nm (d) detection of bands with Rf value

Figure 4.11 shows that separation of the extract in chloroform:methanol 1:10 over 5.5 cm resulted in three bands with Rf values 0.03, 0.17 and 0.6 indicating the presence of highly polar compounds.

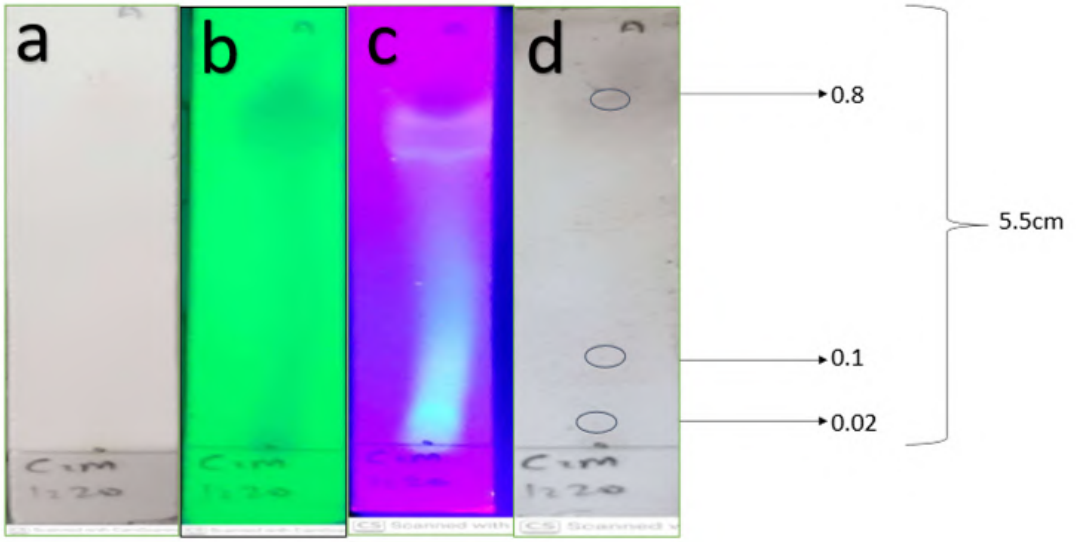


FIGURE 4.12: TLC chromatogram of *A. membranaceous* with chloroform:methanol of ratio 1:20 (a) visible light (b) UV 360nm (c) UV 254nm (d) detection of bands with Rf value

Figure 4.12 shows that separation of the extract in chloroform:methanol 1:20 over 5.5 cm resulted in three bands with Rf values 0.02, 0.1 and 0.8, indicating the presence of highly polar to less polar compounds.

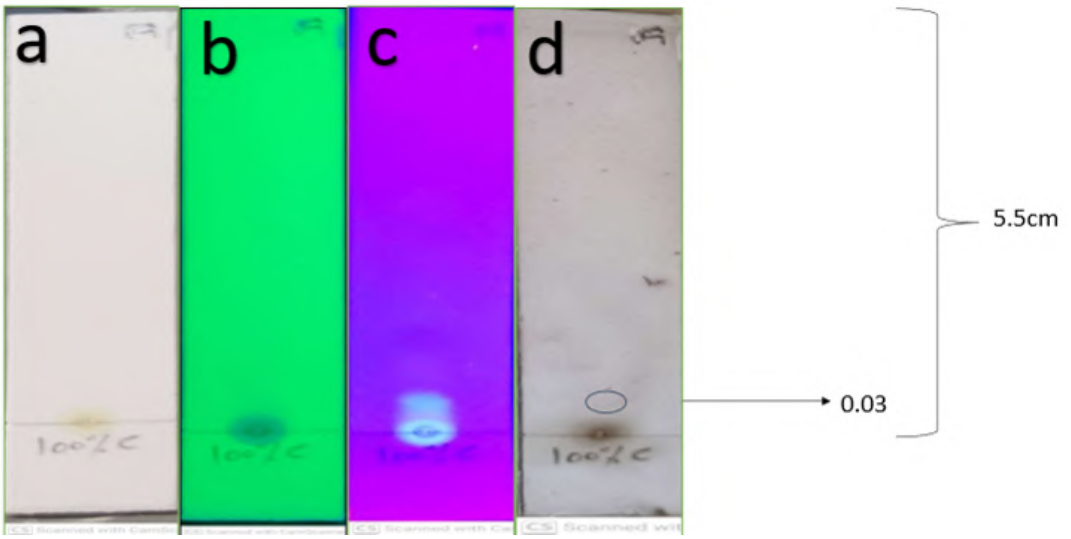


FIGURE 4.13: TLC chromatogram of *A. membranaceous* with 100% chloroform (a) visible light (b) UV 360nm (c) UV 254nm (d) detection of bands with Rf value

Figure 4.13 shows that separation of the extract in 100% chloroform over 5.5 cm resulted in one band with Rf value 0.03, indicating the presence of highly polar compounds.

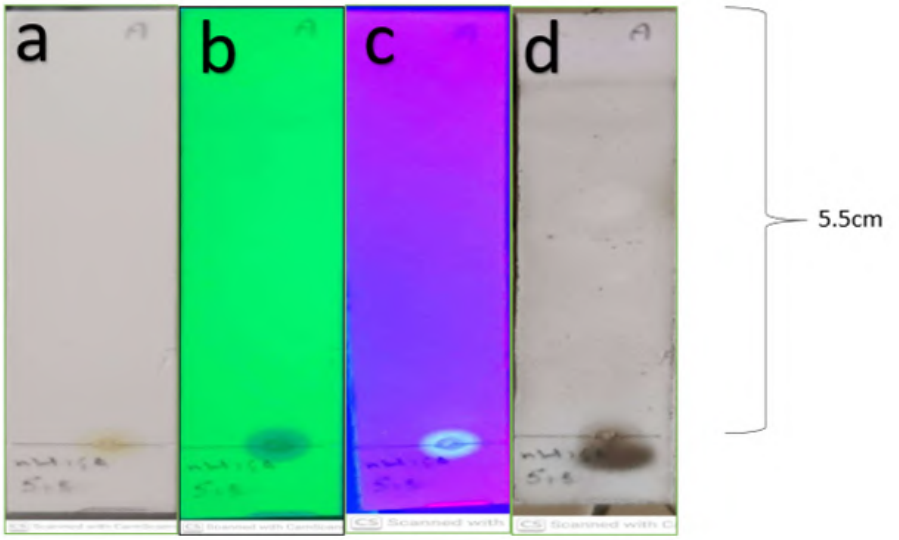


FIGURE 4.14: TLC chromatogram of *A. membranaceous* with n-hexane:ethyl acetate of ratio 5:5 (a) visible light (b) UV 360nm (c) UV 254nm (d) detection of bands with Rf value

Figure 4.14 shows that separation of the extract in n-hexane:ethyl acetate 5:5 over 5.5 cm resulted in no band, indicating that this solvent system is not suitable for *A. membranaceous*.

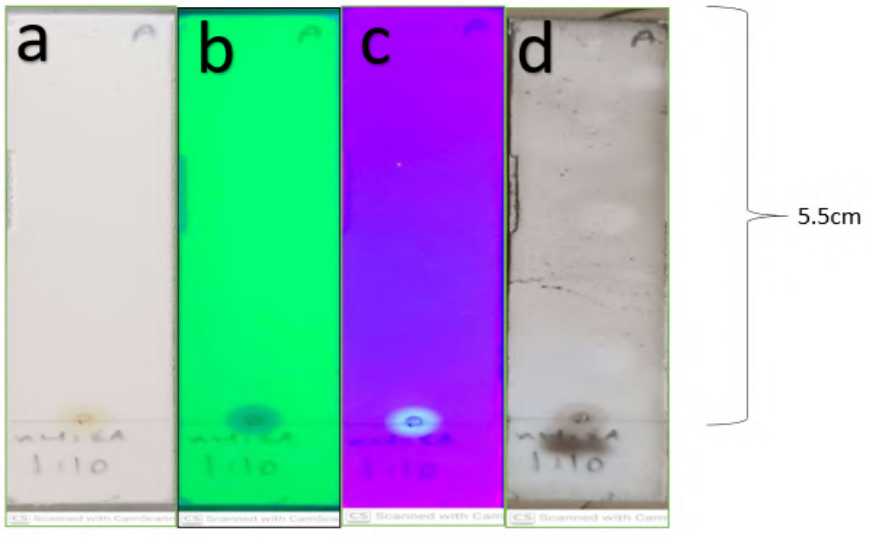


FIGURE 4.15: TLC chromatogram of *A. membranaceous* with n-hexane:ethyl acetate of ratio 1:10 (a) visible light (b) UV 360nm (c) UV 254nm (d) detection of bands with Rf value

Figure 4.15 shows that in n-hexane:ethyl acetate 1:10 over 5.5 cm distance, there is no separation of compounds as no band is visible in any UV light or dye-treated TLC plate, indicating that the n-hexane:ethylacetate with 1:10 is not suitable for A.membranaceous extract.

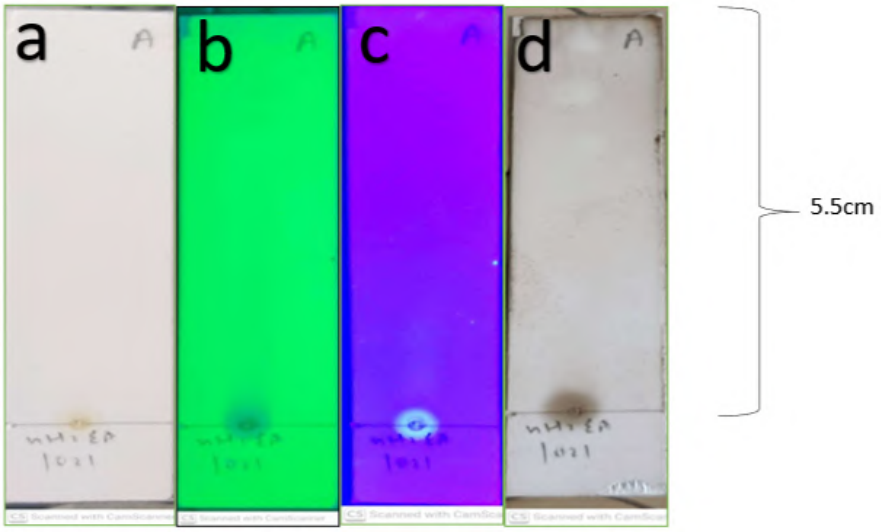


FIGURE 4.16: TLC chromatogram of *A. membranaceous* with n-hexane:ethyl acetate of ratio 10:1 (a) visible light (b) UV 360nm (c) UV 254nm (d) detection of bands with Rf value

Figure 4.16 shows that separation of the extract in n-hexane:ethyl acetate 10:1 over 5.5 cm resulted in no band, indicating that this solvent system is not suitable for *A. membranaceous*.

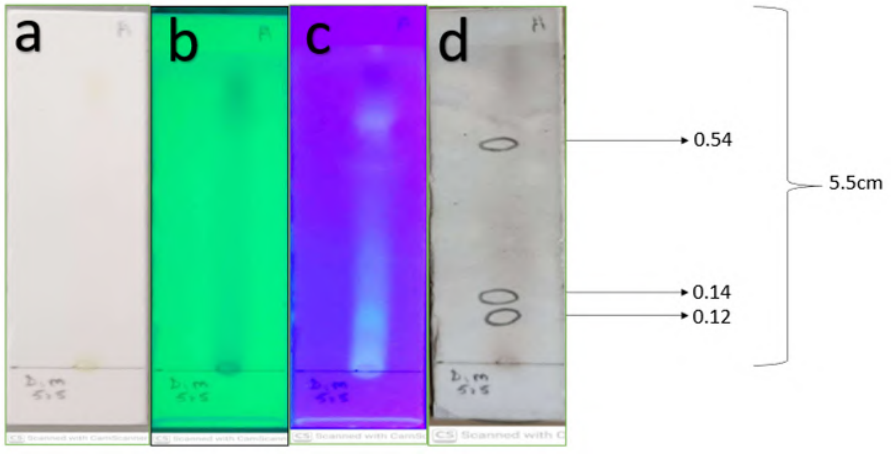


FIGURE 4.17: TLC chromatogram of *A. membranaceous* with dichloromethane:methanol of ratio 5:5 (a) visible light (b) UV 360nm (c) UV 254nm (d) detection of bands with Rf value

Figure 4.17 shows that separation of the extract in dichloromethane:methanol 5:5 over 5.5 cm resulted in three bands with Rf values 0.12, 0.14 and 0.54, indicating the presence of highly polar compounds.

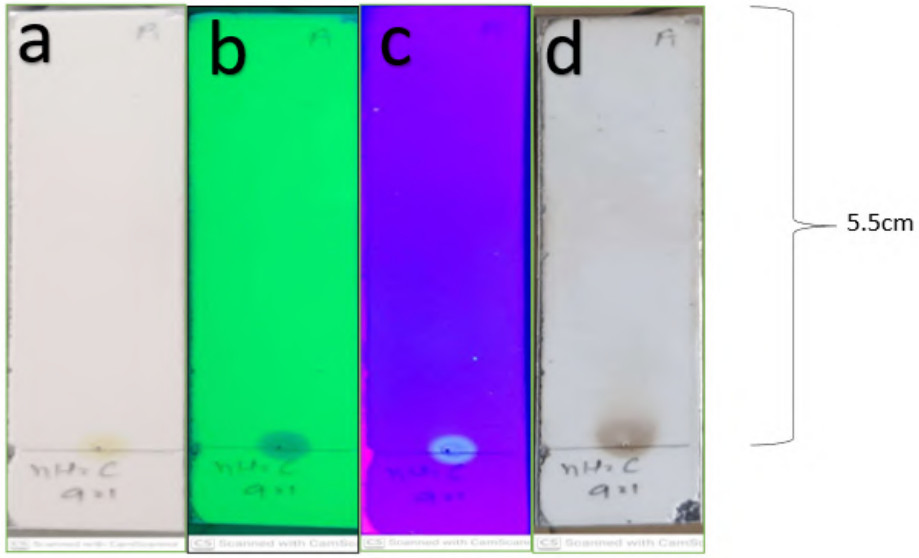


FIGURE 4.18: TLC chromatogram of *A. membranaceous* with n-hexane: chloroform of ratio 9:1 (a) visible light (b) UV 360nm (c) UV 254nm (d) detection of bands with Rf value

Figure 4.18 shows that in n-hexane:chloroform 9:1 over 5.5 cm distance, there is no separation of compounds as no band is visible in any UV light or dye-treated TLC plate, indicating that the n-hexane:chloroform with 9:1 is not suitable for *A. membranaceous* extract.

A detailed analysis of the above chromatograms shows that different ratios of n-hexane/chloroform, dichloromethane/methanol, and n-hexane/ethyl acetate were tried, but they didn't show any variety of compounds, and some showed no bands, thus indicating that these are not suitable solvent systems for compound analysis of *A. membranaceous*.

The chloroform/methanol proved as good solvent system for *A. membranaceous*, as its different ratios gave potential results with a variety of highly polar to moderately polar and less polar compounds, showing that this solvent system can be used for further analysis of *A. membranaceous* phytocompounds.

### 4.3.2 Column Chromatography

After performing the TLC of *A. membranaceous* with several solvent systems, column chromatography was initiated. As *A. membranaceous* showed good results with chloroform/methanol ratios, so this solvent system was used further for column chromatography.

10 grams of *A. membranaceous* concentrated extract was used for the column chromatography and different combinations of chloroform/methanol were used i.e., 100% methanol, C:M 1:5, 1:10, 1:20, 5:1, 10:1, 20:1, 1:1 and 100% chloroform. The mobile phase of different proportions of this solvent system was allowed to flow down and was collected as fractions as shown in the figure 4.19.


FIGURE 4.19: Column chromatography of *A. membranaceous* (a) column packed with solvent system (b) fractions of all combinations

As nine combinations were used to run the column, there was a total of nine fractions obtained. Each fraction consists of four 20ml test tubes. These fractions were further analyzed by TLC with a solvent system of chloroform/methanol with a ratio of 10:1. The chromatograms obtained were visualized in visible light, UV

360 and UV 254. Band detection was done by application of dye and Rf values were calculated as shown in figures below.

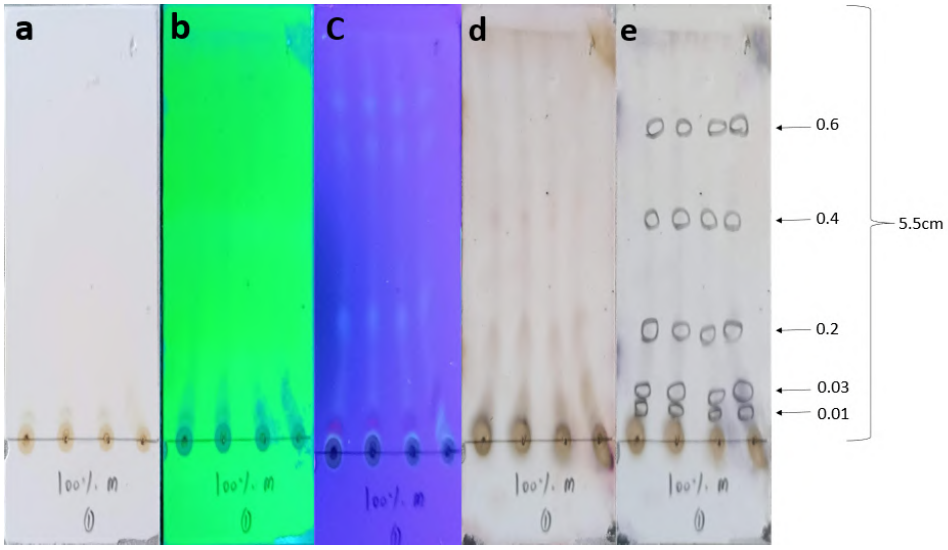


FIGURE 4.20: TLC chromatogram of *A. membranaceous* with 100% methanol (a) visible light (b) UV 360nm (c) UV 254nm (d) dye-treated plate (e) detection of bands with Rf value

Figure 4.20 shows that separation of the extract in 100% methanol over 5.5 cm resulted in five bands with Rf values 0.01, 0.03, 0.2, 0.4 and 0.6, indicating the presence of highly polar to moderately polar compounds.

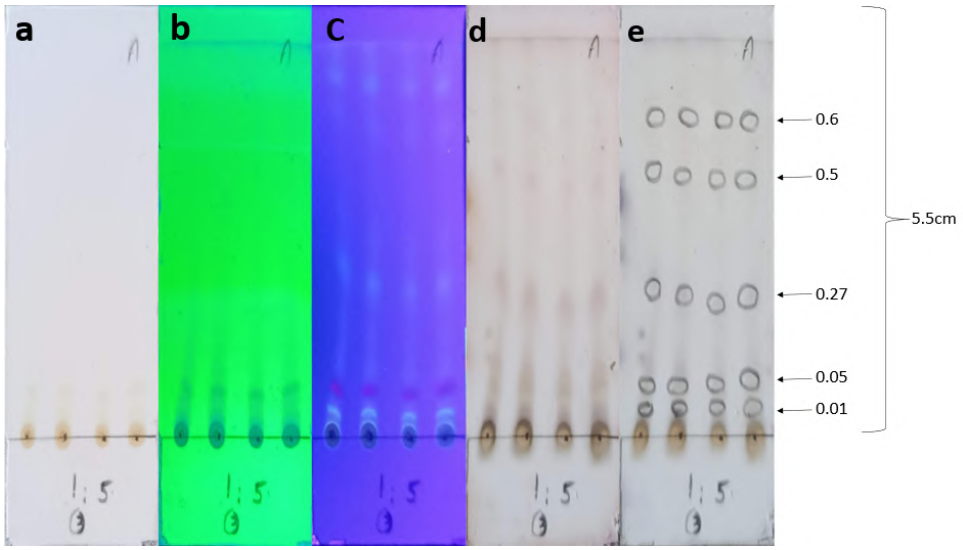


FIGURE 4.21: TLC chromatogram of *A. membranaceous* with chloroform:methanol of ratio 1:5 (a) visible light (b) UV 360nm (c) UV 254nm (d) dye-treated plate (e) detection of bands with Rf value.

Figure 4.21 shows that separation of the extract in chloroform:methanol 1:5 over 5.5 cm resulted in five bands with Rf values 0.01, 0.05, 0.27, 0.5 and 0.6, indicating the presence of highly polar to moderately polar and non-polar compounds.

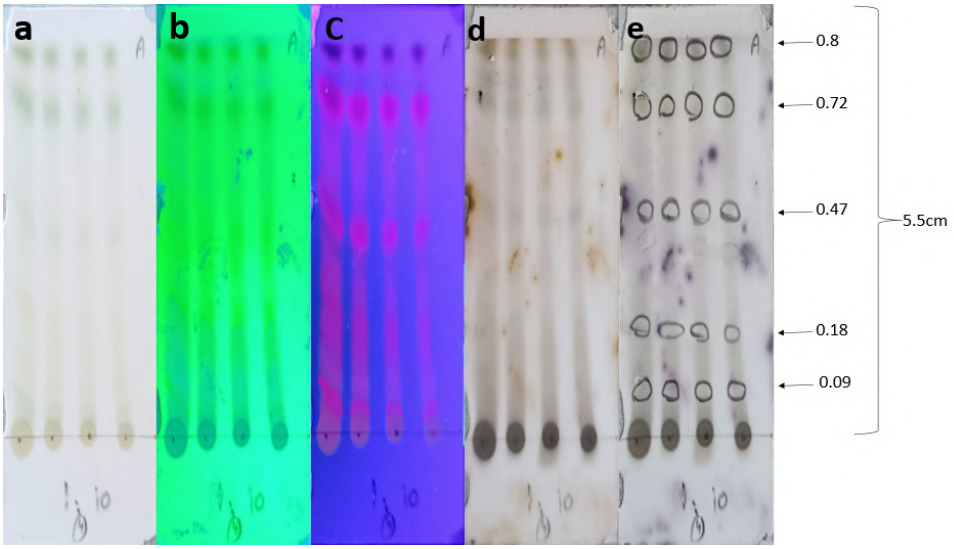


FIGURE 4.22: TLC chromatogram of *A. membranaceous* with chloroform:methanol of ratio 1:10 (a) visible light (b) UV 360nm (c) UV 254nm (d) dye-treated plate (e) detection of bands with Rf value.

Figure 4.22 shows that separation of the extract in chloroform:methanol 1:10 over 5.5 cm resulted in bands bands with Rf values 0.09, 0.18, 0.47, 0.72 and 0.8, indicating the presence of highly polar to moderately polar and less-polar compounds.

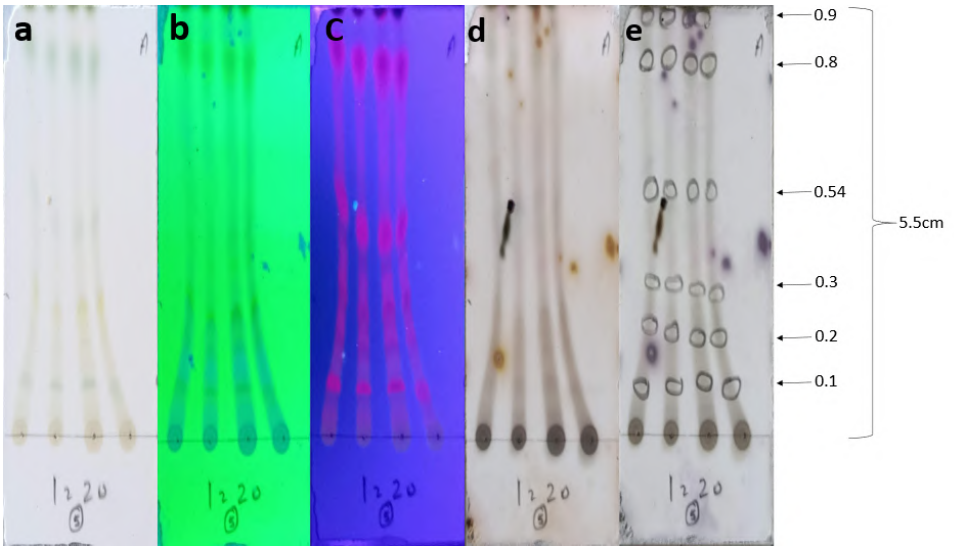


FIGURE 4.23: TLC chromatogram of *A. membranaceous* with chloroform:methanol of ratio 1:20 (a) visible light (b) UV 360nm (c) UV 254nm (d) dye-treated plate (e) detection of bands with Rf value.

Figure 4.23 shows that separation of the extract in chloroform:methanol 1:20 over 5.5 cm resulted in six bands with Rf values 0.1, 0.2, 0.3, 0.54, 0.8 and 0.9, indicating the presence of highly polar to moderately polar and non-polar compounds.

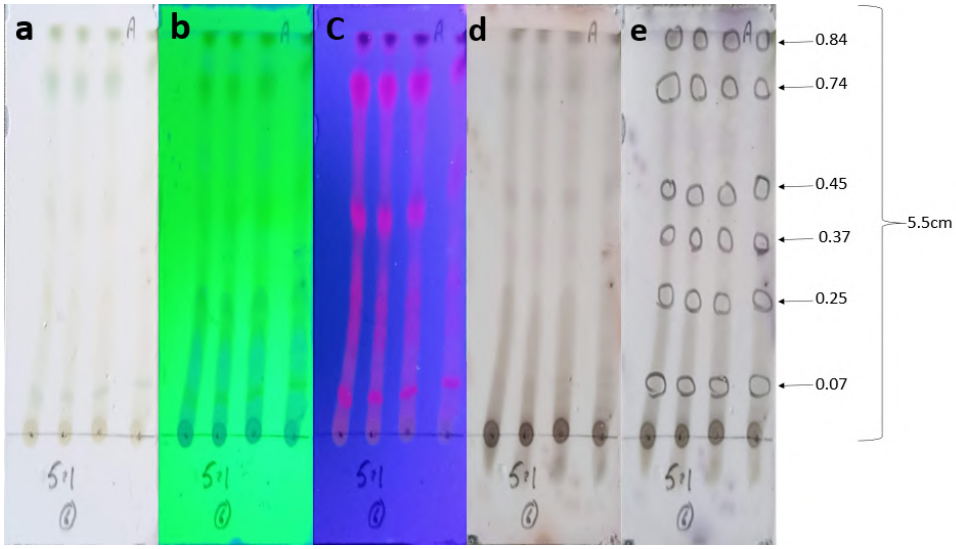


FIGURE 4.24: TLC chromatogram of *A. membranaceous* with chloroform:methanol of ratio 5:1 (a) visible light (b) UV 360nm (c) UV 254nm (d) dye-treated plate (e) detection of bands with Rf value

Figure 4.24 shows that separation of the extract in chloroform:methanol 5:1 over 5.5 cm resulted in six bands with Rf values 0.07, 0.25, 0.37, 0.45, 0.74 and 0.84,indicating the presence of highly polar to moderately polar and less polar compounds.

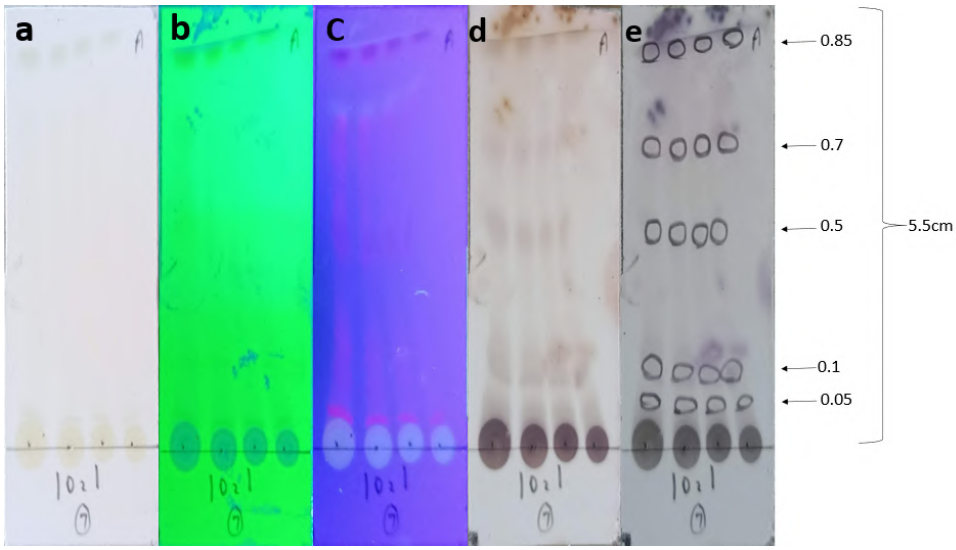


FIGURE 4.25: TLC chromatogram of *A. membranaceous* with chloroform:methanol of ratio 10:1 (a) visible light (b) UV 360nm (c) UV 254nm (d) dye-treated plate (e) detection of bands with Rf value.

Figure 4.25 shows that separation of the extract in chloroform:methanol 10:1 over 5.5 cm resulted in five bands with Rf values 0.05, 0.1, 0.5, 0.7 and 0.85, indicating the presence of highly polar to moderately polar and less polar compounds.

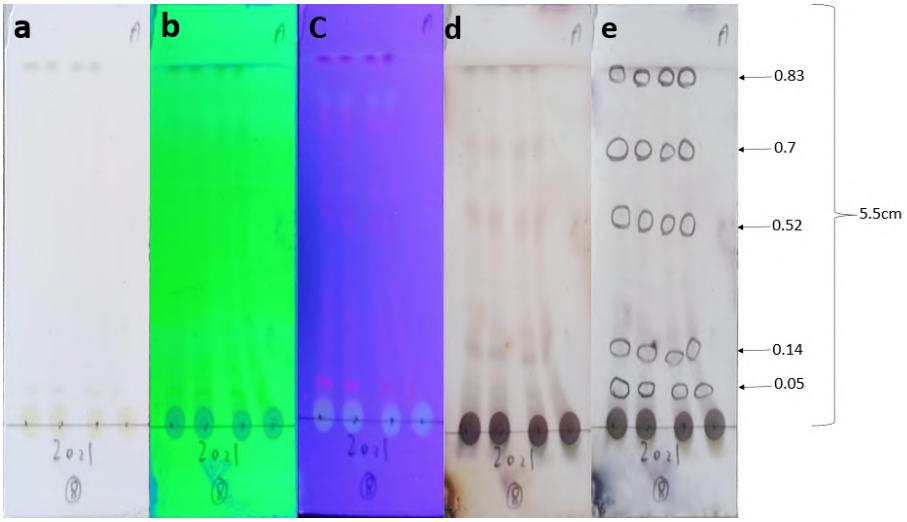


FIGURE 4.26: TLC chromatogram of *A. membranaceous* with chloroform:methanol of ratio 20:1 (a) visible light (b) UV 360nm (c) UV 254nm (d) dye-treated plate (e) detection of bands with Rf value

Figure 4.26 shows that separation of the extract in chloroform:methanol 20:1 over 5.5 cm resulted in five bands with Rf values 0.05, 0.14, 0.52, 0.7 and 0.83, indicating the presence of highly polar to moderately and less polar compounds.

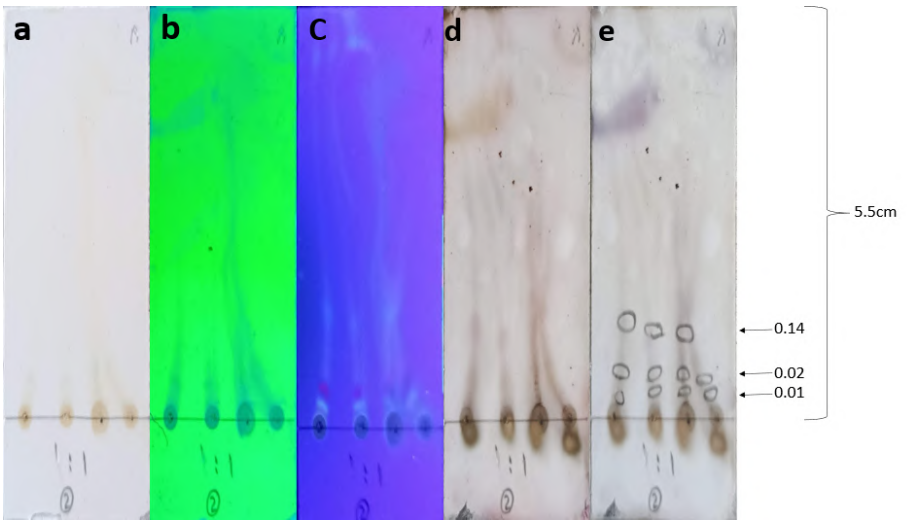


FIGURE 4.27: TLC chromatogram of *A. membranaceous* with chloroform:methanol of ratio 1:1 (a) visible light (b) UV 360nm (c) UV 254nm (d) dye-treated plate (e) detection of bands with Rf value

Figure 4.27 shows that separation of the extract in chloroform:methanol 1:1 over 5.5 cm resulted in three bands with Rf values 0.01, 0.02 and 0.14, indicating the presence of highly polar compounds.

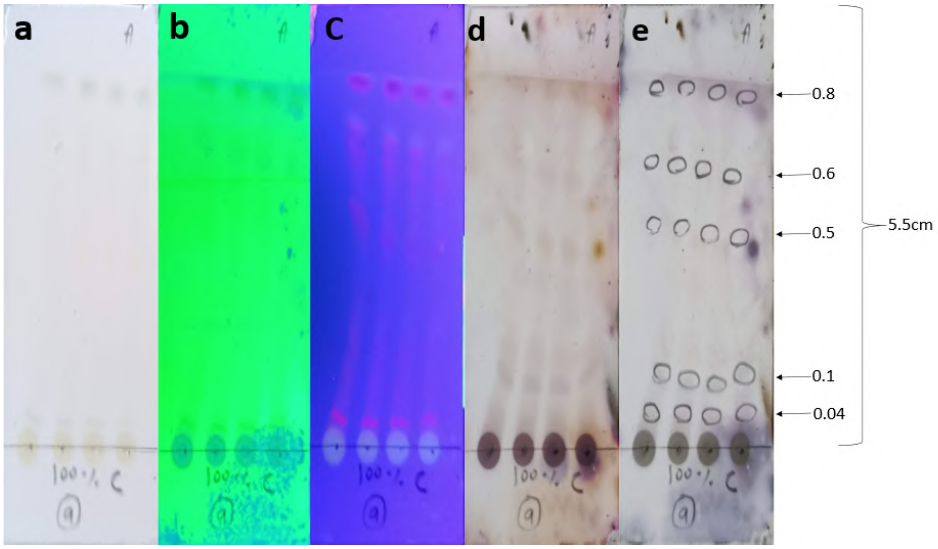


FIGURE 4.28: TLC chromatogram of *A. membranaceous* with 100% chloroform (a) visible light (b) UV 360nm (c) UV 254nm (d) dye-treated plate (e) detection of bands with Rf value

Figure 4.28 shows that separation of the extract in 100% chloroform over 5.5 cm resulted in five bands with Rf values of 0.04, 0.1, 0.5, 0.6 and 0.8, indicating the presence of highly polar to moderately and less polar compounds.

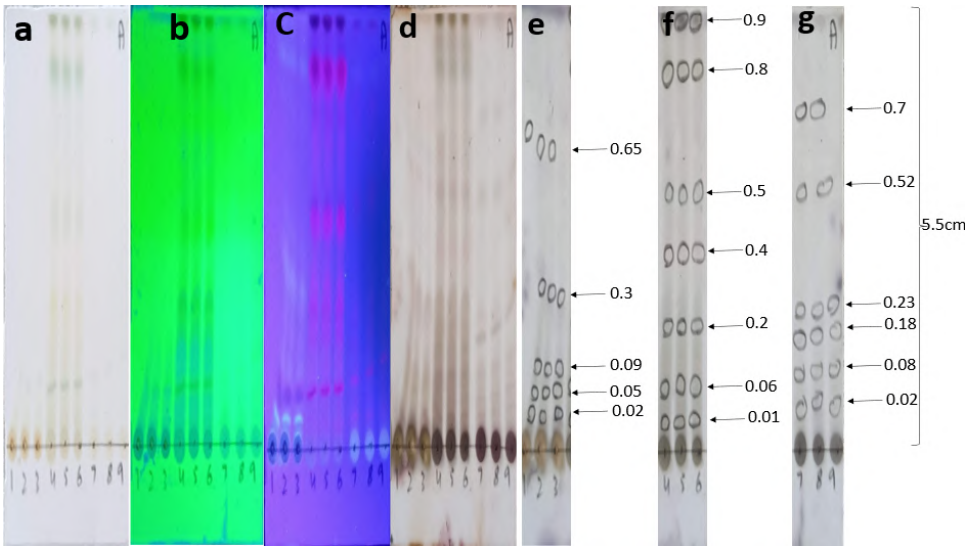


FIGURE 4.29: TLC chromatogram of *A. membranaceous* with all combined fractions (a) visible light (b) UV 360nm (c) UV 254nm (d) dye-treated plate (e) detection of bands with Rf value of fractions 1,2,3 (f) Rf value of fractions 4,5,6 (g) Rf value of fractions 7, 8 and 9

The analysis of chromatograms of the above combinations shows that all four elutes in a single combination share the same number and Rf value of bands, so these four elutes of all individual combinations were mixed to a single fraction. So there were a total of nine fractions named as F1, F2, F3, F4, F5, F6, F7, F8 and F9. These individual fractions were analyzed by TLC as shown in figure 4.29.

Figure 4.29 shows that TLC analysis of nine combined fractions showed that first three fractions F1, F2 and F3 showed five similar bands with Rf values of 0.02, 0.05, 0.09, 0.3 and 0.65 indicating the presence of highly polar to moderately polar compounds. Similarly F4, F5 and F6 showed seven similar bands with Rf values 0.01, 0.06, 0.2, 0.4, 0.5, 0.8 and 0.9 indicating the presence of highly polar to moderately polar and less and non- polar compounds. F7, F8 and F9 shared six similar bands with Rf values 0.02, 0.08, 0.18, 0.23, 0.52 and 0.7 indicating the presence of highly polar to moderately polar compounds.

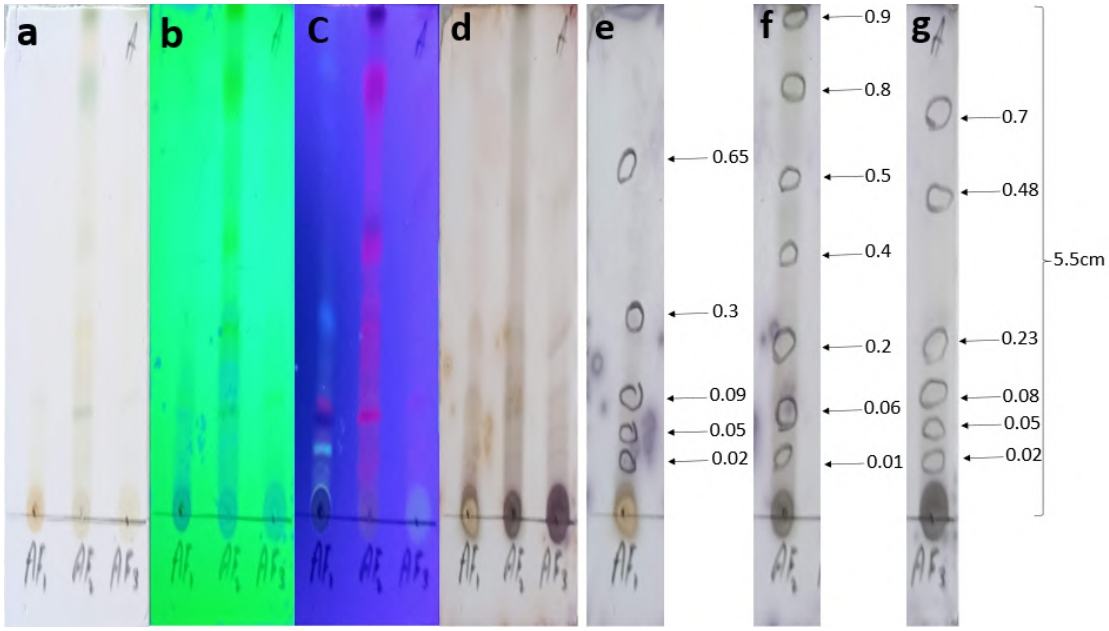


FIGURE 4.30: TLC chromatogram of *A. membranaceous* with super fractions (a) visible light (b) UV 360nm (c) UV 254nm (d) dye-treated plate (e) detection of bands with Rf values for *A. membranaceous* super-fraction 1, AF1 (f) *A. membranaceous* super-fraction 2, AF2 (g) *A. membranaceous* super-fraction 3, AF3

On basis of similarity of bands fractions were combined to form super-fractions. F1, F2 and F3 were combined to form *A. membranaceous* super-fraction 1 and


FIGURE 4.31: Concentrated super-fractions (a) AF1 (b) AF2 (c) AF3

named as AF1. F4, F5 and F6 were combined as *A. membranaceous* super-fraction 2 and named as AF2, while F7, F8 and F9 were combined to form *A. membranaceous* super-fraction 3 and named as AF3. These super-fractions were further analyzed by TLC, as shown in figure 4.30.

Figure 4.30 shows the TLC analysis of super-fractions. AF1 showed five bands with Rf values of 0.02, 0.05, 0.09, 0.3 and 0.65 indicating the presence of highly polar to moderately polar compounds.

Similarly, AF2 showed seven bands with Rf values 0.01, 0.06, 0.2, 0.4, 0.5, 0.8 and 0.9, indicating the presence of highly polar to moderately polar and less polar to non-polar compounds. AF3 showed six bands with Rf values 0.02, 0.05, 0.08, 0.23, 0.48 and 0.7, indicating the presence of highly polar to moderately and less polar compounds.

These super-fractions were evaporated and concentrated. The mass of AF1 is 4.8, the mass of AF2 is 2.2 and the mass of AF3 is 2.1. The yield of super-fraction AF1 is 48, for AF2 it is 22 and for AF3 it is 21 as shown in figure 4.31.

The details of column chromatography, including solvent system along with proportions, mixing of fractions, concentrated weights and yield of super-fractions is given in table 4.1.

Table 4.1: Details of column chromatography

| **Name of Plant** | **Amount used for column(g)** | **Solvent system** | **Proportions of mobile phase to run the column** | **No of elutes collected in test tube** | **Number of fractions obtained** | **TLC Solvent system along with proportion** | **Fractions mixed on basis of TLC** | **Mixed fractions TLC solvent systems with proportion** | **Mixing of fractions to make super-fractions** | **Mass of each super-fraction (g)** | **Yield of each super-fraction (%)** |
|---|---|---|---|---|---|---|---|---|---|---|---|
| *Astragalus membranaceous* | 10 | Chloroform : methanol | 100% methanol | 4 | 9 | Chloroform : methanol | F1 | Chloroform : methanol 10:1 | F1 + F2 + F3 = AF1 | AF1 = 4.8 | AF1 = 48 |
| | | | 1:01 | 4 | | 10:01 | F2 | | F4 + F5 + F6 = AF2 | AF2 = 2.2 | AF2 = 22 |
| | | | 1:5 | 4 | | | F3 | | F7 + F8 + F9 = AF3 | AF3 = 2.1 | AF3 = 21 |
| | | | 1:10 | 4 | | | F4 | | | | |
| | | | 1:20 | 4 | | | F5 | | | | |
| | | | 5:01 | 4 | | | F6 | | | | |
| | | | 10:01 | 4 | | | F7 | | | | |
| | | | 20:01 | 4 | | | F8 | | | | |
| | | | 100% chloroform | 4 | | | F9 | | | | |

The concentrated super-fractions were stored at 4°C and used for further LC-MS, and in vitro experimentation.

#### 4.3.2.1 Bioactivity Assays of Super-fractions

### i. 2, 2 - Diphenyl - 1 - Picrylhydrazyl Radical Scavenging Assay

The DPPH free radical scavenging assay was used to assess the antioxidant activity of *A. membranaceous* super-fractions. For each super-fraction, 100 $\mu$l was combined with 3ml of DPPH solution to create a 1mg/ml dilution. Antioxidant activity was demonstrated by the color shift from deep violet to pale yellow brought on by the methanolic leaf extract, as shown in figure 4.32.

FIGURE 4.32: DPPH assay of A. membranaceous super-fractions

Following thirty minutes of stabilization, the absorbance at 517 nm was measured, and the antioxidant activity percentage was computed using the formula [(Ac - As) / Ac] × 100]. The experiment was repeated in triplicate. All readings along with average and percentage scavenging inhibition, are given in table 4.2.

TABLE 4.2: Scavenging activity of *A. membranaceous* super-fractions

| **Plant name** | **Control** | **Name of super-fraction** | **DPPH Value 1** | **DPPH Value 2** | **DPPH Value 3** | **Average DPPH** | **Scavenging activity (%)** |
|---|---|---|---|---|---|---|---|
| *A. membranaceous* | 0.701 | AF1 | 0.151 | 0.15 | 0.151 | 0.15 | 78.63 |
| | | AF2 | 3:24 | 0.141 | 0.143 | 3:24 | 79.74 |

**Table 4.2 – continued from previous page**

| Plant name | Control | Name of super-fraction | DPPH Value 1 | DPPH Value 2 | DPPH Value 3 | Average DPPH | Scavenging activity (%) |
|---|---|---|---|---|---|---|---|
| | | AF3 | 0.153 | 0.154 | 0.152 | 0.153 | 78.16 |

The results show that AF2 has the highest scavenging activity, i.e., 79.74%, followed by AF1 (78.63%) and AF3 (78.16%). This trend is shown in the graph below.

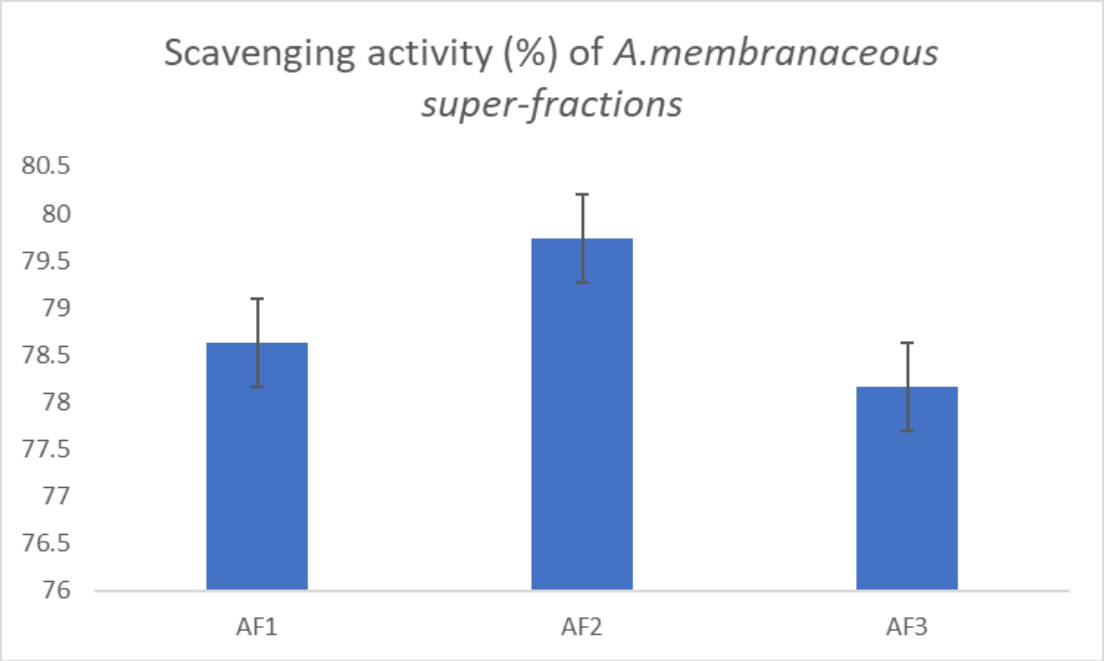


FIGURE 4.33: DPPH profile of *A. membranaceous* super-fractions

### ii. Total Phenolic Concentration

The FC method was used to determine the total phenolic content of the *A. membranaceous* super-fractions, and a calibration curve was created using gallic acid. The standard curve was used to create a regression equation, which was then used to quantify the amount of gallic acid in the super-fractions: y= 0.0632x+0.2211, R2 = 0.8958, where x is the equivalent gallic acid (mg/ml) and y is the absorbance. The absorbance values (0.189, 0.321, 0.592, 0.489, 0.479, 0.653, 0.691, 0.654, 0.778, 0.784, 0.896, 1.057) increase as the concentration of Gallic acid increases (0 to 12

mg/ml). This implied that the amount of light absorbed at 765 nm and the concentration of gallic acid in the solution were directly correlated as shown in figure 4.34 below.

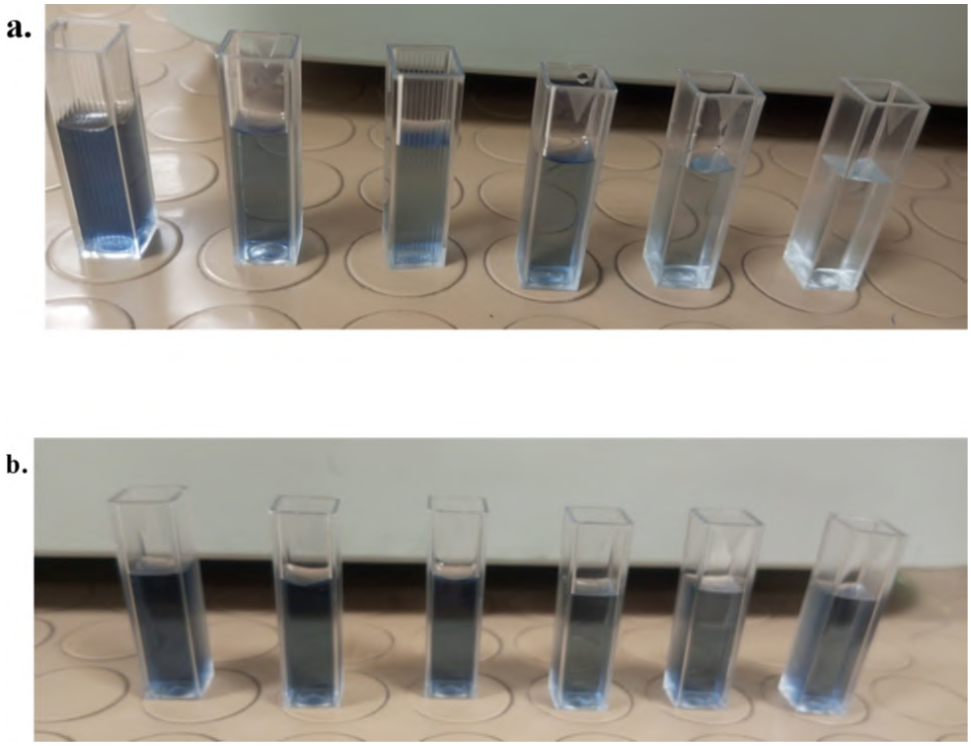


FIGURE 4.34: The curve formed by plotting the absorbance values against different concentrations of gallic acid is shown in the graph below.

Phenolic concentrations were measured by mixing 270 $\mu$L of each super-fraction dilution with 10% FC reagent and 7.5% $Na_2CO_3$ as shown in figure 4.36 and the absorbance was again measured at 765 nm.

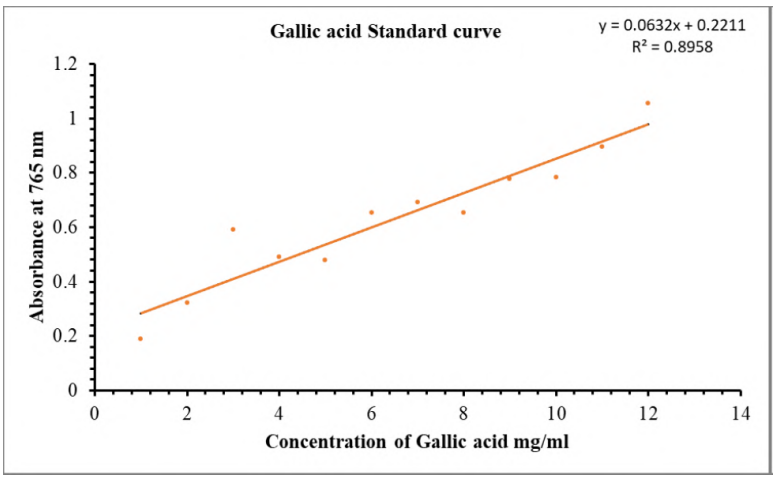


FIGURE 4.35: TPC assay of *A. membranaceous* super-fractions

Phenolic concentrations were observed in the super-fractions of *A. membranaceous* and shown in table 4.3. AF1 exhibited absorbance up to 0.398. AF2 exhibited absorbance up to 0.520 while AF3 exhibited absorbance up to 0.374.

TABLE 4.3: Absorbance of *A. membranaceous* super-fractions at 765 nm

| **Plants name** | **Name of Super-fractions** | **TPC 1** | **TPC 2** | **TPC 3** | **Average TPC** |
|---|---|---|---|---|---|
| *A. membranaceous* | AF1 | 0.39 | 9:33 | 0.406 | 0.398 |
| | AF2 | 0.51 | 0.52 | 0.53 | 0.52 |
| | AF3 | 0.36 | 8:58 | 0.388 | 0.374 |

The curve shown in figure 4.35 above helps quantify the total phenolic content in *A. membranaceous*'s super-fractions. By measuring the absorbance of the sample at the same wavelength (765 nm) and comparing it to the standard curve, the concentration of phenolic compounds in *A. membranaceous*'s super-fractions could be estimated.

The absorbance values of 0.398, 0.520, and 0.374 for AF1, AF2 and AF3, respectively, were calibrated using the Gallic acid standard curve and it indicated the concentration of phenolic content as shown in graph below.

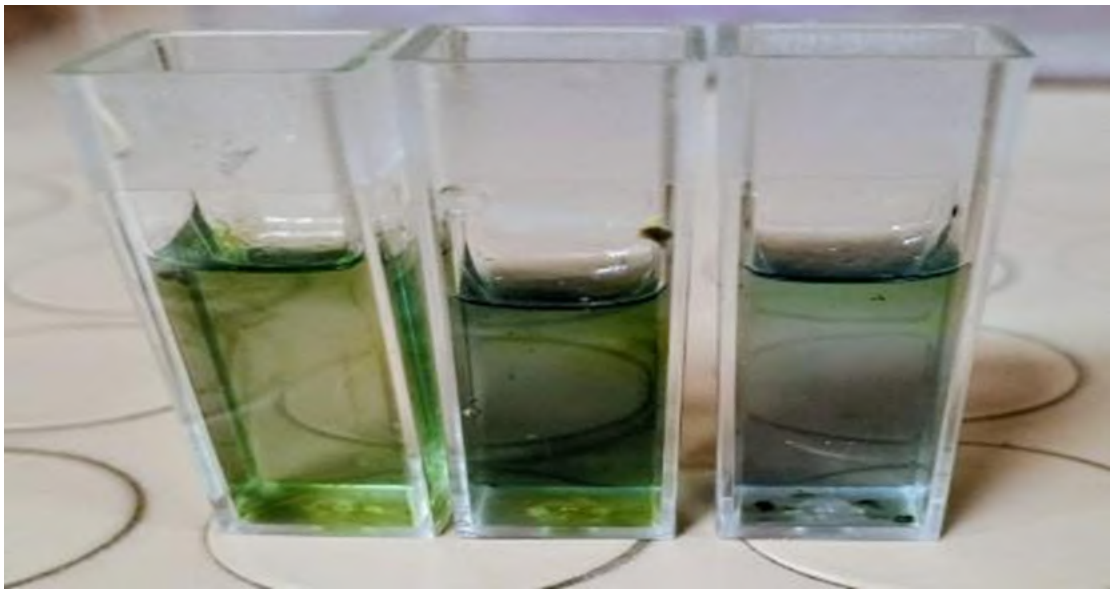

FIGURE 4.36: Phenolic concentration in *A. membranaceous* super-fractions

It was found that the phenolic concentration in AF1 with an absorbance of 0.398 was 2.7 mg GAE/g. Similarly, the phenolic concentration in AF2 with an absorbance of 0.520 was 4.4 mg GAE/g, and the phenolic concentration in AF3 with an absorbance of 0.374 was 2.2 mg GAE/g. The table 4.4 shows the concentration of phenolic acids in A. membranaceous super-fractions.

TABLE 4.4: Phenolic concentration in *A. membranaceous* super-fractions

| **Sample** | **Absorbance** | **Phenolic concentration (mg GAE/g)** |
|---|---|---|
| AF1 | 0.697 | 2.7 |
| AF2 | 0.327 | 4.4 |
| AF3 | 0.341 | 2.2 |

According to table, AF2 has the highest phenolic content, i.e., 4.4 mg GAE/g, followed by AF1, which has 2.7 mg GAE/g, and AF3, which has 2.2 mg GAE/g. This trend is shown in the graph below.

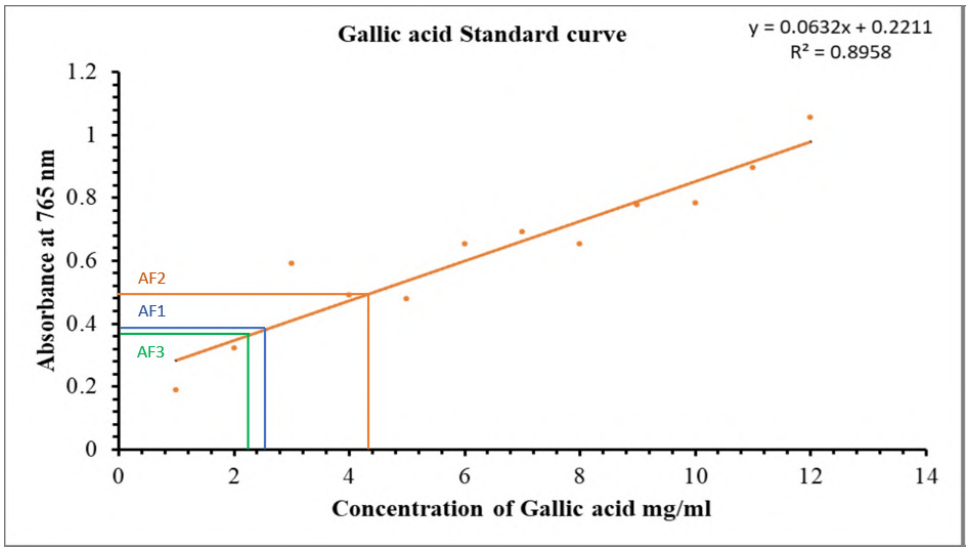


FIGURE 4.37: TPC profile of A. membranaceous super-fractions

### iii. Inhibition of Alpha-amylase

Inhibiting alpha-amylase is vital for diabetes management and starch digestion. This study explored the effects of *A. membranaceous* super-fractions on alpha-amylase using a specific assay, where phosphate buffer, super-fraction dilution, and the alpha-amylase were combined with starch as shown in figure 4.39.

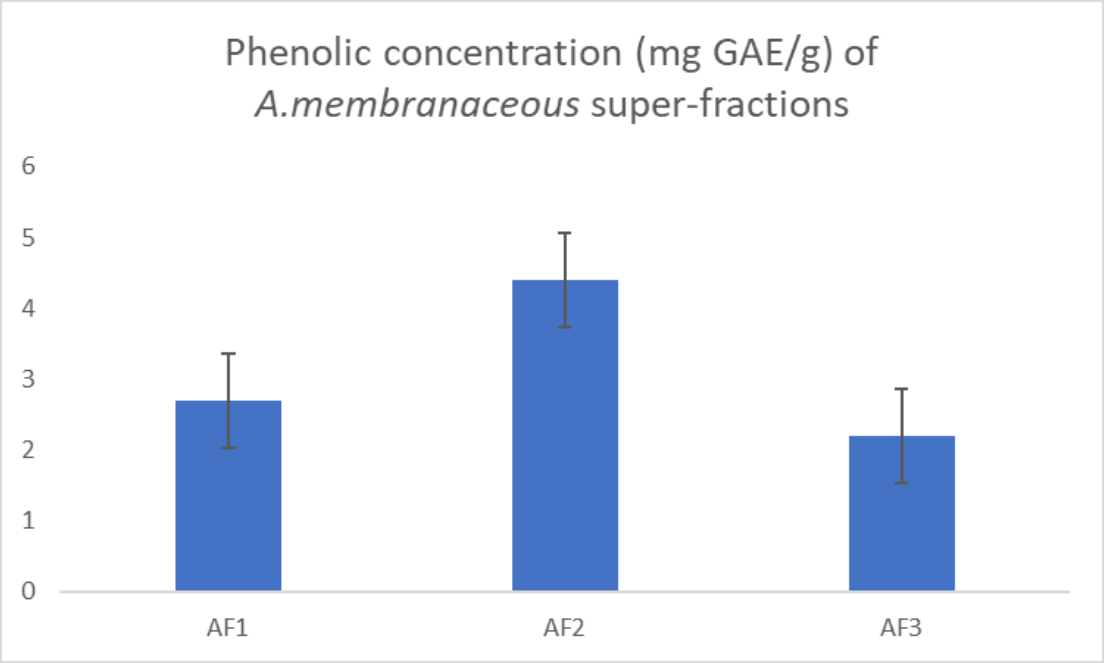


FIGURE 4.38: Alpha-amylase assay of *A. membranaceous* super-fractions

### iv. Inhibition of Alpha-amylase

Inhibiting alpha-amylase is vital for diabetes management and starch digestion. This study explored the effects of *A. membranaceous* super-fractions on alpha-amylase using a specific assay, where phosphate buffer, super-fraction dilution, and the alpha-amylase were combined with starch as shown in figure 4.39.

FIGURE 4.39: Alpha-amylase inhibition of *A. membranaceous* super-fractions

Acarbose served as the positive control, with the reaction halted using the DNSA reagent. The absorbance was measured at 540 nm and the inhibition percentage was calculated as shown in table 4.5.

TABLE 4.5: Alpha-amylase inhibition of *A. membranaceous* super-fractions

| **Plant name** | **Control** | **Name of super-fractions** | **Alpha-amylase 1** | **Alpha-amylase 2** | **Alpha-amylase 3** | **Average** | **Alpha-amylase inhibition (%)** |
|---|---|---|---|---|---|---|---|
| *A. membranaceous* | 0.971 | **AF1** | 13:53 | 0.546 | 0.512 | 13:04 | 43.87 |
| | | AF2 | 0.25 | 0.249 | 0.253 | 0.25 | 74.25 |
| | | AF3 | 16:37 | 0.636 | 0.609 | 0.646 | 33.39 |

According to the percentage inhibition value, the AF2 showed 74.25% inhibition, indicating it is the most effective at inhibiting alpha-amylase activity among the three samples. AF1 has 43.87% alpha-amylase inhibition, while AF3 has 33.39% alpha-amylase inhibition. This trend is shown in the graph below.

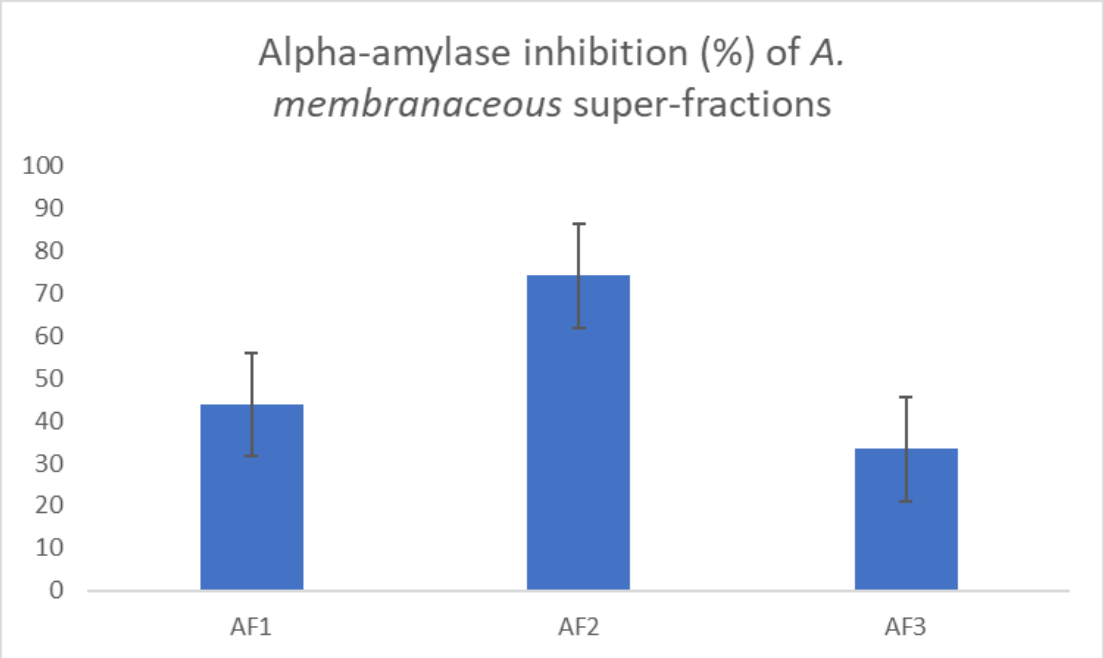


FIGURE 4.40: Alpha-amylase inhibition of *A. membranaceous* super-fractions

### v. Alpha-glucosidase Inhibition

To conduct the alpha-glucosidase assay, super-fraction dilution, phosphate buffer (pH 6.9), and $\alpha$-glucosidase solution were mixed, followed by the addition of PNPG solution and incubation as shown in the figure 4.41.

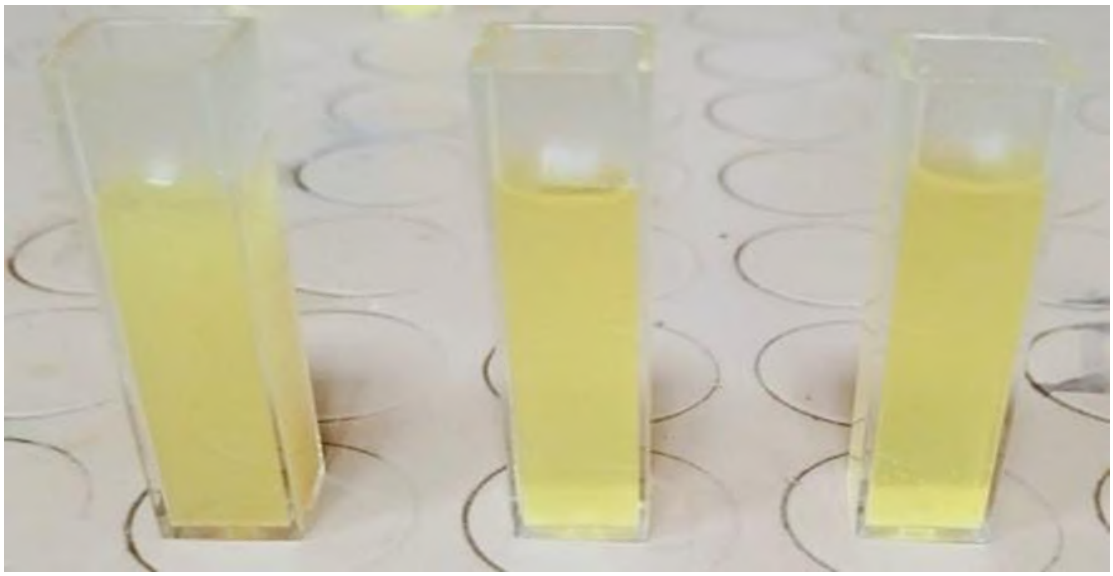

FIGURE 4.41: Alpha-glucosidase assay of *A. membranaceous* super-fractions

Absorbance was measured at 405 nm using a spectrophotometer before and after incubation, using acarbose as a positive control, and the inhibition percentage was calculated as shown in table 4.6.

TABLE 4.6: Alpha-glucosidase inhibition of *A. membranaceous* super-fractions

| **Plant name** | **Control** | **Name of super-fractions** | **Alpha glucosidase 1** | **Alpha glucosidase 2** | **Alpha glucosidase 3** | **Avg** | **Alpha-glucosidase inhibition (%)** |
|---|---|---|---|---|---|---|---|
| *A. membranaceous* | 0.531 | AF1 | 0.498 | 0.428 | 0.303 | 0.409 | 22.94 |
| | | AF2 | 7:42 | 0.258 | 0.276 | 0.285 | 46.24 |
| | | AF3 | 9:36 | 0.52 | 0.64 | 0.52 | 2.07 |

According to the percentage inhibition value, the AF2 showed 46.24% inhibition, indicating it is the most effective at inhibiting alpha-glucosidase activity among

the three samples. AF1 has 22.94% alpha-glucosidase inhibition, while AF3 has 2.07% alpha-glucosidase inhibition. This trend is shown in the graph below.

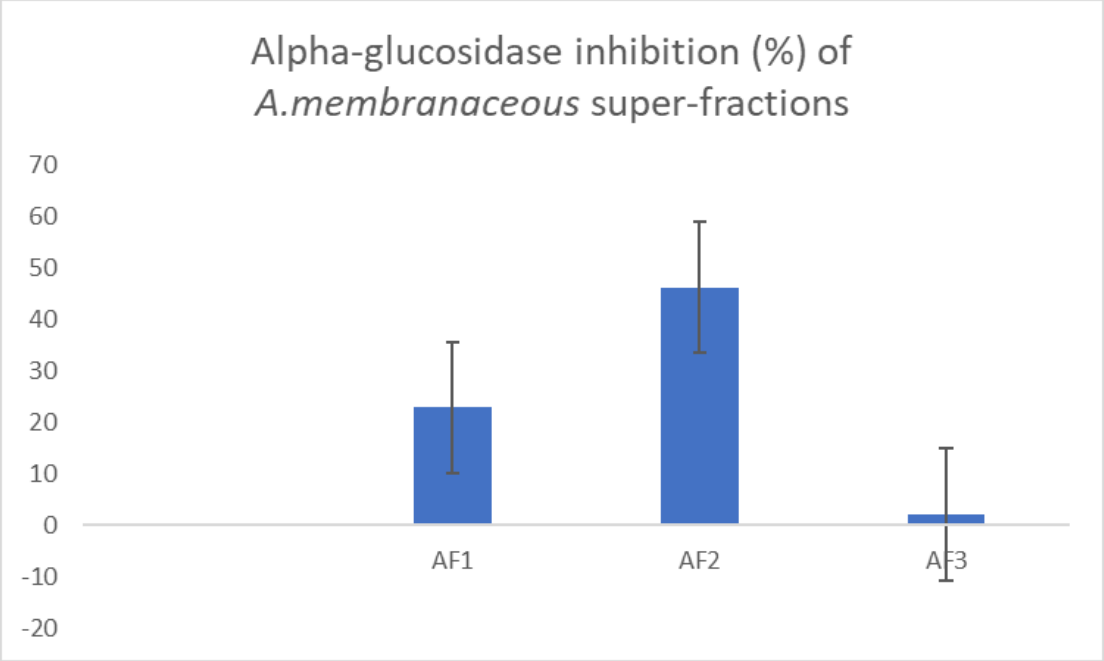


FIGURE 4.42: Alpha-glucosidase inhibition of *A. membranaceous* super-fractions

### 4.3.3 High-Performance Liquid Chromatography - Mass Spectrometry

The LCMS analysis used a Triple Quadrupole Mass Spectrometer with a heated electrospray ionization source. Samples were prepared using methanol and introduced through a direct insertion technique. Multiple peaks were selected for analysis during the fragmentation phase. The compounds obtained after LC-MS data analysis along with molecular weight, fragmentation peaks and structure are given in table 4.7 below.

Table shows the compounds obtained after LC-MS data analysis. These compounds were selected on the basis of molecular weight and fragmentation pattern. Aristolone, medicarpin and vasicine were obtained in AF1, while riboflavin was present in AF2 super-fraction. These compounds were further evaluated through molecular docking.

TABLE 4.7: Compounds obtained after LC-MS data analysis

| **Molecular Weight** | **Fragmentation Peaks** | **Type of fraction** | **Compound** | **Structure** |
|---|---|---|---|---|
| 218.33 | 219, 218, 204, 199, 186, 185, 184, 172, 168, 159, 148, 146, 133, 131, 129, 117, 115, 104, 91, 83, 81, 70, 69, 67, 55 | AF1 | Aristolone | 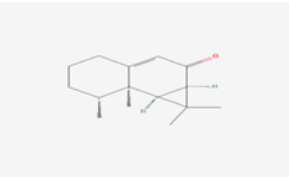 |
| 270.28 | 270, 235, 225, 205, 180, 162, 149, 122, 115, 97, 91, 82, 69, 59 | AF1 | Medicarpin | 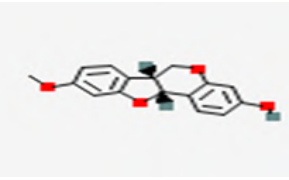 |
| 376.4 | 376/377, 241/40, 305, 281, 237, 227, 215, 195, 190, 178, 161, 135, 119, 100, 88, 62 | AF2 | Riboflavin | 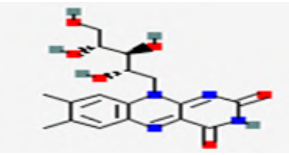 |
| 188.23 | 189, 173, 171, 169, 168, 154, 153, 143, 139, 131, 130, 118, 117, 116, 115, 106, 103, 93, 91, 90, 89, 88, 78, 77, 76, 70, 64 | AF1 | Vasicine | 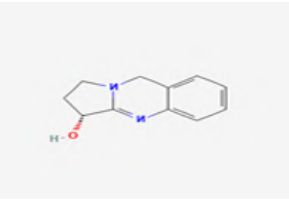 |

## 4.4 In silico Evaluation of *A. membranaceous* Phytocompounds

### 4.4.1 3D Structure Prediction and Refinement of Selected Proteins

The peroxisome proliferator-activated receptor-$\gamma$ (PPAR-$\gamma$), pancreatic and duodenal homeobox 1 (PDX-1), insulin receptor substrate-2 (IRS-2), phosphatidylinositol 3-kinase alpha (PI3K-$\alpha$), and protein kinase B (Akt2) were selected as

target proteins for their potential roles in the development of Type 2 Diabetes. 3D structure and FASTA sequence of target proteins i.e. PI3K-$\alpha$, Akt2 and PPAR-$\gamma$ was taken from PDB under PDB IDs 5M6U, 8Q61 and 5GTN respectively. While the 3D structure and FASTA sequence of PDX-1 and IRS-2 were obtained from AlphaFold under IDs P52945 and Q9YAH2, respectively. Using PyMol, the protein structures were refined by eliminating any ligands and water molecules. To obtain a stable conformation the absent polar hydrogens were added, and other atoms were removed to prevent overlaps and the modified file was saved in PDB format. The refined structures of target proteins are shown in figure 4.43 below.

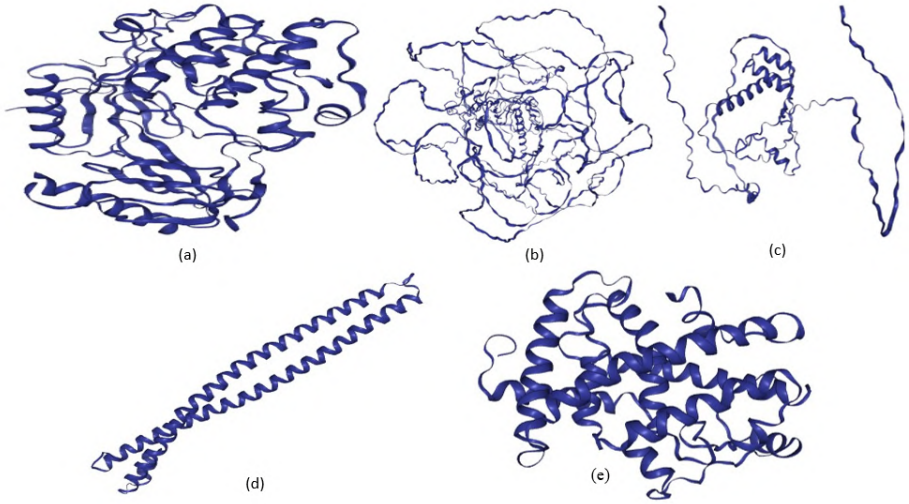


FIGURE 4.43: Structures of refined target proteins (a) Akt2 (b) IRS-2 (c) PDX-1 (d) PI3K-$\alpha$ (e) PPAR-$\gamma$

### 4.4.2 Physicochemical Characterization of Target Proteins

We utilized an online tool called ProtParam to forecast a variety of parameters, including the molecular and structural properties of specific proteins. Table 4.8 lists the physicochemical characteristics of target proteins.

TABLE 4.8: The target proteins' physicochemical characteristics

| S. No. | Target Proteins | MW | PI | NR | PR | Ext Co1. | Ext Co2. | Instability Index | Aliphatic Index | GRAVY |
|---|---|---|---|---|---|---|---|---|---|---|
| 1 | Akt2 | 55897.9 | 21:21 | 74 | 66 | 67185 | 66810 | 34.81 | 76.89 | -0.468 |
| 2 | PI3K-$\alpha$ | 83557.3 | 18:28 | 109 | 96 | 999505 | 99130 | 48.33 | 81.34 | -0.712 |
| 3 | PPAR-$\gamma$ | 32242.41 | 8:38 | 40 | 32 | 11920 | 11920 | 44.57 | 105.8 | -0.117 |
| 4 | IRS-2 | 137334.06 | 21:36 | 105 | 121 | 94880 | 93630 | 70.45 | 58.54 | -0.506 |

**Table 4.8 continued from previous page**

| S. No. | Target Proteins | MW | PI | NR | PR | Ext Co1. | Ext Co2. | Instability Index | Aliphatic Index | GRAVY |
|---|---|---|---|---|---|---|---|---|---|---|
| 5 | PDX-1 | 30770.99 | 2:24 | 31 | 31 | 39545 | 39420 | 78.54 | 61.87 | -0.671 |

All proteins exhibit molecular weights ranging from approximately 30 kDa to 137 kDa, with isoelectric points varying from 5.36 to 8.90, suggesting they are likely soluble under physiological conditions. The instability index values are relatively out of range except for Akt2.

Moreover, the proportionate volume of the aliphatic side chains is represented by the aliphatic index, and this index is high for all proteins, indicating the tendency to be thermostable. Additionally, the GRAVY value is negative, indicating that the proteins are hydrophilic and help in interactions with the aqueous environment. Overall, these properties suggest that the proteins are well-suited for their biological roles.

### 4.4.3 Active Site Identification

The dogsitescorer software, which determines the number of pockets that can be bound and gives details on their surface area and volume, was utilized to determine the active sites of the proteins. Figure 4.44 below illustrates the areas and volumes of target proteins. The coloured areas depict the active sites available for a particular protein.

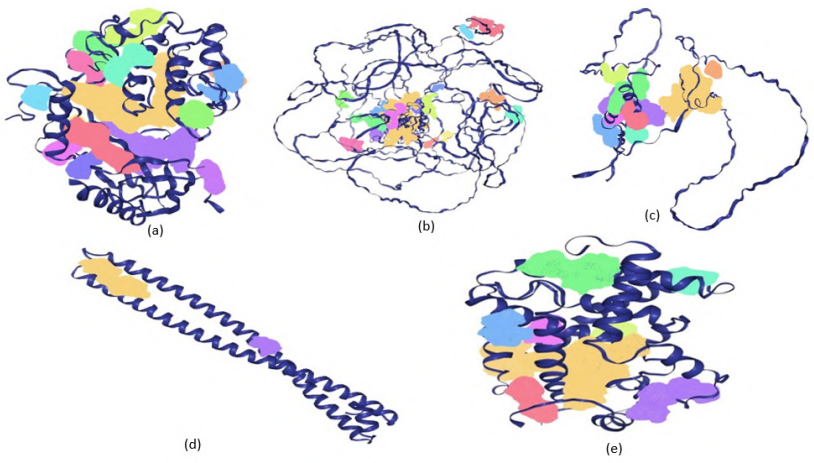


FIGURE 4.44: Active sites of refined target proteins (a) Akt2 (b) IRS-2 (c) PDX-1 (d) PI3K-$\alpha$ (e) PPAR-$\gamma$

Dogsitescorer data depict different numbers of pockets for each protein. Every pocket has different surface area and volume. According to this data, the Akt2 consists of fifteen pockets, PDX-1 consists of nine pockets. PI3K-$\alpha$ consists of two pockets, PPAR-$\gamma$ consists of eighteen pockets, and IRS-2 consists of eight pockets.

### 4.4.4 Retrieval of Chemical Structure of the Ligands

The largest chemical database in the world, PubChem, was searched for ligands. These ligands' 3D structures were extracted in SDF format from the PubChem database. After downloading the structures, the next step performed was minimizing the energy of these ligands. This step is an important one as we can't use simply the downloaded structure as the ligands are unstable and it can directly affect the docking vina scores. The refined structures of ligands obtained after energy minimization along with other information are given in table 4.9.

TABLE 4.9: Chemical structure of ligands

| **Ligand Names** | **Mol weights** | **Formulas** | **Mol Structures** | **Canonical Smiles** |
|---|---|---|---|---|
| Aristolone | 218.33 | $C_{15}H_{22}O$ | 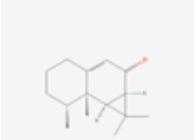 | C[C@@H]1CCCC2=CC(=O)[C@@H]3[C@H]([C@@]12C)C3(C)C |
| Medicarpin | 270.28 | $C_{16}H_{14}O_4$ | 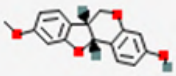 | COC1=CC2=C(C=C1)[C@@H]3COC4=C([C@@H]3O2)C=CC(=C4)O |
| Riboflavin | 376.4 | $C_{17}H_{20}N_4O_6$ | 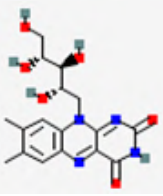 | CC1=CC2=C(C=C1C)N(C3=NC(=O)NC(=O)C3=N2)C[C@@H]([C@@H]([C@@H](CO)O)O)O |
| Vasicine | 188.23 | $C_{11}H_{12}N_2O$ | 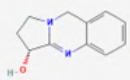 | C1CN2CC3=CC=CC=C3N=C2[C@H]1O |

### 4.4.5 Virtual Screening of Ligands

For compounds to be separated as both drug-like and nondrug-like virtual screening and pharmacokinetic properties are followed. The Lipinski rule addresses specific parameters, including molecular weight ($\leq$ 500), log P ($\leq$ 5), H-bond donors ($\leq$ 5), H-bond acceptors ($\leq$ 10), and rotatable bonds ($\leq$ 10). Orally active chemicals must adhere to these guidelines.

The manner of administration affects the drug-like. When a chemical satisfies three or more requirements, it is classified as a drug; if it violates more than two, its absorption is poor [150]. Virtual screening of ligands is shown is table 4.10.

TABLE 4.10: Virtual screening of ligands

| **S.No** | **Ligand Name** | **Mol Weight** | **Log P value** | **Rotatable Bonds** | **H-bond Acceptors** | **H-bond Donors** |
|---|---|---|---|---|---|---|
| 1. | Aristolone | 218.34 | 3.594 | 0 | 1 | **0** |
| 2. | Medicarpin | 270.284 | 3.0105 | 1 | 4 | 1 |
| 3. | Riboflavin | 376.369 | -1.72356 | 5 | 9 | 5 |
| 4. | Vasicine | 188.23 | 1.2968 | 0 | 3 | 1 |

According to table 4.10, the molecular weight, log P value, hydrogen bond donors, acceptors and rotatable bonds are in range for all ligands. Overall, all ligands are following all lipinski rules so they can be processed further.

### 4.4.6 ADMET Analysis of Ligands

A second investigation was conducted utilizing the online program pkCSM to ascertain ligands' ADMET characteristics as a pharmacokinetic metric following the Lipinski rule. There are two general words in pharmacology: pharmacodynamics and pharmacokinetics.

Within the field of pharmacology, pharmacodynamics examines how medications affect the body. In pharmacokinetics, we investigate how medications are absorbed, distributed, metabolized, and excreted [151].

#### 4.4.6.1 Absorption Properties of Ligands

The absorption parameters reveal important criteria for evaluating the bioavailability of compounds. For water solubility, the higher the number, the better the solubility, helping with absorption. In the case of $CaCO_2$ permeability, a desirable number should be above 0, and when above 1, permeability and absorption are high. For intestinal absorption, desirable values should be above 50%, representing good absorption in human metabolism. For skin permeation, desirable values should be above -2, helping with absorption. Finally, being an P-Glycoprotein substrate is desirable when "Yes" as it can be preferably transported by P-Glycoprotein, depending on the case. Ideally, for P-glycoprotein inhibitors, a "No" status is preferred to avoid potential drug interactions that could compromise therapeutic efficacy [152]. The absorption properties of ligands are given in table 4.11.

TABLE 4.11: Absorption properties of ligands

| **Ligand Name** | **Water solubility** | **$CaCO_2$ Permeability** | **Intestinal absorption (human)** | **Skin permeability** | **P - glycoprotein substrate** | **P - glycoprotein I inhibitor** | **P - glycoprotein II inhibitor** |
|---|---|---|---|---|---|---|---|
| Aristolone | -4.426 | 1.291 | 98.879 | -2.191 | No | No | No |
| Medicarpin | -3.459 | 1.246 | 95.188 | -2.819 | No | No | No |
| Riboflavin | -2.029 | 1.679 | 85.107 | -2.767 | No | No | No |
| Vasicine | -2.433 | 1.595 | 86.22 | -2-827 | No | No | No |

According to table 4.11, all ligands have good water solubility. Caco2 permeability is in range for all ligands. Intestinal absorption for all ligands is above 50. Skin permeability is also in range. No ligand is an inhibitor or substrate of P-glycoprotein

#### 4.4.6.2 Distribution Properties of Ligands

The theoretical volume or VDss indicates the entire dosage of the medication that must be dispersed evenly to produce a concentration similar to that of blood plasma. For VDss a good value is typically greater than 0.5 L/kg, indicating

favorable distribution in body tissues. The fraction unbound (Fu) should ideally be above 0.1, which signifies a significant proportion of the drug is available for therapeutic action. The blood-brain barrier reduces the amount of exogenous substances that can reach the brain directly while protecting it.

Regarding BBB permeability (log BB), values greater than 0 suggest the ability to cross the blood-brain barrier. For CNS permeability (log PS), values closer to 0, ideally above -2 are preferred, as they indicate potential for penetration into the central nervous system [153].

Table 4.12 shows the distribution properties of ligands. The table indicates all ligands have safe range which is given below.

TABLE 4.12: Distribution properties of ligands

| **Ligand Name** | **VDss (human)** | **Fraction unbound (human) Fu** | **BBB permeability log BB** | **CNS permeability log PS** |
|---|---|---|---|---|
| Aristolone | 0.451 | 0.201 | 0.072 | -1.958 |
| Medicarpin | 0.065 | 0.14 | 0.024 | -1.838 |
| Riboflavin | 0.196 | 0.676 | -1.552 | -2.144 |
| Vasicine | 0.08 | 0.4 | -0.127 | -2.159 |

The above table 4.12 shows that all ligands have positive VDSS values. The fraction unbound values, BBB and CNS permeability is approximately in range for all ligands.

### 4.4.7 Metabolism Properties of Ligands

The enzyme cytochrome P450 is in charge of the liver's detoxification process. Many drugs get deactivated by this enzyme but certain drugs are capable of activating. This enzyme's inhibitors can directly affect the metabolism of the drug hence should not be used. Similarly, CYP2D6 and CYP3A4 are responsible for the drugs' metabolism. Inhibition of these affects the pharmacokinetics of the drug in use [154].

The ligand metabolism prediction is shown below. The metabolic characteristics of ligands are displayed in table 4.13.

TABLE 4.13: Metabolism properties of ligands

| **Ligand Name** | **CYP2D6 substrate** | **CYP3A4 substrate** | **CYP1A2 inhibitor** | **CYP2C19 inhibitor** | **CYP2C9 inhibitor** | **CYP2D6 inhibitor** | **CYP3A4 inhibitor** |
|---|---|---|---|---|---|---|---|
| Aristolone | No | No | No | No | No | No | No |
| Medicarpin | No | No | Yes | Yes | Yes | No | Yes |
| Riboflavin | No | No | No | No | No | No | No |
| Vasicine | No | No | No | No | No | No | No |

The metabolic properties of the ligands as shown in table 4.13, indicate that none of the compounds are substrates for the CYP2D6 and CYP3A4 enzymes which suggests they are not metabolized by these pathways. This is beneficial as it reduces potential drug interactions that could arise from competition for these important metabolic enzymes. Medicarpin shows inhibition of the CYP enzymes, which can lead to increased levels of drugs metabolized by this enzyme.

#### 4.4.7.1 Excretion Properties of Ligands

Two organs are involved in drug excretion, the liver, which is engaged in biliary excretion, and the kidneys, which are involved in renal excretion. Excretion may also include other organs, such as the lungs in the case of volatile or gaseous substances. Moreover, drugs can be expelled through tears, saliva, and perspiration [155]. The excretion values of the ligands are given in table 4.14.

TABLE 4.14: Excretion properties of ligands

| **Ligand Name** | **Total Clearance** | **Renal OCT2 substrate** |
|---|---|---|
| Aristolone | 0.913 | No |
| Medicarpin | 0.273 | No |
| Riboflavin | 0.7 | No |
| Vasicine | 0.58 | No |

According to table 4.14, the total clearance values for the compounds are in range. Notably, all compounds are classified as non-substrates for renal OCT2, which

implies that they do not rely on this renal transport mechanism for excretion. This is beneficial as it minimizes the risk of interactions with other drugs that may utilize the same pathway.

#### 4.4.7.2 Toxicity Properties of Ligands

By using pkCSM we determined the toxicity of the ligands. AMES toxicity test is used to test the mutagenic potential of the compound by using bacteria. If it shows a positive response, then the ligand is mutagenic which can also act as a carcinogen. The toxicity of *T. Pyriformis* (protozoa bacterium) is used as a toxic endpoint in the *T. Pyriformis* toxicity method. Any value >-0.5 log ug/L is considered toxic [156]. The values predicted in the Minnow toxicity test are used to represent the concentration at which the compound could cause the death of 50% of the minnows. The value below 0.5 mM is regarded as acute toxic. The expected log value of the oral rat chronic toxicity test's lowest recorded adverse effect is correlated with the drug concentration that requires a specific duration of treatment, expressed in log mg/kg bw/day. A hepatotoxicity test predicts that if a compound could affect liver functioning or not. Higher maximum tolerated dose (MRTD) values indicate better safety [157]. The toxicity values of all ligands are given in table 4.15.

TABLE 4.15: Toxicity values of ligands

| **Ligand Name** | **AMES toxicity** | **Max tolerated dose (human)** | **hERG I inhibitor** | **hERG II inhibitor** | **Oral rat acute toxicity (LD50)** | **Oral rat chronic toxicity (LOAEL)** | **Hepato toxicity** | **Skin sensitization** | ***T. pyriformis* toxicity** | **Minnow toxicity** |
|---|---|---|---|---|---|---|---|---|---|---|
| Aristolone | No | 0.078 | No | No | 1.681 | 1.246 | No | **No** | 1.276 | 0.598 |
| Medicarpin | No | 0.102 | No | No | 2.512 | 1.875 | No | No | 0.688 | 0.657 |

**Table 4.15 continued from previous page**

| **Ligand Name** | **AMES toxicity** | **Max tolerated dose (human)** | **hERG I inhibitor** | **hERG II inhibitor** | **Oral rat acute toxicity (LD50)** | **Oral rat chronic toxicity (LOAEL)** | **Hepato toxicity** | **Skin sensitization** | ***T. pyriformis* toxicity** | **Minnow toxicity** |
|---|---|---|---|---|---|---|---|---|---|---|
| Riboflavin | No | 0.712 | No | No | 2.17 | 3.864 | No | No | 0.285 | 4.528 |
| Vasicine | No | 0.204 | No | No | 2.697 | 1.427 | No | No | 0.736 | 1.86 |

According to table 4.15, no inhibition of hERG I or hERG II was seen in any ligand. None of the ligands demonstrated hepatotoxicity, AMES toxicity, or skin sensitization. MRTD value is also positive for all ligands. *T. pyriformis* activity and minnow toxicity values are also in range for all ligands.

## 4.5 Molecular Docking

To carry out docking, the three-dimensional structures of the protein and ligands are used. An online blind auto docking program called CB dock is utilized for this. CB Dock computes the cavity sizes and predicts the protein binding locations. CB Dock provides us with the top five possess and receptor models upon docking. Based on the cavity size and the vina score, the optimal position was chosen among these five [158]. Target proteins and ligands were used in molecular docking. Ligands are in SDF format, while the proteins are in PDB format. After verifying the input files, CB Dock uses Open Babel and MGL tools to transform them into files in the pdbqt format. Next, CB dock determines the receptor's cavities as well as the diameters and centers of the top five cavities. The protein-ligand interaction's high-affinity score determines which of the five optimal conformations

is the best [159]. The scores obtained after the docking of proteins and ligands are shown in tables 4.16.

TABLE 4.16: Docking score of ligand-protein complexes

| **S. No** | **Ligands** | **Target Proteins** | | | | |
|---|---|---|---|---|---|---|
| | | Akt2 | IRS-2 | PDX-1 | PI3K-$\alpha$ | PPAR-$\gamma$ |
| 1. | Aristolone | -8 | -5.8 | -5.5 | -6.4 | -6.9 |
| 2. | Medicarpin | -8.3 | -6.3 | -6.3 | -6.5 | -8.3 |
| 3. | Riboflavin | -9.1 | -6.8 | -6.2 | -5.9 | -8.1 |
| 4. | Vasicine | -7.3 | -5.9 | -5.4 | -5.5 | -7.3 |

Table 4.16 shows the docking result of receptors with ligands. It shows that riboflavin has the highest binding score of -9.1 with Akt2, followed by -8.1 with PPAR-$\gamma$.

### 4.5.1 Analysis of Docked Complexes via Discovery Studio

To understand docking data, ligand and protein interaction was estimated. Hydrogen bonding, alkyl and van der waals interactions are the main types of interactions that were investigated. Discovery Studio 2025 Client was used to analyze these interactions between proteins and ligands.

The saved conformations for the ligand-receptor complex of each molecule were analyzed in detail. This program creates schematic representations of the protein-ligand interactions between the specified ligands in the PDB file automatically [160].

Numerous interactions between the ten ligands and the three target proteins were seen in the docked data, which were submitted in PDB format. The docked complexes and ligand-receptor interactions are depicted in the following diagrams. The (a) part of the figure represents the docking complex, while (b) part of the figure provides information about the interaction between protein and ligand.

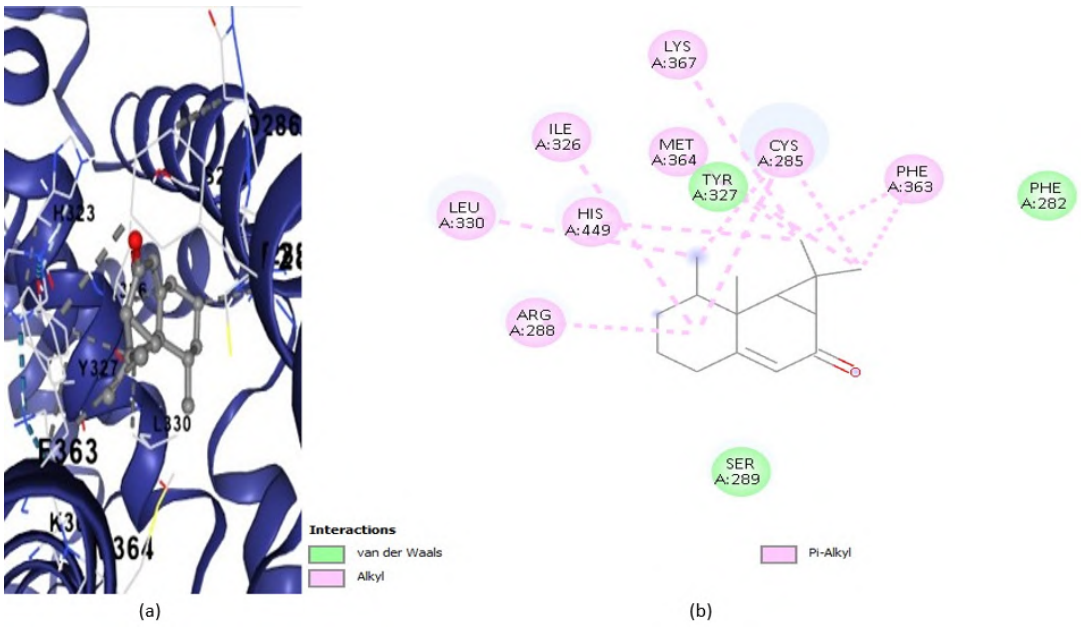


FIGURE 4.45: Analysis of dock complexes of aristilone with PPAR-$\gamma$

Figure 4.45 shows the interaction of aristilone with PPAR-$\gamma$. It shows there are eleven alkyl bonds and three van der waals interactions.

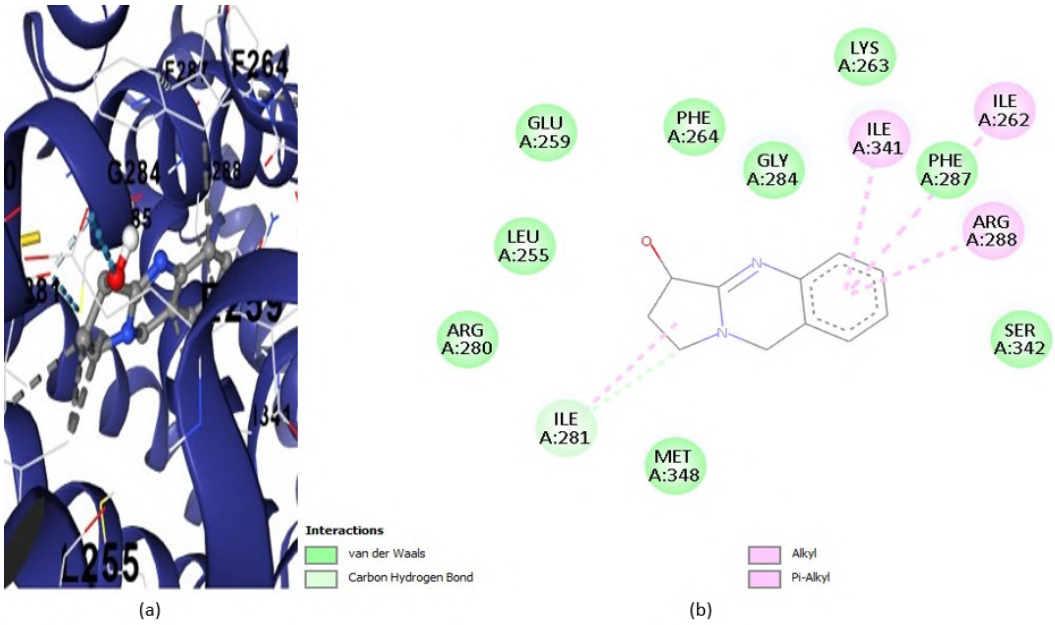


FIGURE 4.46: Analysis of dock complexes of vascine with PPAR-$\gamma$

Figure 4.46 shows the interaction of vascine with PPAR-$\gamma$. It shows there are three alkyl bonds, one carbon hydrogen bond and nine van der waals interactions.

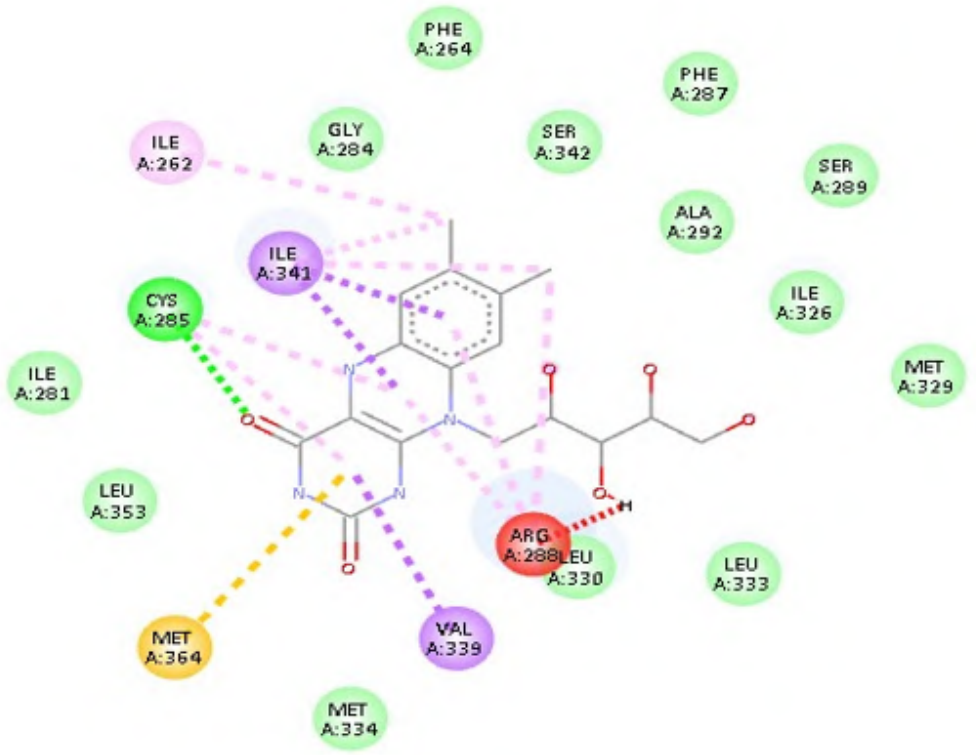


FIGURE 4.47: Analysis of dock complexes of riboflavin with PPAR-$\gamma$

Figure 4.47 shows the interaction of riboflavin with PPAR-$\gamma$. It shows there is one alkyl bond, one conventional hydrogen bond and thirteen van der waals interactions.

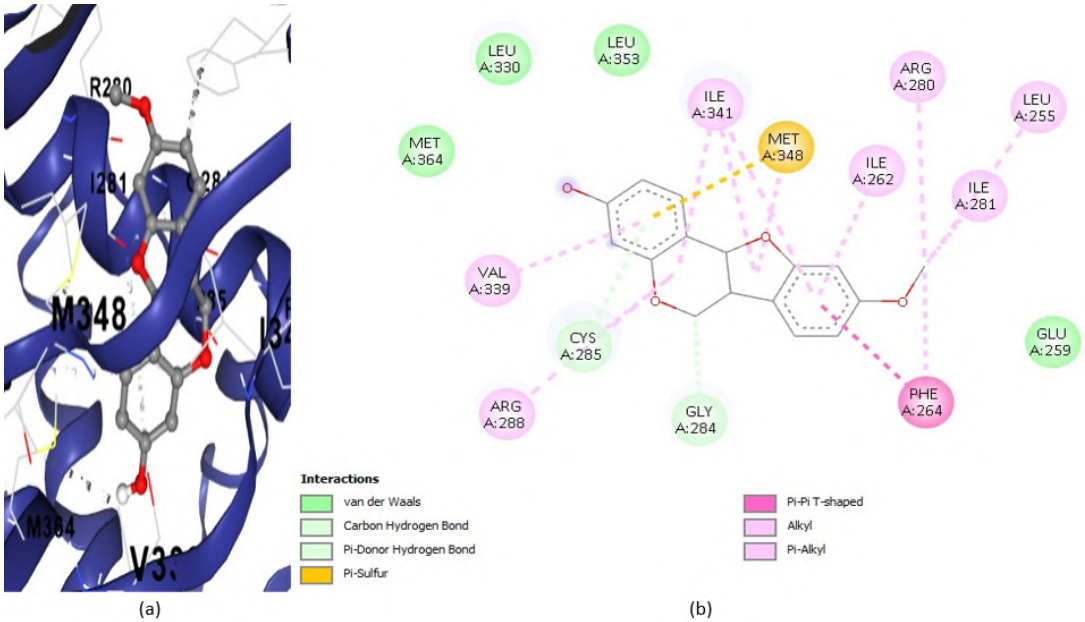


FIGURE 4.48: Analysis of dock complexes of metacarpin with PPAR-$\gamma$

Figure 4.48 shows the interaction of metacarpin with PPAR-$\gamma$. It shows there are nine alkyl bonds, two carbon hydrogen bond and four van der waals interactions.

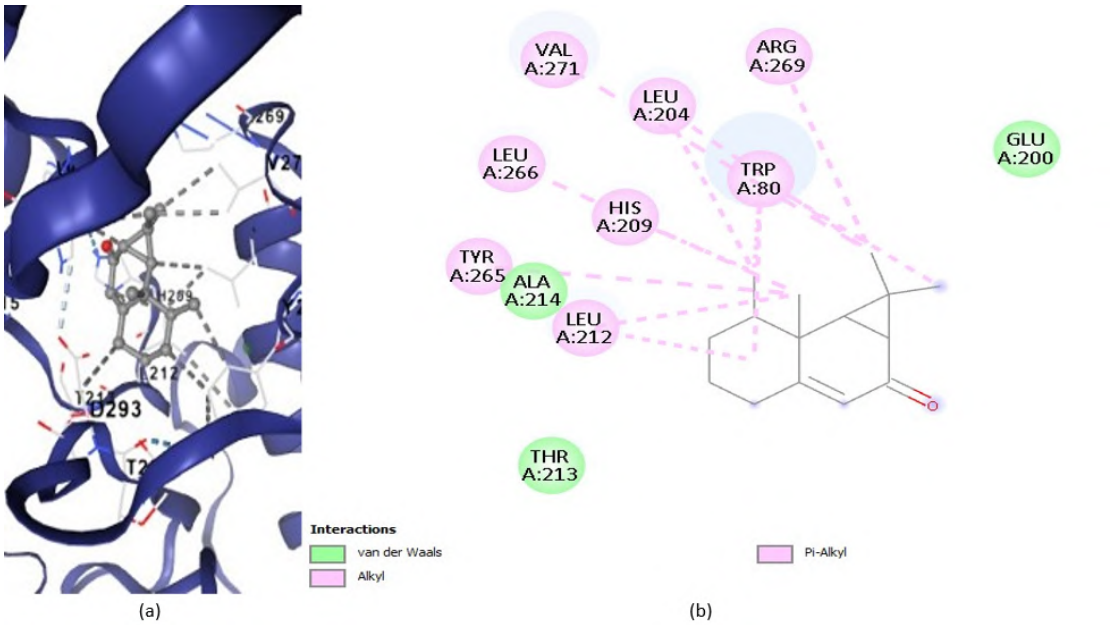


FIGURE 4.49: Analysis of dock complexes of aristilone with Akt2

Figure 4.49 shows the interaction of aristilone with Akt2. It shows there are nine alkyl bonds and three van der waals interactions.

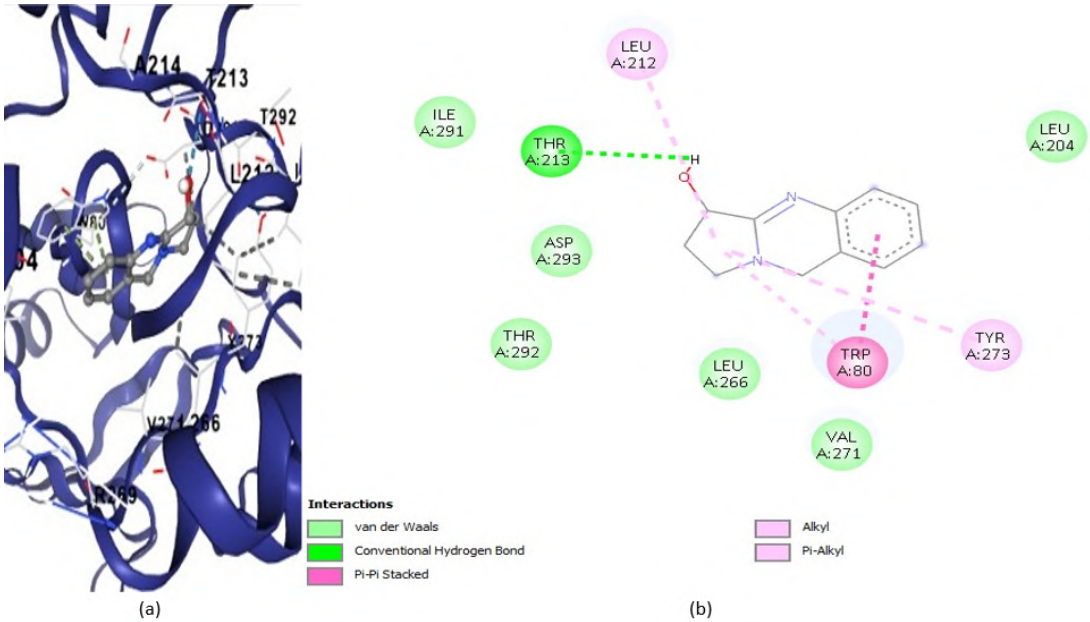


FIGURE 4.50: Analysis of dock complexes of vascine with Akt2

Figure 4.50 shows the interaction of vascine with Akt2. It shows there are two alkyl bonds, one conventional hydrogen bond and six van der waals interactions.

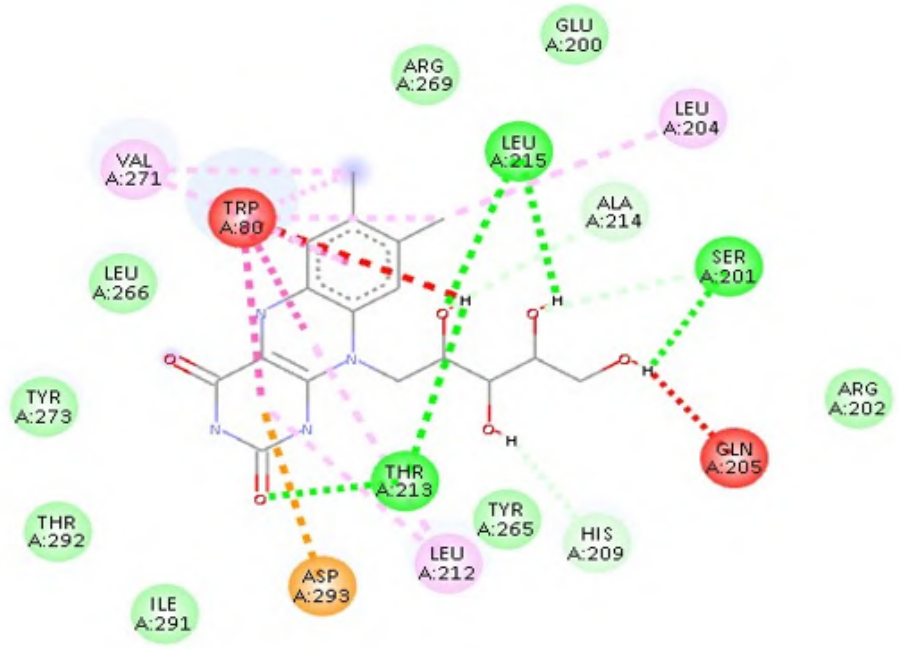


FIGURE 4.51: Analysis of dock complexes of riboflavin with Akt2

Figure 4.51 shows the interaction of riboflavin with Akt2. It shows there are three alkyl bonds, four conventional hydrogen bonds, one pi-anion, two carbon hydrogen bonds, eight van der waals and two unfavorable interactions.

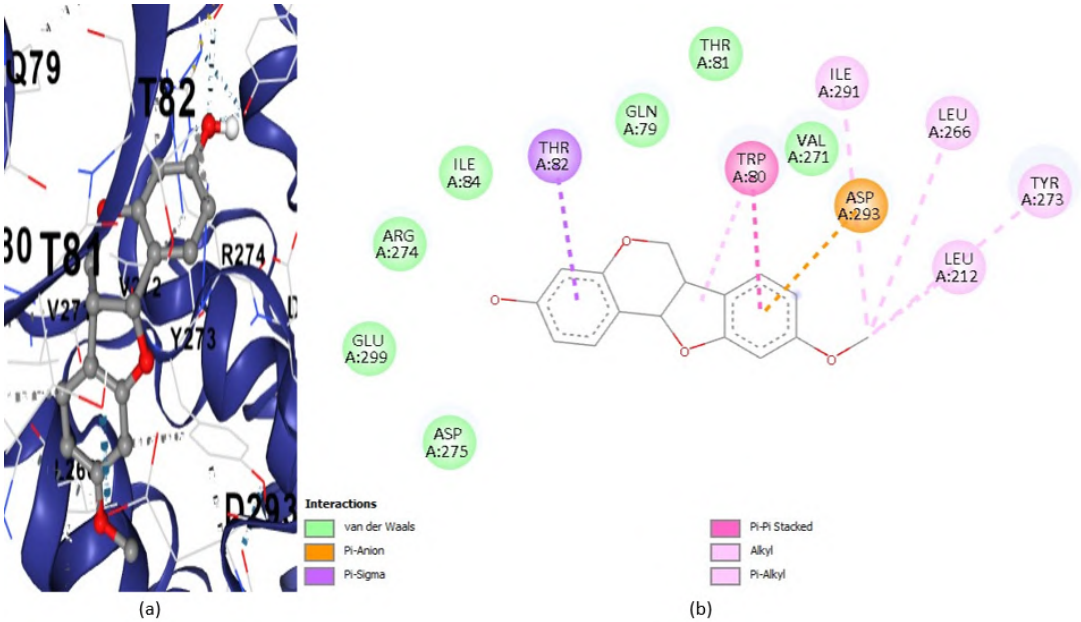


FIGURE 4.52: Analysis of dock complexes of metacarpin with Akt2

Figure 4.52 shows the interaction of metacarpin with Akt2. It shows there are four alkyl bonds and seven van der waals interactions.

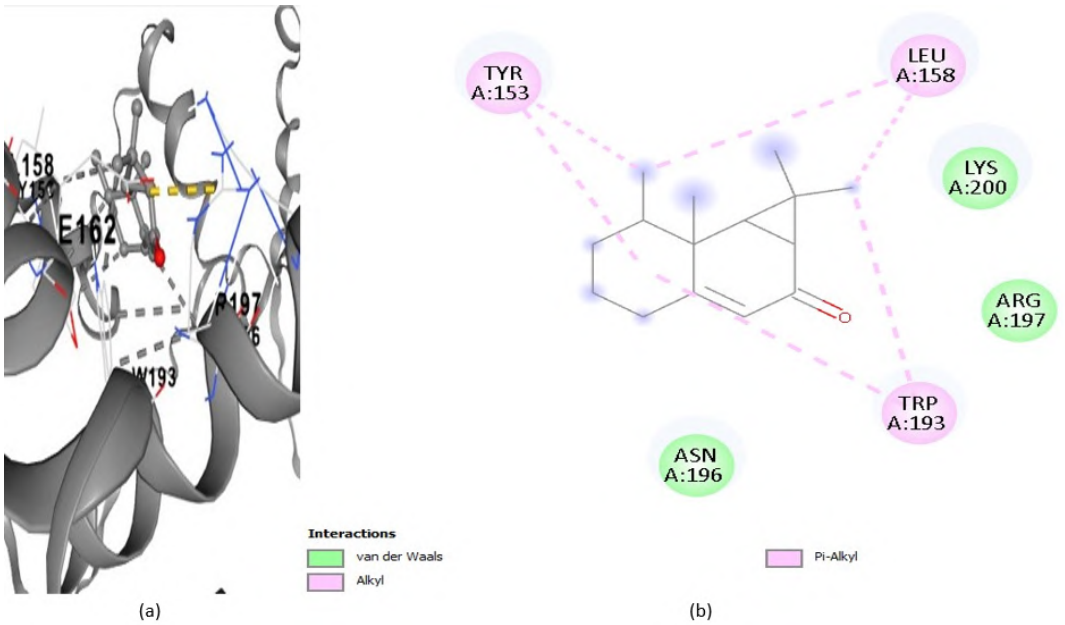


FIGURE 4.53: Analysis of dock complexes of aristilone with PDX-1

Figure 4.53 shows the interaction of aristilone with PDX-1. It shows there are six alkyl bonds and three van der waals interactions.

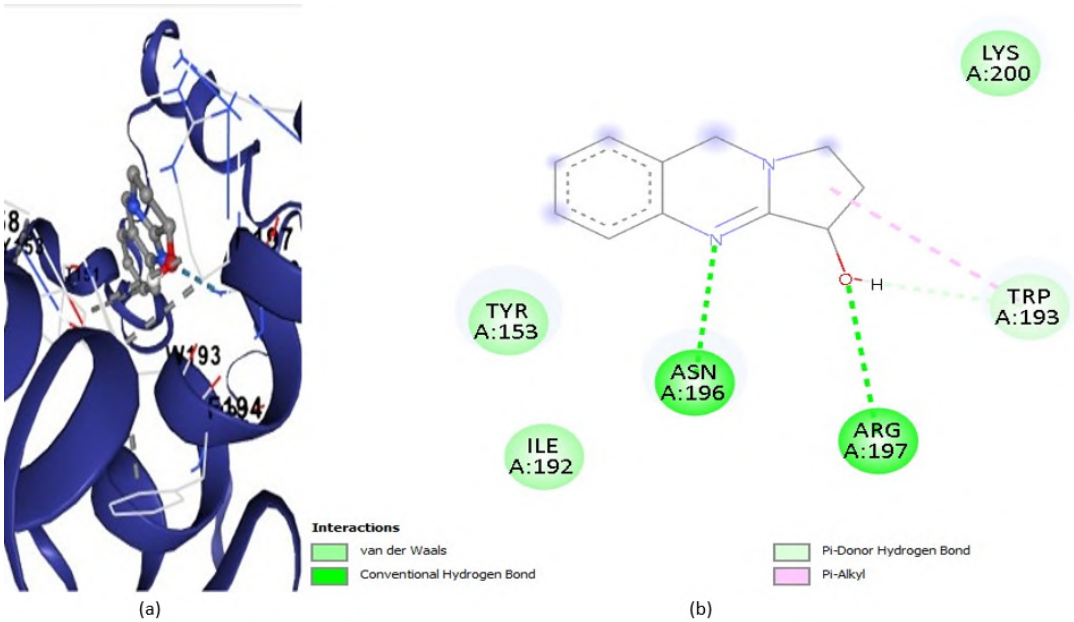


FIGURE 4.54: Analysis of dock complexes of vascine with PDX-1

Figure 4.54 shows the interaction of vascine with PDX-1. It shows there are two conventional hydrogen bonds, one donor hydrogen bond and three van der waals interactions.

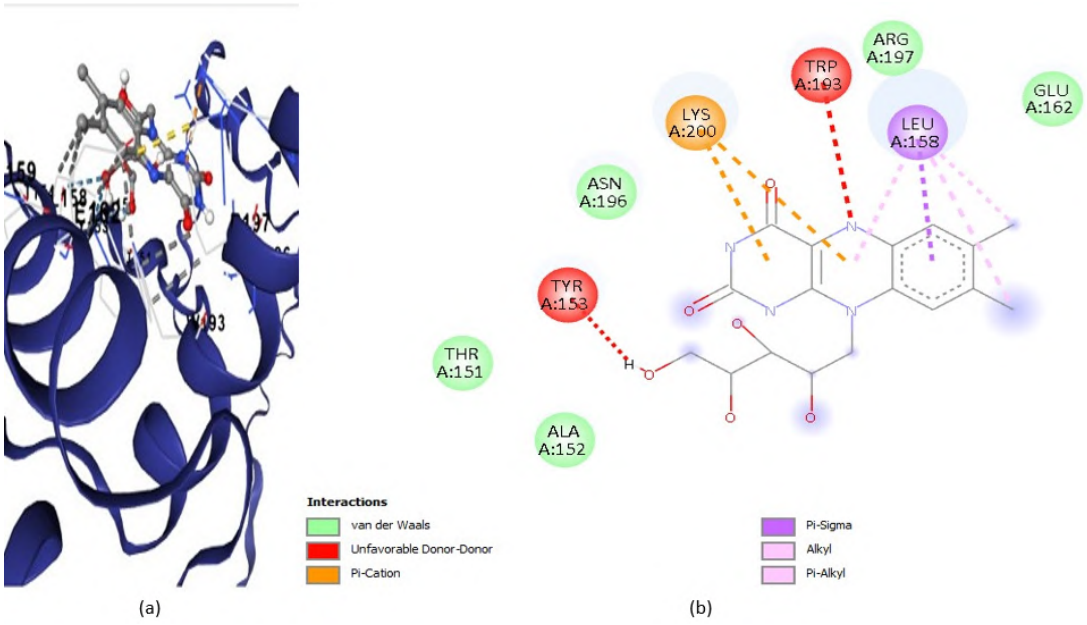


FIGURE 4.55: Analysis of dock complexes of riboflavin with PDX-1

Figure 4.55 shows the interaction of riboflavin with PDX-1. It shows there are five van der waals interactions.

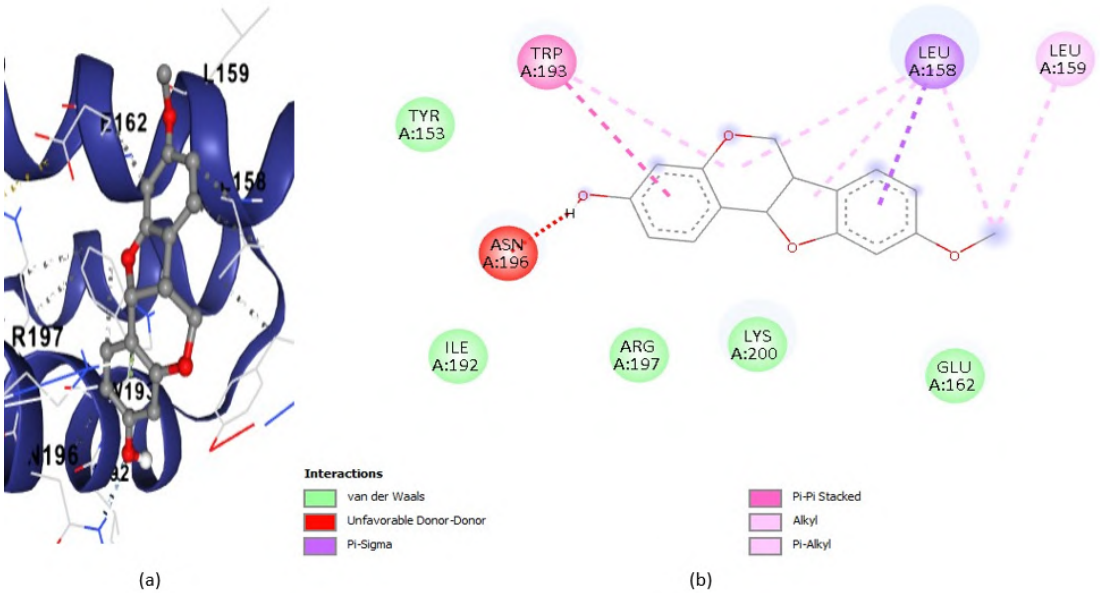


FIGURE 4.56: Analysis of dock complexes of metacarpin with PDX-1

Figure 4.56 shows the interaction of metacarpin with PDX-1. It shows there is one alkyl bond and five van der waals interactions.

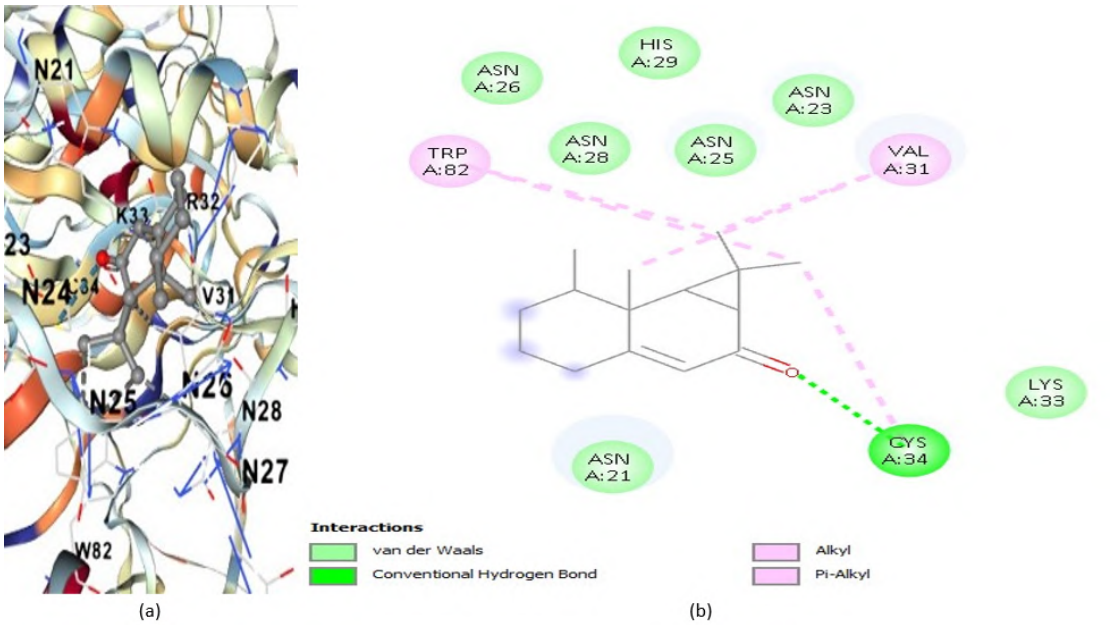


FIGURE 4.57: Analysis of dock complexes of aristilone with IRS-2

Figure 4.57 shows the interaction of aristilone with IRS-2. It shows there are three alkyl bonds, one conventional hydrogen bond and seven van der waals interactions.

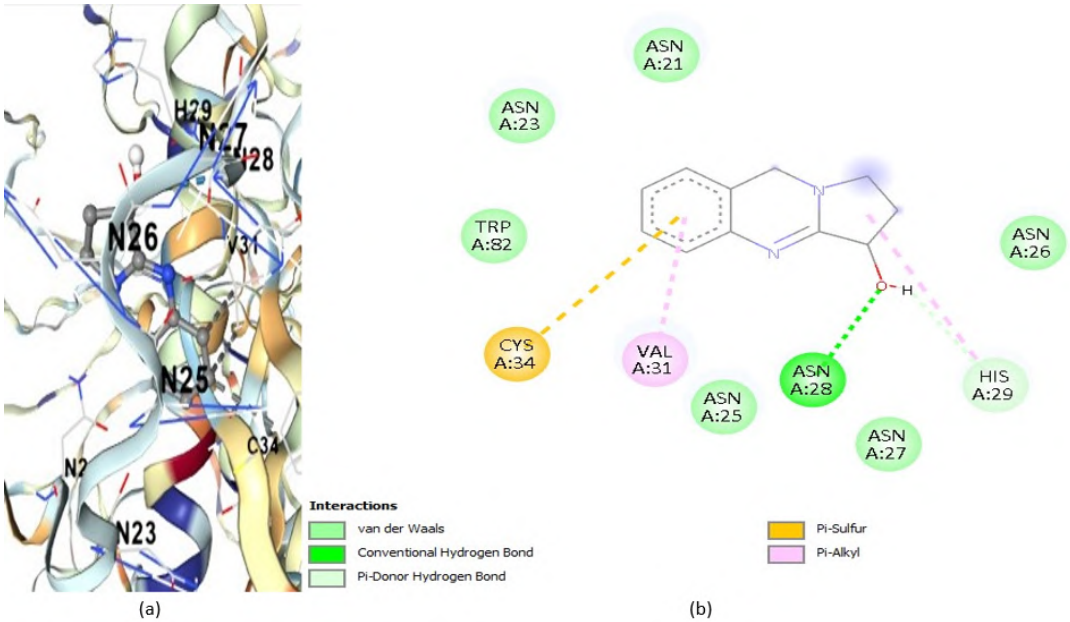


FIGURE 4.58: Analysis of dock complexes of vascine with IRS-2

Figure 4.58 shows the interaction of vascine with IRS-2. It shows there is one alkyl bond, one conventional hydrogen bond, one donor hydrogen bond and six van der waals interactions.

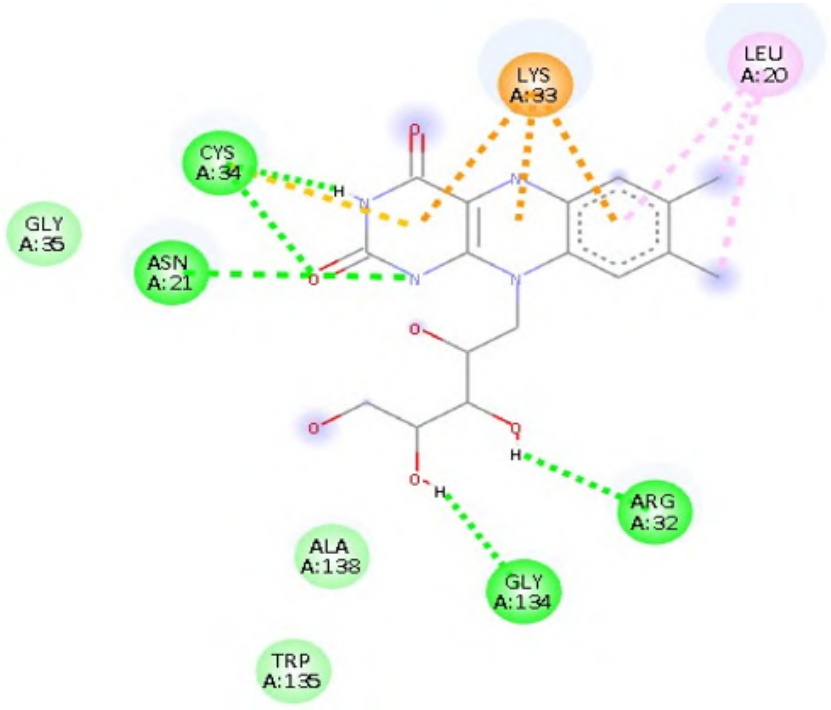


FIGURE 4.59: Analysis of dock complexes of riboflavin with IRS-2

Figure 4.59 shows the interaction of riboflavin with IRS-2. It shows there are three alkyl bonds, five conventional hydrogen bonds and three van der waals interactions.

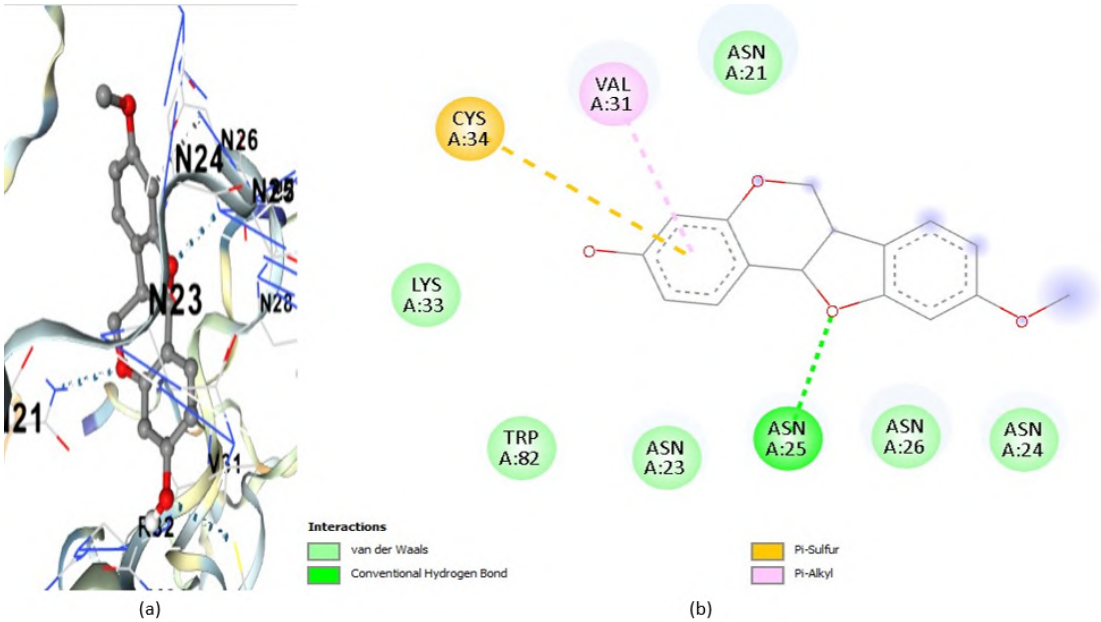


FIGURE 4.60: Analysis of dock complexes of metacarpin with IRS-2

Figure 4.60 shows the interaction of metacarpin with IRS-2. It shows there is one alkyl bond, one conventional hydrogen bond and six van der waals interactions.

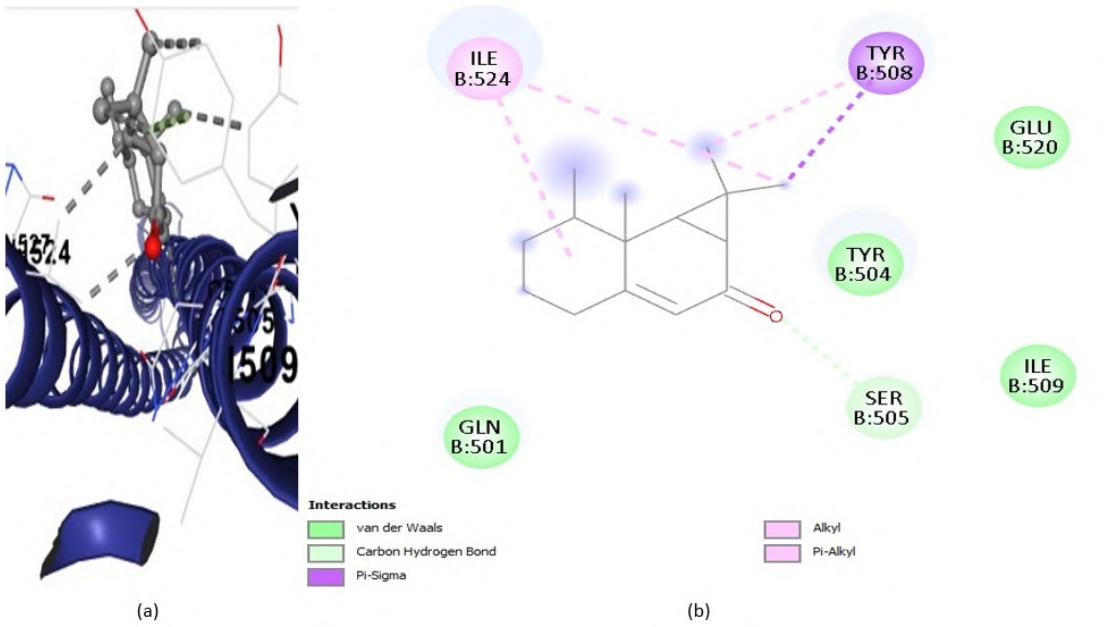


FIGURE 4.61: Analysis of dock complexes of aristilone with PI3K-$\alpha$

Figure 4.61 shows the interaction of aristilone with PI3K-$\alpha$. It shows there are two alkyl bonds, one carbon hydrogen bond and four van der waals interactions.

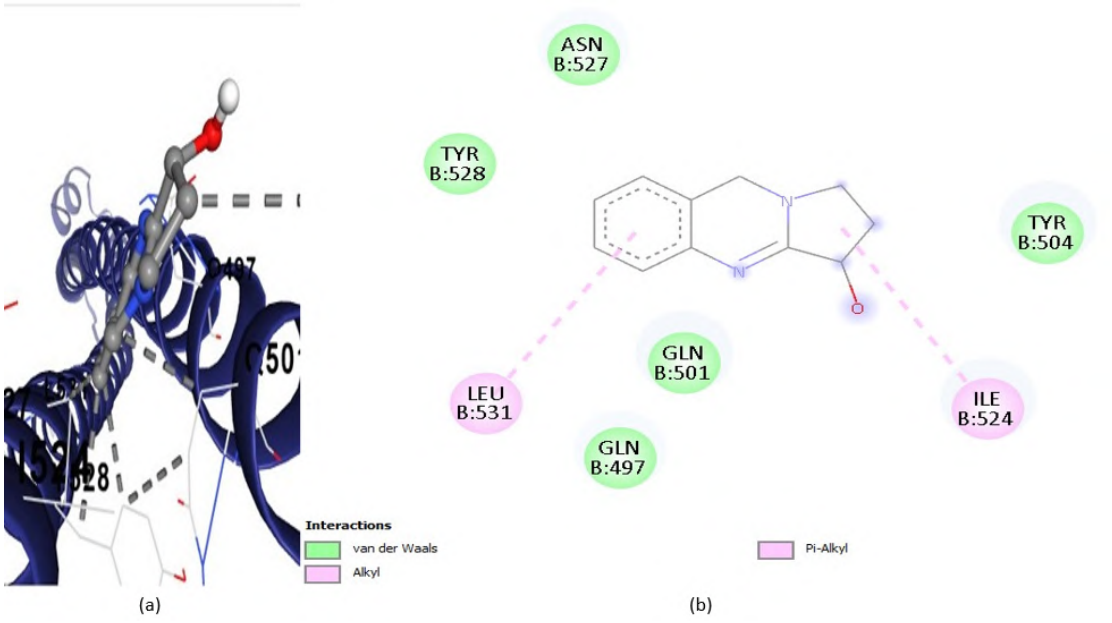


FIGURE 4.62: Analysis of dock complexes of vascine with PI3K-$\alpha$

Figure 4.62 shows the interaction of vascine with PI3K-$\alpha$. It shows there are two alkyl bonds and five van der waals interactions.

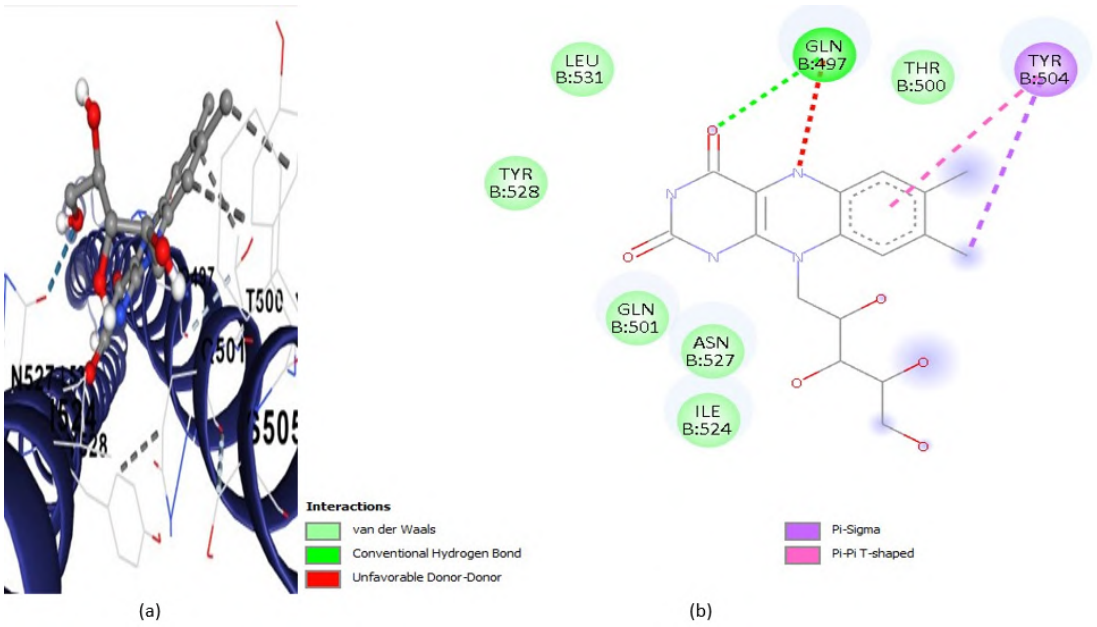


FIGURE 4.63: Analysis of dock complexes of riboflavin with PI3K-$\alpha$

Figure 4.63 shows the interaction of riboflavin with PI3K-$\alpha$. It shows there is one conventional hydrogen bond and six van der waals interactions.

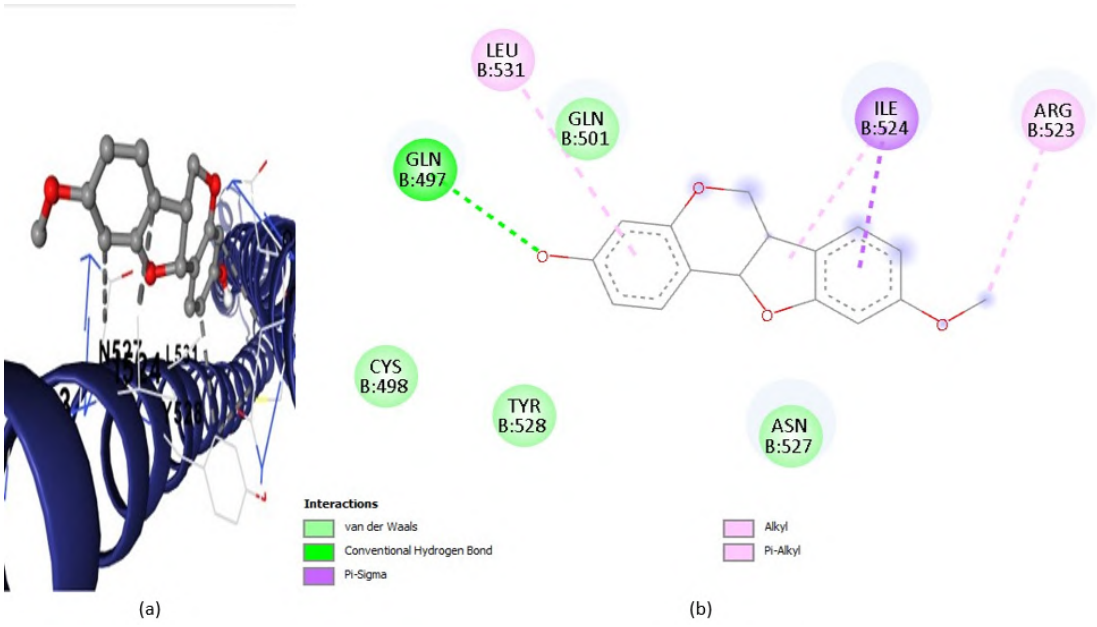


FIGURE 4.64: Analysis of dock complexes of metacarpin with PI3K-$\alpha$

Figure 4.64 shows the interaction of metacarpin with PI3K-$\alpha$. It shows there is one conventional hydrogen bond, two alkyl bonds and four van der waals interactions.

### 4.5.2 Lead Compound Identification

The ligands' pharmacokinetic and physicochemical properties determine their fate as either drug or non-drug compounds. Lipinski's rule is the first filter and pharmacokinetics is the second filter for this identification. All ligands were seen obeying the lipinski rule of five so they all got selected for docking.

The next knockout stage is pharmacokinetic screening and docking score. In this screening, riboflavin from super-fraction AF2 was selected as lead compound because it showed the best ADMET values concerning high water solubility, good intestinal absorption, and minimal toxicity. Docking score of riboflavin is also good against all receptors and highest i.e. -9.1 against Akt2 receptor.

Additionally, riboflavin has a significant quantity of residues having van der waals interactions, alkyl bonds and hydrogen bonds, so riboflavin was selected as the lead compound.

### 4.5.3 Reference Anti-diabetic Drug Identification

Metformin is a commonly used medication for diabetes. It works by reducing hepatic glucose production and increasing insulin sensitivity. It activates AMP-activated protein kinase, which inhibits gluconeogenic enzymes, decreasing glucose production in the liver.

Additionally, it enhances glucose uptake in muscle and fat tissues by promoting GLUT4 translocation to the cell membrane. It may also reduce intestinal glucose absorption and alter gut microbiota, contributing to its glucose-lowering effect. Metformin is effective in lowering blood glucose levels without significant hypoglycemia, though it can cause gastrointestinal side effects and, rarely, lactic acidosis [161].

#### 4.5.3.1 Metformin and Lead Compound Comparison

Metformin's effective mechanism of action and favorable safety profile make it an ideal reference drug for comparative studies, providing a solid foundation for evaluating new potential therapeutic agents such as riboflavin in the context of IRS protein sensitivity and glucose metabolism.

#### 4.5.3.2 Metformin Structure Prediction

First of all metformin structure was downloaded in SDF format from PubChem. Then its energy was minimized by using chem3D pro to get the refined structure. The chemical formula of metformin is C4H11N5 and its refined structure is given in figure 4.65.

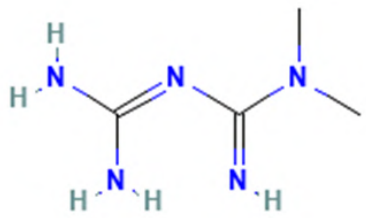


FIGURE 4.65: Structure of metformin

#### 4.5.3.3 Lipinski Rule Comparison

The metformin and riboflavin were compared to observe their response to the lipinski rule and to evaluate their pharmacokinetic properties, to assess their bioavailability, safety, efficacy, and drug-likeness. The comparison is given in table 4.17.

TABLE 4.17: The lipinski rule of five comparison

| **Ligands** | **Log P value** | **Molecular weight** | **H-bond donor** | **H-bond acceptor** | **Rotatable bonds** |
|---|---|---|---|---|---|
| Metformin | -1.24 | 129.167 | 3 | 1 | 0 |
| Riboflavin | -1.72 | 3766.369 | 5 | 9 | 5 |

Table 4.17 shows that both metformin and riboflavin are following lipinski rule.

#### 4.5.3.4 ADMET Properties Comparison

The ADMET qualities were used to evaluate the drug's and the lead chemical's absorption, distribution, metabolism, excretion, and toxicity to identify a better drug candidate.

### i. The Absorption Properties Comparison

A comparison between metformin and riboflavin for checking absorbance models is given in table 4.18.

TABLE 4.18: Absorption properties comparison

| | Absorption Properties | | | | | | |
|---|---|---|---|---|---|---|---|
| **Ligand Name** | **Water solubility** | **$CaCO_2$ Permeability** | **Intestinal absorption (human)** | **Skin permeability** | **P - glycoprotein substrate** | **P - glycoprotein I inhibitor** | **P - glycoprotein II inhibitor** |
| Metformin | -2.707 | -0.339 | 59.401 | -2.735 | Yes | No | No |
| Riboflavin | -2.029 | 1.679 | 85.107 | -2.767 | No | No | No |

Table 4.18 shows that both metformin and riboflavin show comparable absorption properties except for intestinal absorption, which is low for metformin.

### ii. Distribution Properties Comparison

The comparison between the distribution properties of metformin and riboflavin is given in table 4.19.

TABLE 4.19: Distribution properties comparison

| | Distribution Properties | | | |
|---|---|---|---|---|
| **Ligand Name** | **VDss (human)** | **Fraction unbound (human) Fu** | **BBB permeability log BB** | **CNS permeability log PS** |
| Metformin | -0.232 | 0.811 | -0.946 | -4.238 |
| Riboflavin | 0.196 | 0.676 | -1.552 | -2.144 |

The above table 4.19 shows the comparative distribution properties of metformin and riboflavin. Both metformin and riboflavin share comparable distribution properties except VDSS, which is negative for metformin.

### iii. Metabolism Properties Comparison

The comparison between the metabolism properties of metformin and riboflavin is given in table 4.20.

TABLE 4.20: Metabolic properties comparison

| **Ligand Name** | **Metabolism Properties** | | | | | | |
|---|---|---|---|---|---|---|---|
| | **CYP2D6 substrate** | **CYP3A4 substrate** | **CYP1A2 inhibitor** | **CYP2C19 inhibitor** | **CYP2C9 inhibitor** | **CYP2D6 inhibitor** | **CYP3A4 inhibitor** |
| Metformin | No | No | No | No | No | No | No |
| Riboflavin | No | No | No | No | No | No | No |

Table 4.20 shows that both metformin and riboflavin share similar metabolism profiles.

### iv. Excretion Properties Comparison

The comparison between the excretion properties of metformin and riboflavin is given in table 4.21.

TABLE 4.21: Excretion properties comparison

| **Ligand Name** | **Excretion Properties** | |
|---|---|---|
| | **Total Clearance** | **Renal OCT2 substrate** |
| Metformin | 0.1 | No |
| Riboflavin | 0.7 | No |

Table 4.21 shows that both metformin and riboflavin have similar excretion profiles.

### v. Toxicity Properties Comparison

The comparison between the toxicity properties of metformin and riboflavin is given in table 4.22.

TABLE 4.22: Toxicity properties comparison

| **Ligand Name** | **Toxicity Properties** | | | | | | | | | |
|---|---|---|---|---|---|---|---|---|---|---|
| | **AMES toxicity** | **Max tolerated dose (human)** | **hERG I inhibitor** | **hERG II inhibitor** | **Oral rat acute toxicity (LD50)** | **Oral rat chronic toxicity (LOAEL)** | **Hepato toxicity** | **Skin sensitization** | ***T. pyriformis* toxicity** | **Minnow toxicity** |
| Metformin | Yes | 0.902 | No | No | 2.453 | 2.158 | No | Yes | 0.25 | 3.972 |
| Riboflavin | No | 0.712 | No | No | 2.17 | 3.864 | No | No | 0.285 | 4.528 |

Table 4.22 shows that both metformin and riboflavin have comparable toxicity profiles except for AMES toxicity and skin sensitization which is shown by the standard drug metformin.

#### 4.5.3.5 Docking Score Comparison

The standard drug metformin and lead compound riboflavin were docked against target proteins and binding values were obtained. The docking score comparison between metformin and riboflavin is displayed in table 4.23.

TABLE 4.23: Docking comparison of metformin and riboflavin

| **S. No** | **Ligands** | **Target Proteins** | | | | |
|---|---|---|---|---|---|---|
| | | **Akt2** | **IRS-2** | **PDX1** | **PI3K-$\alpha$** | **PPAR-$\gamma$** |
| 1. | Metformin | -5.5 | -4.5 | -3.7 | -3.9 | -5.1 |
| 2. | Riboflavin | -9.1 | -6.8 | -6.2 | -5.9 | -8.1 |

As can be shown in table 4.23, the vina scores of the lead compound riboflavin are significantly greater than those of the standard drug metformin. The docking scores of metformin against target proteins Akt2, IRS-2, PDX1, PI3K-$\alpha$ and

PPAR-$\gamma$ are -5.5, -4.5, -3.7, -3.9 and -5.1, respectively, while for riboflavin these scores are -9.1, -6.8, -6.2, -5.9 and -8.1 respectively. These results show that the lead compound riboflavin with highest docking score i.e., -9.1 has more binding efficiency than the standard drug metformin with docking score -5.5.

#### 4.5.3.6 Docking Analysis Comparison

Discovery studio evaluated the docking results depending upon the number of interactions between ligand and protein. The following figure shows the docking analysis of standard drug metformin with highest docking score -5.5 against target protein Akt2.

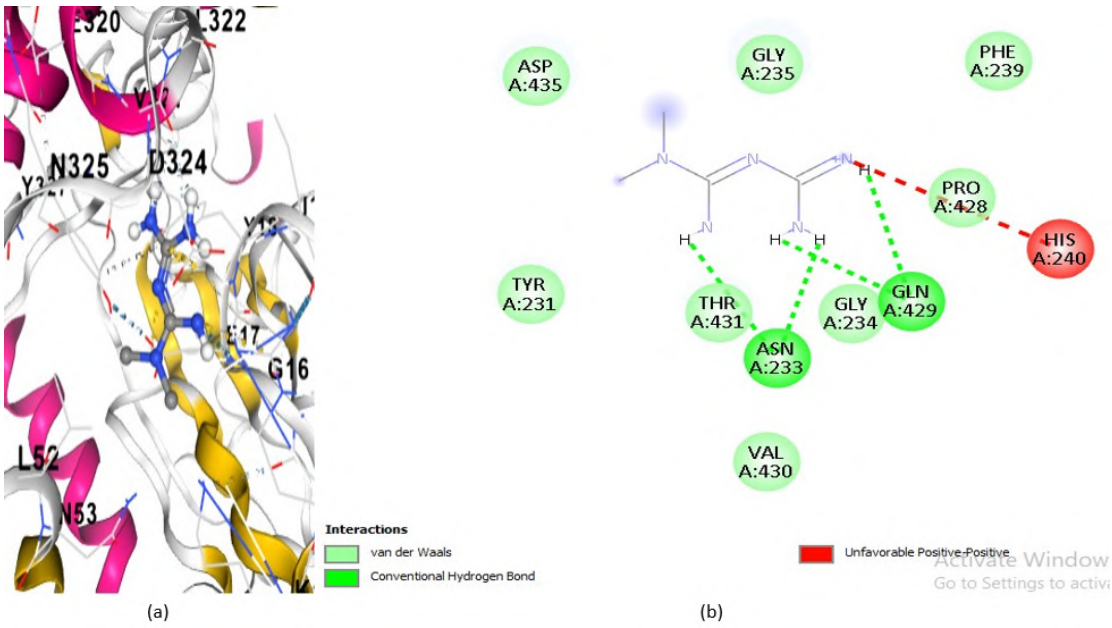


FIGURE 4.66: Docking interaction of metformin with target protein Akt2

Figure 4.66 shows the interaction of metformin with the target protein Akt2. It shows there are four conventional hydrogen bonds, eight van der waals and one unfavorable interaction. Whereas in the case of riboflavin interacting with Akt2, figure 4.51 above, it shows there are three alkyl bonds, four conventional hydrogen bonds, one pi-anion, two carbon hydrogen bonds and eight van der waals interactions. The data demonstrate that both riboflavin and metformin share a robust interaction profile, but the presence of unfavorable interaction in metformin

might reduce its overall stability. Also riboflavin contains alkyl bonds and carbon-hydrogen bonds, which are not present in metformin.

Overall, the comparison of metformin and riboflavin shows that both share comparable lipinski rules and ADMET analysis. But the docking scores and receptor-ligand interaction profile of the lead compound riboflavin are better than those of the standard drug metformin. It shows that riboflavin from super-fraction AF2 can act as a promising anti-diabetic therapeutic candidate in the future.

## 4.6 Discussion

The findings of the current study on the fractionation of Astragalus membranaceus extract, obtained through column chromatography, yield significant insights into the medicinal properties of this plant, particularly regarding its antioxidant and antidiabetic activities. These results align well with a substantial body of existing literature, thereby reinforcing the traditional medicinal use of *A. membranaceus*. This validation is crucial as it bridges the gap between traditional knowledge and modern scientific research, underscoring the potential importance of this herb in both ethnomedicine and contemporary therapeutic applications [162].

The antioxidant activity observed in the active fractions of *A. membranaceus* corroborates previous studies that highlighted the leaf extracts' remarkable abilities to mitigate oxidative stress. Antioxidants play a vital role in protecting cellular systems from oxidative damage, a critical factor exacerbated in various pathological conditions, including diabetes. Oxidative stress results from an imbalance between the production of free radicals and the body's ability to counteract their harmful effects, leading to cellular damage. The significant reduction of lipid peroxidation and enhancement of antioxidant enzyme levels in tissues characterized by diabetic conditions further point to the extract's protective functions. This evidence not only supports the role of *A. membranaceus* in managing oxidative stress but also suggests that it may provide a dual benefit of reducing clinical manifestations associated with diabetes and its complications. The discovery of

potent antioxidants within the extract could thus open new avenues for therapeutic applications in preventing oxidative stress-related diseases [150].

In the context of diabetes, which is often accompanied by complications such as dyslipidemia and cardiovascular diseases, the effectiveness of *A. membranaceus* in diminishing blood glucose levels through various mechanisms warrants closer examination. Numerous studies have historically documented the antidiabetic effects of *A. membranaceus*, showcasing its effectiveness in reducing blood glucose levels in various animal models subjected to diabetes-inducing agents like alloxan or streptozotocin. Our findings are consistent with this literature, particularly regarding the efficacy of the aqueous extract of the plant's roots in managing both hyperglycemia and dyslipidemia. The synchronous regulation of these conditions is paramount in diabetes management, as the presence of dyslipidemia significantly contributes to cardiovascular complications associated with the disease. The potential of *A. membranaceus* to act as a holistic therapeutic agent, balancing multiple metabolic parameters, reinforces its importance in comprehensive diabetes management protocols, potentially reducing the reliance on pharmaceutical interventions and minimizing the side effects associated with long-term drug use [163].

Moreover, our comparative analysis of different extract fractions reveals noteworthy observations regarding the efficacy of younger extracts over older ones. This finding aligns with the understanding that younger plant materials tend to possess higher concentrations of bioactive compounds, which can vary significantly in potency due to differences in their phytochemical constituents. These variations may influence the biological activity of the extracts and could lead to more effective treatments. The importance of this finding is further amplified when we consider that the efficacy of herbal medicine often relies upon the cultivation practices, harvest time, and the specific conditions under which the plant is grown. Understanding and optimizing these factors could vastly improve the therapeutic contributions of *A. membranaceus* [151].

In exploring the clinical implications of these findings, it is imperative to acknowledge the robust evidence showcasing the effectiveness of *A. membranaceus* not

only in laboratory settings but also in clinical environments. In vivo studies using standardized aqueous extracts of *A. membranaceus* roots and twigs have demonstrated beneficial effects, including enhanced blood sugar regulation and improved vascular functionality, even when used alongside standard antidiabetic medications such as metformin. This translational aspect of our findings highlights the critical need for further clinical trials to comprehensively understand the dynamics of *A. membranaceus* in diabetic care settings. By establishing a clearer interaction between herbal and conventional medicine, we can facilitate a more integrative approach to treatment, which is likely to enhance patient outcomes and tailor therapies more precisely to individual patient needs [164].

The mechanisms underlying the hypoglycemic effects of *A. membranaceus* appear to be multifaceted and complex. Numerous studies suggest that these benefits may stem from enhanced insulin sensitivity, improved functionality of pancreatic $\beta$-cells, and reduced oxidative stress. Additionally, the presence of various bioactive compounds, including flavonoids and polysaccharides, may contribute to these effects, thereby emphasizing the significance of conducting further research to elucidate the precise pathways involved. In this context, understanding the pharmacokinetics and pharmacodynamics of these compounds will be essential for their optimization in clinical applications. Moreover, the potential for antiserotonergic properties to influence glucose regulation adds another layer to our understanding of this plant's therapeutic potential, suggesting areas for future research that could uncover novel mechanisms of action [152].

While existing literature often emphasizes the properties of crude extracts or isolated compounds, the fractionation approach taken in this study signifies an important shift toward more refined phytochemical research. By dissecting the bioactive properties of various fractions of the leaf extract, this research not only isolates compounds with potent antioxidant and antidiabetic activities but also highlights the necessity of understanding the interactions among these bioactive compounds within complex mixtures. Investigating these interactions can lead to a clearer understanding of how these compounds work synergistically, potentially enhancing their therapeutic effects. The fractionation technique employed here facilitates a

thorough exploration of the chemical constituents that drive therapeutic effects, enabling researchers to build a comprehensive profile of the extract's medicinal properties [165].

In doing so, our study provides valuable information that could promote the development of standardized herbal medicines. Standardization is a critical aspect of herbal medicine, as it can ensure consistency in efficacy, safety, and quality across different formulations. Furthermore, isolating specific bioactive compounds could lead to the creation of more targeted therapeutic strategies, allowing for more refined and effective interventions in clinical settings. This focus on precision medicine aligns with modern healthcare's shift toward personalized approaches, where treatments can be tailored to meet individual patient profiles, thereby enhancing therapeutic efficacy and minimizing adverse effects [153].

Moreover, with the continuing global rise of chronic diseases and the limitations of conventional pharmacotherapy, the exploration of *A. membranaceus* offers a promising avenue for research into alternative or complementary therapies. The integration of this herb into mainstream clinical practice could provide a more holistic approach to health and disease management. It could empower patients by offering them natural alternatives to synthetic medications, potentially improving adherence to treatment regimens and overall quality of life [166].

In conclusion, the current study robustly confirms the traditional and scientific justifications for investigating the medicinal properties of *A. membranaceus*. As a rich source of bioactive compounds, this herb has the potential to make substantial contributions to natural product research and the development of novel therapeutic agents. Future studies should aim to elucidate the specific mechanisms of action of the identified fractions and explore their synergistic effects when combined with conventional therapies. Research into the long-term safety and efficacy of these treatments will also be vital to quantify their potential impact on public health [154].

Furthermore, in light of its antioxidant and antidiabetic properties, it would be beneficial to explore the role of *A. membranaceus* in other metabolic conditions,

such as obesity and metabolic syndrome, to fully elucidate its potential in promoting health and preventing disease. The implications for public health are significant; by promoting effective herbal treatments, we can potentially lower healthcare costs associated with chronic disease management and enhance the well-being of populations at risk [167].

Through these scientific explorations, we can ensure that the benefits of *A. membranaceus* are not only recognized but systematically integrated into patient care paradigms. This integration could significantly improve the quality of life for those affected by chronic conditions such as diabetes, highlighting the necessity for continued, in-depth research in this area [155]. Ultimately, by embracing both ancient wisdom and modern scientific inquiry, we can foster a more comprehensive understanding of *A. membranaceus* and its vital role in contemporary medicine. Such an approach will help pave the way for innovative botanical therapies that align with future health trends aimed at enhancing preventive care and improving the health outcomes of individuals across diverse populations.

# Chapter 5

# Conclusion and Future Prospects

This study highlights the enormous potential of *Astragalus membranaceus* leaf extract as an antidiabetic and antioxidant agent, particularly through the method of fractionation. The results lend strong support to the utilization of *A. membranaceus* in traditional medicine, demonstrating that the AF2 super-fraction possesses a potent ability to regulate glucose levels and combat oxidative stress. These findings not only align with existing literature but also provide a scientifically validated basis for the traditional applications of this herb, encouraging its broader acceptance in both herbal and clinical pharmaceutical contexts. The corroboration of traditional uses with empirical evidence emphasizes the significance of integrating ethnobotanical knowledge with modern scientific methodologies.

In addition to the observed antioxidant and antidiabetic properties, an in silico study suggests that the riboflavin molecule found in the AF2 fraction may bind to target proteins, indicating its potential as a promising anti-diabetic medication in the future. The ability of riboflavin to influence various metabolic pathways through specific protein interactions opens new avenues for drug development. This discovery highlights the importance of exploring individual constituents within herbal extracts as they may have unique therapeutic roles that could be harnessed for effective treatment strategies in diabetes management. Such an approach not only enhances our understanding of the herb's bioactive

compounds but also prioritizes the development of standardized extracts that can be reliably used in clinical settings.

However, while these preliminary findings are encouraging, further studies are essential to confirm the efficacy and safety of *A. membranaceus* extracts in vivo and clinical settings. Future research should prioritize the use of diabetes-specific pancreatic cell lines, such as INS cell lines, to ascertain the bioactivity of different fractions and clarify their mechanisms of action. This research will provide critical insights into how the extract interacts with insulin signaling pathways and other metabolic processes. Such understanding is essential for developing therapeutic strategies that exploit these bioactive compounds effectively.

Moreover, future studies should investigate the detailed profiles of the active substances responsible for the observed antidiabetic and antioxidant activities. Understanding their chemical structures, concentrations, and potential synergistic effects when combined with other bioactive compounds will be crucial for optimizing formulations that maximize therapeutic benefits. Identifying the mechanisms through which these compounds exert their effects will allow researchers to tailor interventions more precisely, potentially increasing efficacy and patient adherence to treatment regimens.

It is also important to explore potential interactions between these herbal compounds and conventional diabetes medications. Evaluating the possibility of synergistic effects when used alongside established antidiabetic therapies could lead to the development of more comprehensive treatment protocols that enhance the overall effectiveness of diabetes management while minimizing the risk of adverse effects. Such integrative approaches are important as they align with the growing emphasis on personalized medicine.

Furthermore, researchers should explore the applications of *A. membranaceus* extracts in the context of functional foods. Incorporating these natural compounds into dietary interventions could enhance their health benefits and contribute to the prevention and management of metabolic disorders such as diabetes. This approach not only promotes healthy eating habits but may also lead to improved

metabolic health in the general population. The increasing consumer interest in functional foods offers a unique opportunity to market *A. membranaceus* as part of a health-promoting diet, emphasizing its natural origins and minimal side effects compared to synthetic drugs.

Overall, the implications of this research extend beyond pharmacological applications. *A. membranaceus* presents an exceptional opportunity to improve public health initiatives aimed at diabetes management and prevention.

By promoting natural therapies, we can enhance the accessibility of effective treatments for diabetes and related diseases, especially in regions where conventional medications may be limited or unaffordable. Advocating for the integration of herbal medicines into healthcare systems could lead to a more holistic approach to managing chronic diseases, providing patients with multiple avenues of care that are tailored to their needs.

In conclusion, this study not only highlights the medicinal value of *A. membranaceus* but also sets the stage for future explorations into its potential as a natural therapeutic agent.

Continued investigation into the active constituents, their mechanisms of action, and their interactions with conventional therapies will unlock new possibilities for diabetes treatment and enhance health outcomes for individuals worldwide. The quest for innovative, effective, and accessible treatment options is more critical than ever.

*A. membranaceus* stands at the forefront of this endeavor, promising substantial contributions to the fight against diabetes and related health challenges. Future research can further explore the feasibility of integrating *A. membranaceus* into existing treatment protocols, focusing not only on its efficacy but also on patient-centered outcomes such as quality of life, cost-effectiveness, and long-term sustainability. By fostering collaboration between traditional medicine practitioners, researchers, and healthcare providers, we can cultivate a comprehensive understanding of this herb, ultimately harnessing it as a valuable resource in the global effort to combat diabetes and enhance public health initiatives.

Through dedicated investigations and collaborative efforts, we can ensure that the benefits of *A. membranaceus* are not only recognized but also systematically integrated into patient care paradigms. This integration has the potential to improve the quality of life for individuals affected by chronic conditions such as diabetes and to support broader community health initiatives. By embracing both the wisdom of traditional practices and the rigor of modern science, we can help ensure that *A. membranaceus* plays a vital role in the development of new, effective strategies for diabetes management and prevention in the future.

In summary, as we look towards future research directions, the potential applications of *A. membranaceus* in functional foods, dietary supplements, and integrative health approaches warrant thorough investigation. By focusing our efforts on these areas, we can unveil its full therapeutic potential, allowing it to make a meaningful impact on public health and wellness in combating diabetes and other related conditions. Ultimately, these combined efforts may lead to a transformative shift in how we approach metabolic health, blending the strengths of traditional herbal medicine with the advancements of modern science.

# Bibliography

[1] E. D. Abel *et al.*, "Diabetes mellitus—progress and opportunities in the evolving epidemic," *Cell*, vol. 187, no. 15, pp. 3789–3820, 2024.

[2] M.-Á. Núñez-Baila, A. Gómez-Aragón, A.-M. Marques-Silva, and J. R. González-López, "Lifestyle in emerging adults with type 1 diabetes mellitus: A qualitative systematic review," *Healthcare*, vol. 12, no. 3, p. 309, 2024.

[3] X. Lu *et al.*, "Type 2 diabetes mellitus in adults: pathogenesis, prevention and therapy," *Signal Transduction and Targeted Therapy*, vol. 9, no. 1, p. 262, 2024.

[4] S. Latha and R. Vijayakumar, "The facts about diabetes mellitus-a review," *Galore International Journal of Health Sciences and Research*, vol. 4, no. 2, pp. 64–75, 2019.

[5] S. Bellary, I. Kyrou, J. E. Brown, and C. J. Bailey, "Type 2 diabetes mellitus in older adults: clinical considerations and management," *Nature Reviews Endocrinology*, vol. 17, no. 9, pp. 534–548, 2021.

[6] E. D. Szmuilowicz, J. L. Josefson, and B. E. Metzger, "Gestational diabetes mellitus," *Endocrinology and Metabolism Clinics*, vol. 48, no. 3, pp. 479–493, 2019.

[7] K. M. Jang, "Maturity-onset diabetes of the young: update and perspectives on diagnosis and treatment," *Yeungnam University Journal of Medicine*, vol. 37, no. 1, pp. 13–21, 2020.

[8] J. Beltrand *et al.*, "Neonatal diabetes mellitus," *Frontiers in Pediatrics*, vol. 8, p. 540718, 2020.

[9] S. K. Bhattamisra *et al.*, "Type-3c diabetes mellitus, diabetes of exocrine pancreas-an update," *Current Diabetes Reviews*, vol. 15, no. 5, pp. 382–394, 2019.

[10] S. Davies, "Latent autoimmune diabetes in adults (lada): What do primary care professionals need to know," *Journal of Diabetes Nursing*, vol. 25, no. 3, 2021.

[11] M. K. Hahn, A. Giacca, and S. Pereira, "In vivo techniques for assessment of insulin sensitivity and glucose metabolism," *Journal of Endocrinology*, vol. 260, no. 3, 2024.

[12] W.-C. Lin, B.-C. Hoe, X. Li, D. Lian, and X. Zeng, "Glucose metabolism-modifying natural materials for potential feed additive development," *Pharmaceutics*, vol. 16, no. 9, p. 1208, 2024.

[13] E. Scoditti, S. Sabatini, F. Carli, and A. Gastaldelli, "Hepatic glucose metabolism in the steatotic liver," *Nature Reviews Gastroenterology & Hepatology*, pp. 1–16, 2024.

[14] L. Lema-Pérez, "Main organs involved in glucose metabolism," in *Risks and Benefits and the Global Diabetes Epidemic*. IntechOpen, 2021.

[15] Q. Jiang *et al.*, "Postprandial regulation of glucose metabolism and insulin signaling pathways in macrobrachium rosenbergii," *Aquaculture Reports*, vol. 39, p. 102501, 2024.

[16] D. E. James, J. Stöckli, and M. J. Birnbaum, "The aetiology and molecular landscape of insulin resistance," *Nature Reviews Molecular Cell Biology*, vol. 22, no. 11, pp. 751–771, 2021.

[17] S. J. Humphrey *et al.*, "Dynamic adipocyte phosphoproteome reveals that akt directly regulates mtorc2," *Cell Metabolism*, vol. 17, no. 6, pp. 1009–1020, 2013.

[18] C. Rask-Madsen and C. R. Kahn, "Tissue–specific insulin signaling, metabolic syndrome, and cardiovascular disease," *Arteriosclerosis, Thrombosis, and Vascular Biology*, vol. 32, no. 9, pp. 2052–2059, 2012.

[19] D. H. Akhtar, U. Iqbal, L. M. Vazquez-Montesino, B. B. Dennis, and A. Ahmed, "Pathogenesis of insulin resistance and atherogenic dyslipidemia in nonalcoholic fatty liver disease," *Journal of Clinical and Translational Hepatology*, vol. 7, no. 4, p. 362, 2019.

[20] D. Leto and A. R. Saltiel, "Traffic control of glut4: regulation of glucose transport by insulin," *Nature Reviews Molecular Cell Biology*, vol. 13, no. 6, pp. 383–396, 2012.

[21] Y. Mugabo and G. E. Lim, "Scaffold proteins: from coordinating signaling pathways to metabolic regulation," *Endocrinology*, vol. 159, no. 11, pp. 3615–3630, 2018.

[22] J.-M. Schwarz, M. Clearfield, and K. Mulligan, "Conversion of sugar to fat: is hepatic de novo lipogenesis leading to metabolic syndrome and associated chronic diseases?" *The Journal of the American Osteopathic Association*, vol. 117, no. 8, pp. 520–527, 2017.

[23] P. Morigny, M. Houssier, E. Mouisel, and D. Langin, "Adipocyte lipolysis and insulin resistance," *Biochimie*, vol. 125, pp. 259–266, 2016.

[24] T. Chen *et al.*, "Mir-27a promotes insulin resistance and mediates glucose metabolism by targeting ppar-gamma-mediated pi3k/akt signaling," *Aging*, vol. 11, no. 18, p. 7510, 2019.

[25] S. Takahashi, T. Tanaka, T. Kodama, and J. Sakai, "Peroxisome proliferator-activated receptor delta (ppar-delta), a novel target site for drug discovery in metabolic syndrome," *Pharmacological Research*, vol. 53, no. 6, pp. 501–507, 2006.

[26] R. Tomar, S. Mishra, J. Sahoo, and S. K. Rath, "Computational investigation of phytochemicals from allamanda cathartica as a potent agonist

of peroxisome proliferator-activated receptor-gamma (ppar-gamma) for the treatment of diabetes mellitus," 2024.

[27] L. Wang *et al.*, "Natural product agonists of peroxisome proliferator-activated receptor gamma (ppar-gamma): a review," *Biochemical Pharmacology*, vol. 92, no. 1, pp. 73–89, 2014.

[28] L. P. Christensen and R. B. El-Houri, "Development of an in vitro screening platform for the identification of partial ppar-gamma agonists as a source for antidiabetic lead compounds," *Molecules*, vol. 23, no. 10, p. 2431, 2018.

[29] H. A. Hamouda, S. M. Mansour, and M. F. Elyamany, "Vitamin d combined with pioglitazone mitigates type-2 diabetes-induced hepatic injury through targeting inflammation, apoptosis, and oxidative stress," *Inflammation*, vol. 45, no. 1, pp. 156–171, 2022.

[30] R. A. DeFronzo, "From the triumvirate to the ominous octet: a new paradigm for the treatment of type 2 diabetes mellitus," *Diabetes*, vol. 58, no. 4, pp. 773–795, 2009.

[31] J. E. Lima, N. C. Moreira, and E. T. Sakamoto-Hojo, "Mechanisms underlying the pathophysiology of type 2 diabetes: From risk factors to oxidative stress, metabolic dysfunction, and hyperglycemia," *Mutation Research/Genetic Toxicology and Environmental Mutagenesis*, vol. 874, p. 503437, 2022.

[32] R. Khalilov and S. Abdullayeva, "Mechanisms of insulin action and insulin resistance," *Advances in Biology & Earth Sciences*, vol. 8, no. 2, 2023.

[33] L. H. Philipson, "Harnessing heterogeneity in type 2 diabetes mellitus," *Nature Reviews Endocrinology*, vol. 16, no. 2, pp. 79–80, 2020.

[34] T. M. Batista, N. Haider, and C. R. Kahn, "Defining the underlying defect in insulin action in type 2 diabetes," *Diabetologia*, vol. 64, pp. 994–1006, 2021.

[35] K. Lyu *et al.*, "A membrane-bound diacylglycerol species induces pkc-epsilon-mediated hepatic insulin resistance," *Cell Metabolism*, vol. 32, no. 4, pp. 654–664, 2020.

[36] M. Raciti, L. V. Lotti, S. Valia, F. Pulcinelli, and L. Di Renzo, "Jnk2 is activated during er stress and promotes cell survival," *Cell Death & Disease*, vol. 3, no. 11, p. e429, 2012.

[37] International Diabetes Federation, "Idf diabetes atlas 11th edition," https://diabetesatlas.org/resources/idf-diabetes-atlas-2025/, 2025, accessed: 2026.

[38] K. Copps and M. White, "Regulation of insulin sensitivity by serine/threonine phosphorylation of insulin receptor substrate proteins irs1 and irs2," *Diabetologia*, vol. 55, pp. 2565–2582, 2012.

[39] P. Lebrun and E. Van Obberghen, "Socs proteins causing trouble in insulin action," *Acta Physiologica*, vol. 192, no. 1, pp. 29–36, 2008.

[40] N. E. Cummings *et al.*, "Restoration of metabolic health by decreased consumption of branched-chain amino acids," *The Journal of Physiology*, vol. 596, no. 4, pp. 623–645, 2018.

[41] D. Cozzone *et al.*, "Isoform-specific defects of insulin stimulation of akt/protein kinase b (pkb) in skeletal muscle cells from type 2 diabetic patients," *Diabetologia*, vol. 51, pp. 512–521, 2008.

[42] T. M. Batista *et al.*, "A cell-autonomous signature of dysregulated protein phosphorylation underlies muscle insulin resistance in type 2 diabetes," *Cell Metabolism*, vol. 32, no. 5, pp. 844–859, 2020.

[43] M. Vujkovic *et al.*, "Discovery of 318 new risk loci for type 2 diabetes and related vascular outcomes among 1.4 million participants in a multi-ancestry meta-analysis," *Nature Genetics*, vol. 52, no. 7, pp. 680–691, 2020.

[44] M. Katayama *et al.*, "Circulating exosomal mir-20b-5p is elevated in type 2 diabetes and could impair insulin action in human skeletal muscle," *Diabetes*, vol. 68, no. 3, pp. 515–526, 2019.

[45] S. R. K. S. Kale, "Diabetes associated complicated disorders and its treatment a review article," *World Journal of Current Medical and Pharmaceutical Research*, pp. 99–106, 2023.

[46] W. Zhang *et al.*, "A review of the pharmacological action of astragalus polysaccharide," *Frontiers in Pharmacology*, vol. 10, p. 1049, 2019.

[47] ——, "Astragalus (huáng qí): Benefits, side effects and dosage," Healthline, 2025, accessed Oct. 28, 2025.

[48] D. Deiss *et al.*, "Astragalus: Usefulness and safety," National Center for Complementary and Integrative Health (NCCIH), 2025, accessed Oct. 28, 2025.

[49] Y. Xu *et al.*, "Astragalus membranaceus: A review of its protection against various diseases," *Phytotherapy Research*, vol. 30, no. 3, pp. 350–358, 2016.

[50] ——, "A review of the botany, phytochemistry, traditional uses, pharmacology, toxicology and clinical applications of astragalus (huangqi)," *Frontiers in Pharmacology*, vol. 14, 2023.

[51] T. S. Jensen *et al.*, "Pharmacological effects of astragalus polysaccharides in treating neurodegenerative diseases," *Frontiers in Pharmacology*, vol. 15, 2024.

[52] ——, "Anti-aging implications of astragalus membranaceus (huangqi)," *Aging and Disease*, vol. 8, no. 6, pp. 868–886, 2017.

[53] D. Deiss *et al.*, "Review of the botanical characteristics, phytochemistry, and pharmacology of astragali radix," *Fitoterapia*, vol. 93, pp. 209–221, 2014.

[54] J. A. Janssen, "Hyperinsulinemia and its pivotal role in aging, obesity, type 2 diabetes, cardiovascular disease and cancer," *International Journal of Molecular Sciences*, vol. 22, no. 15, p. 7797, 2021.

[55] D. O. Soyoye, O. O. Abiodun, R. T. Ikem, B. A. Kolawole, and A. O. Akintomide, "Diabetes and peripheral artery disease: A review," *World Journal of Diabetes*, vol. 12, no. 6, p. 827, 2021.

[56] S. Thipsawat, "Early detection of diabetic nephropathy in patient with type 2 diabetes mellitus: A review of the literature," *Diabetes and Vascular Disease Research*, vol. 18, no. 6, p. 14791641211058856, 2021.

[57] T. S. Jensen *et al.*, "Painful and non-painful diabetic neuropathy, diagnostic challenges and implications for future management," *Brain*, vol. 144, no. 6, pp. 1632–1645, 2021.

[58] T. Salmen, B. M. Mihai, R. A. Iarca, B. A. Stan, V. Dima, and R. E. Bohiltea, "Diabetes mellitus and periodontal disease," *Romanian Journal of Stomatology*, vol. 67, pp. 244–246, 2021.

[59] M. Monteiro-Soares, J. Vale-Lima, J. Martiniano, S. Pinheiro-Torres, V. Dias, and E. J. Boyko, "A systematic review with meta-analysis of the impact of access and quality of diabetic foot care delivery in preventing lower extremity amputation," *Journal of Diabetes and its Complications*, vol. 35, no. 4, p. 107837, 2021.

[60] R. Krishnan, R. Subramanian, and R. Selvarajan, "Technological and therapeutic approaches to type 2 diabetes management," 2023.

[61] T. Haak *et al.*, "Flash glucose-sensing technology as a replacement for blood glucose monitoring for the management of insulin-treated type 2 diabetes: a multicenter, open-label randomized controlled trial," *Diabetes Therapy*, vol. 8, pp. 55–73, 2017.

[62] D. Deiss *et al.*, "Clinical practice recommendations on the routine use of eversense, the first long-term implantable continuous glucose monitoring system," *Diabetes Technology & Therapeutics*, vol. 21, no. 5, pp. 254–264, 2019.

[63] F. Grosser *et al.*, "Design of the davos study: Diabetes smartphone app, a fully automatic transmission of data from the blood glucose meter and insulin pens using wireless technology to enhance diabetes self-management," *Journal of Diabetes Science and Technology*, vol. 17, no. 3, pp. 742–750, 2023.

[64] D. C. Klonoff and D. Kerr, "Smart pens will improve insulin therapy," *Journal of Diabetes Science and Technology*, vol. 12, no. 3, pp. 551–553, 2018.

[65] S. Schlesinger, M. Neuenschwander, A. Ballon, U. Nöthlings, and J. Barbaresko, "Adherence to healthy lifestyles and incidence of diabetes and mortality among individuals with diabetes: a systematic review and meta-analysis of prospective studies," *Journal of Epidemiology and Community Health*, vol. 74, no. 5, pp. 481–487, 2020.

[66] E. Sanchez-Rangel and S. E. Inzucchi, "Metformin: clinical use in type 2 diabetes," *Diabetologia*, vol. 60, pp. 1586–1593, 2017.

[67] N. Thangavel, M. Al Bratty, S. Akhtar Javed, W. Ahsan, and H. A. Alhazmi, "Targeting peroxisome proliferator-activated receptors using thiazolidinediones: strategy for design of novel antidiabetic drugs," *International Journal of Medicinal Chemistry*, vol. 2017, p. 1069718, 2017.

[68] C. L. Roumie *et al.*, "Comparative effectiveness of sulfonylurea and metformin monotherapy on cardiovascular events in type 2 diabetes mellitus: a cohort study," *Annals of Internal Medicine*, vol. 157, no. 9, pp. 601–610, 2012.

[69] S. L. Kristensen *et al.*, "Cardiovascular, mortality, and kidney outcomes with glp-1 receptor agonists in patients with type 2 diabetes: a systematic review and meta-analysis of cardiovascular outcome trials," *The Lancet Diabetes & Endocrinology*, vol. 7, no. 10, pp. 776–785, 2019.

[70] R. Nistala and V. Savin, "Diabetes, hypertension, and chronic kidney disease progression: role of dpp4," *American Journal of Physiology-Renal Physiology*, vol. 312, no. 4, pp. F661–F670, 2017.

[71] S. Kalra, "Alpha glucosidase inhibitors," *Journal of the Pakistan Medical Association*, vol. 64, no. 4, pp. 474–476, 2014.

[72] B. M. Bonora, A. Avogaro, and G. P. Fadini, "Extraglycemic effects of sglt2 inhibitors: a review of the evidence," *Diabetes, Metabolic Syndrome and Obesity: Targets and Therapy*, vol. 13, pp. 161–174, 2020.

[73] L. Hieronymus and S. Griffin, "Role of amylin in type 1 and type 2 diabetes," *The Diabetes Educator*, vol. 41, no. 1_suppl, pp. 47S–56S, 2015.

[74] M. A. Nauck and D. A. D'Alessio, "Tirzepatide, a dual gip/glp-1 receptor co-agonist for the treatment of type 2 diabetes with unmatched effectiveness regarding glycaemic control and body weight reduction," *Cardiovascular Diabetology*, vol. 21, no. 1, p. 169, 2022.

[75] C. S. Marathe, C. K. Rayner, T. Wu, K. L. Jones, and M. Horowitz, "Gastrointestinal disorders in diabetes," in *Endotext*. MDtext, Inc., 2024.

[76] R. DeFronzo, G. A. Fleming, K. Chen, and T. A. Bicsak, "Metformin-associated lactic acidosis: Current perspectives on causes and risk," *Metabolism*, vol. 65, no. 2, pp. 20–29, 2016.

[77] C. R. Triggle and H. Ding, "Cardiovascular impact of drugs used in the treatment of diabetes," *Therapeutic Advances in Chronic Disease*, vol. 5, no. 6, pp. 245–268, 2014.

[78] C. V. Dave *et al.*, "Sodium-glucose cotransporter-2 inhibitors and the risk for severe urinary tract infections: a population-based cohort study," *Annals of Internal Medicine*, vol. 171, no. 4, pp. 248–256, 2019.

[79] R. M. DiSogra and J. Meece, "Auditory and vestibular side effects of fda-approved drugs for diabetes," in *Seminars in Hearing*, vol. 40, no. 04, 2019, pp. 315–326.

[80] N. M. George, P. M. Sangolli, A. Thulaseedharan, and S. Dominic, "Cutaneous adverse drug reactions to antidiabetic medications and medical devices used in management of diabetes mellitus," *Journal of Skin and Stem Cell*, vol. 11, no. 2, 2024.

[81] L. Wilson and J. J. Saseen, "Gouty arthritis: a review of acute management and prevention," *Pharmacotherapy: The Journal of Human Pharmacology and Drug Therapy*, vol. 36, no. 8, pp. 906–922, 2016.

[82] B. Jacob and R. Narendhirakannan, "Role of medicinal plants in the management of diabetes mellitus: a review," *3 Biotech*, vol. 9, p. 4, 2019.

[83] B. Salehi *et al.*, "Antidiabetic potential of medicinal plants and their active components," *Biomolecules*, vol. 9, no. 10, p. 551, 2019.

[84] G. Kavishankar, N. Lakshmidevi, S. M. Murthy, H. Prakash, and S. Niranjana, "Diabetes and medicinal plants-a review," *International Journal of Pharmaceutical and Biomedical Sciences*, vol. 2, no. 3, pp. 65–80, 2011.

[85] B. Moradi, S. Abbaszadeh, S. Shahsavari, M. Alizadeh, and F. Beyranvand, "The most useful medicinal herbs to treat diabetes," *Biomedical Research and Therapy*, vol. 5, no. 8, pp. 2538–2551, 2018.

[86] P. Ansari *et al.*, "Pharmacologically active phytomolecules isolated from traditional antidiabetic plants and their therapeutic role for the management of diabetes mellitus," *Molecules*, vol. 27, no. 13, p. 4278, 2022.

[87] Adedapo and I. Ogunmiluyi, "The use of natural products in the management of diabetes: The current trends," *Journal of Drug Delivery and Therapeutics*, vol. 10, no. 1, pp. 153–162, 2020.

[88] P. Ansari *et al.*, "Plant-based diets and phytochemicals in the management of diabetes mellitus and prevention of its complications: a review," *Nutrients*, vol. 16, no. 21, p. 3709, 2024.

[89] V. D. Kappel *et al.*, "Involvement of glut-4 in the stimulatory effect of rutin on glucose uptake in rat soleus muscle," *Journal of Pharmacy and Pharmacology*, vol. 65, no. 8, pp. 1179–1186, 2013.

[90] F. Li, C. Zhao, and L. Wang, "Molecular-targeted agents combination therapy for cancer: developments and potentials," *International Journal of Cancer*, vol. 134, no. 6, pp. 1257–1269, 2014.

[91] R. C. R. Latha and P. Daisy, "Insulin-secretagogue, antihyperlipidemic and other protective effects of gallic acid isolated from terminalia bellerica roxb.

in streptozotocin-induced diabetic rats," *Chemico-Biological Interactions*, vol. 189, no. 1-2, pp. 112–118, 2011.

[92] M. D. Girón *et al.*, "Salacia oblonga extract increases glucose transporter 4-mediated glucose uptake in l6 rat myotubes: role of mangiferin," *Clinical Nutrition*, vol. 28, no. 5, pp. 565–574, 2009.

[93] P. K. Prabhakar and M. Doble, "Effect of natural products on commercial oral antidiabetic drugs in enhancing 2-deoxyglucose uptake by 3t3-l1 adipocytes," *Therapeutic Advances in Endocrinology and Metabolism*, vol. 2, no. 3, pp. 103–114, 2011.

[94] M. Liu, K. Wu, X. Mao, Y. Wu, and J. Ouyang, "Astragalus polysaccharide improves insulin sensitivity in kkay mice: regulation of pkb/glut4 signaling in skeletal muscle," *Journal of Ethnopharmacology*, vol. 127, no. 1, pp. 32–37, 2010.

[95] S. H. Cheong *et al.*, "Daidzein promotes glucose uptake through glucose transporter 4 translocation to plasma membrane in l6 myocytes and improves glucose homeostasis in type 2 diabetic model mice," *The Journal of Nutritional Biochemistry*, vol. 25, no. 2, pp. 136–143, 2014.

[96] M. F. Khan, P. Dixit, N. Jaiswal, A. K. Tamrakar, A. K. Srivastava, and R. Maurya, "Chemical constituents of kigelia pinnata twigs and their glut4 translocation modulatory effect in skeletal muscle cells," *Fitoterapia*, vol. 83, no. 1, pp. 125–129, 2012.

[97] M. F. Khan *et al.*, "Design and synthesis of lupeol analogues and their glucose uptake stimulatory effect in l6 skeletal muscle cells," *Bioorganic & Medicinal Chemistry Letters*, vol. 24, no. 12, pp. 2674–2679, 2014.

[98] Y. He *et al.*, "Ursolic acid increases glucose uptake through the pi3k signaling pathway in adipocytes," *PLoS One*, vol. 9, no. 10, p. e110711, 2014.

[99] D. H. Priscilla, M. Jayakumar, and K. Thirumurugan, "Flavanone naringenin: An effective antihyperglycemic and antihyperlipidemic nutraceutical

agent on high fat diet fed streptozotocin induced type 2 diabetic rats," *Journal of Functional Foods*, vol. 14, pp. 363–373, 2015.

[100] C. Zhu *et al.*, "Effects of marine collagen peptides on glucose metabolism and insulin resistance in type 2 diabetic rats," *Journal of Food Science and Technology*, vol. 54, pp. 2260–2269, 2017.

[101] J. Runtuwene *et al.*, "Rosmarinic acid ameliorates hyperglycemia and insulin sensitivity in diabetic rats, potentially by modulating the expression of pepck and glut4," *Drug Design, Development and Therapy*, vol. 10, pp. 2193–2202, 2016.

[102] T. Wang *et al.*, "Baicalin and its metabolites suppresses gluconeogenesis through activation of ampk or akt in insulin resistant hepg-2 cells," *European Journal of Medicinal Chemistry*, vol. 141, pp. 92–100, 2017.

[103] F.-L. Hsu *et al.*, "Antidiabetic effects of pterosin a, a small-molecular-weight natural product, on diabetic mouse models," *Diabetes*, vol. 62, no. 2, pp. 628–638, 2013.

[104] G. M. Do *et al.*, "Resveratrol ameliorates diabetes-related metabolic changes via activation of amp-activated protein kinase and its downstream targets in db/db mice," *Molecular Nutrition & Food Research*, vol. 56, no. 8, pp. 1282–1291, 2012.

[105] K. W. Ong, A. Hsu, and B. K. H. Tan, "Anti-diabetic and anti-lipidemic effects of chlorogenic acid are mediated by ampk activation," *Biochemical Pharmacology*, vol. 85, no. 9, pp. 1341–1351, 2013.

[106] J. Sun *et al.*, "Hypoglycemic effect and mechanism of honokiol on type 2 diabetic mice," *Drug Design, Development and Therapy*, vol. 9, pp. 6327–6342, 2015.

[107] H. Alkhalidy *et al.*, "Small molecule kaempferol promotes insulin sensitivity and preserved pancreatic beta-cell mass in middle-aged obese diabetic mice," *Journal of Diabetes Research*, vol. 2015, p. 532984, 2015.

[108] P. Kalhotra, V. C. Chittepu, G. Osorio-Revilla, and T. Gallardo-Velázquez, "Discovery of galangin as a potential dpp-4 inhibitor that improves insulin-stimulated skeletal muscle glucose uptake: a combinational therapy for diabetes," *International Journal of Molecular Sciences*, vol. 20, no. 5, p. 1228, 2019.

[109] S. R. Klopfenstein *et al.*, "1, 2, 3, 4-tetrahydroisoquinolinyl sulfamic acids as phosphatase ptp1b inhibitors," *Bioorganic & Medicinal Chemistry Letters*, vol. 16, no. 6, pp. 1574–1578, 2006.

[110] M. Rehan and O. S. Bajouh, "Virtual screening of naphthoquinone analogs for potent inhibitors against the cancer-signaling pi3k/akt/mtor pathway," *Journal of Cellular Biochemistry*, vol. 120, no. 2, pp. 1328–1339, 2019.

[111] S. S. Swain and R. N. Padhy, "In vitro antibacterial efficacy of plants used by an indian aboriginal tribe against pathogenic bacteria isolated from clinical samples," *Journal of Taibah University Medical Sciences*, vol. 10, no. 4, pp. 379–390, 2015.

[112] R. K. Mishra *et al.*, "In silico modeling-based identification of glucose transporter 4 (glut4)-selective inhibitors for cancer therapy," *Journal of Biological Chemistry*, vol. 290, no. 23, pp. 14 441–14 453, 2015.

[113] R. M. DiSogra and J. Meece, "Auditory and vestibular side effects of fda-approved drugs for diabetes," in *Seminars in Hearing*, vol. 40, no. 4. Thieme Medical Publishers, 2019, pp. 315–326.

[114] N. M. George, P. M. Sangolli, A. Thulaseedharan, and S. Dominic, "Cutaneous adverse drug reactions to antidiabetic medications and medical devices used in management of diabetes mellitus," *Journal of Skin and Stem Cell*, vol. 11, no. 2, 2024.

[115] L. Wilson and J. J. Saseen, "Gouty arthritis: a review of acute management and prevention," *Pharmacotherapy: The Journal of Human Pharmacology and Drug Therapy*, vol. 36, no. 8, pp. 906–922, 2016.

[116] Y. Zhang *et al.*, "Review of astragalus membranaceus polysaccharides: Extraction, structural characterization and biological activities," *Journal of Integrative Agriculture*, 2024.

[117] L. Wang *et al.*, "Beneficial effects of astragalus membranaceus (fisch.) bunge on allergic airway inflammation," *International Journal of Molecular Sciences*, 2023.

[118] WebMD, "Astragalus – uses, side effects, and more," https://www.webmd.com, 2025, accessed Oct. 28, 2025.

[119] X. Li *et al.*, "Astragaloside iv derived from astragalus membranaceus – pharmacological effects, pharmacokinetics and toxicity," *Life Sciences*, vol. 232, p. 116635, 2019.

[120] H. Chen *et al.*, "Exploring the role and mechanism of astragalus membranaceus in wound healing and fibrotic diseases," *Scientific Reports*, vol. 13, p. 12345, 2023.

[121] M. Schmidt *et al.*, "Astragalus (chinese herbal) in sports: supplementation potential in athletes," *MDPI*, 2024.

[122] A. Johnson *et al.*, "The anti-cancerous activity of adaptogenic herb astragalus: a review," *Phytomedicine*, 2021.

[123] R. Kumar *et al.*, "Exploring the role of astragalus for gut health, immune system, and antioxidant status," *Animal Frontiers*, 2024.

[124] A. N. Alamgir, "Herbal drugs: their collection, preservation, and preparation; evaluation, quality control, and standardization of herbal drugs," in *Therapeutic Use of Medicinal Plants and Their Extracts: Volume 1: Pharmacognosy*. Cham: Springer International Publishing, sep 2017, pp. 453–495.

[125] D. Lee, D. H. Lee, S. Choi, J. S. Lee, D. S. Jang, and K. S. Kang, "Identification and isolation of active compounds from Astragalus membranaceus

that improve insulin secretion by regulating pancreatic $\beta$-cell metabolism," *Biomolecules*, vol. 9, no. 10, p. 618, oct 2019.

[126] M. Zych and A. Pyka Pajak, "TLC in the analysis of plant material," *Processes*, vol. 13, no. 11, p. 3497, oct 2025.

[127] X. M. Luan, Q. H. Sun, Y. Yang, R. Rong, and X. Wang, "Improvement of polarity-based solvent system for countercurrent chromatography in the guidance of solvent selectivity: n-hexane/ethyl acetate/alcohol solvents/water as an example," *Journal of Chromatography A*, vol. 1736, p. 465389, nov 2024.

[128] T. Kowalska and M. Sajewicz, "Thin-layer chromatography (TLC) in the screening of botanicals—its versatile potential and selected applications," *Molecules*, vol. 27, no. 19, p. 6607, oct 2022.

[129] D. Mayasari, Y. B. Murti, S. U. Pratiwi, and S. Sudarsono, "Antibacterial activity and TLC-densitometric analysis of secondary metabolites in the leaves of the traditional herb, Melastoma malabathricum L." *Borneo Journal of Pharmacy*, vol. 5, no. 4, pp. 334–344, nov 2022.

[130] L. Y. Ning, A. A. Azmi, D. F. Syamsumir, W. I. Ismail, and M. Maulidiani, "Phytochemical screening, TLC profile and $^{1}$H NMR analysis of Passiflora foetida extracts," *Universiti Malaysia Terengganu Journal of Undergraduate Research*, vol. 5, no. 2, pp. 65–74, apr 2023.

[131] P. K. Zarzycki, "Staining and derivatization techniques for visualization in planar chromatography," in *Instrumental Thin-Layer Chromatography*. Elsevier, jan 2023, pp. 213–257.

[132] R. Pungle, S. H. Nile, N. Makwana, R. Singh, R. P. Singh, and A. S. Kharat, "Green synthesis of silver nanoparticles using the Tridax procumbens plant extract and screening of its antimicrobial and anticancer activities," *Oxidative Medicine and Cellular Longevity*, vol. 2022, p. 9671594, 2022.

[133] S. A. Jafri, Z. M. Khalid, M. R. Khan, S. Ashraf, N. Ahmad, A. M. Karami *et al.*, "Evaluation of some essential traditional medicinal plants for their

potential free scavenging and antioxidant properties," *Journal of King Saud University-Science*, vol. 35, no. 3, p. 102562, apr 2023.

[134] G. J. Molole, A. Gure, and N. Abdissa, "Determination of total phenolic content and antioxidant activity of Commiphora mollis (Oliv.) Engl. resin," *BMC Chemistry*, vol. 16, no. 1, p. 48, jun 2022.

[135] S. A. Jaber, "In vitro alpha-amylase and alpha-glucosidase inhibitory activity and in vivo antidiabetic activity of Quercus coccifera (Oak tree) leaves extracts," *Saudi Journal of Biological Sciences*, vol. 30, no. 7, p. 103688, jul 2023.

[136] Y. Elouafy, A. El Yadini, S. Mortada, M. Hnini, H. Harhar, A. Khalid *et al.*, "Antioxidant, antimicrobial, and $\alpha$-glucosidase inhibitory activities of saponin extracts from walnut (Juglans regia L.) leaves," *Asian Pacific Journal of Tropical Biomedicine*, vol. 13, no. 2, pp. 60–69, feb 2023.

[137] B. Chibuye, I. Sen Singh, L. Chimuka, and K. K. Maseka, "Phytochemical and LCMS/MS screening, total phenolic and flavonoid content and antioxidant activity of the leaves of Diospyros batokana (Ebenaceae)," *MS Screening, Total Phenolic and Flavonoid Content and Antioxidant Activity of the Leaves of Diospyros Batokana (Ebenaceae)*, 2023.

[138] S. K. Burley, H. M. Berman, G. J. Kleywegt, J. L. Markley, H. Nakamura, and S. Velankar, "Protein data bank (pdb): the single global macromolecular structure archive," in *Protein Crystallography: Methods and Protocols*, 2017, pp. 627–641.

[139] W. L. DeLano, "PyMOL: An open-source molecular graphics tool," *CCP4 Newsletter on Protein Crystallography*, vol. 40, no. 1, pp. 82–92, 2002.

[140] R. Azimi, M. Ozgul, M. C. Kenney, and B. D. Kuppermann, "Bioinformatic analysis of small humanin like peptides using AlphaFold-2 and Expasy ProtParam," *Investigative Ophthalmology & Visual Science*, vol. 65, no. 7, pp. 1320–1320, 2024.

[141] A. Volkamer, D. Kuhn, F. Rippmann, and M. Rarey, "DoGSiteScorer: a web server for automatic binding site prediction, analysis and druggability assessment," *Bioinformatics*, vol. 28, no. 15, pp. 2074–2075, 2012.

[142] M. Butkiewicz, E. W. Lowe, and J. Meiler, "Benchmarking ligand-based virtual high-throughput screening with the PubChem database," *Molecules*, vol. 18, no. 1, pp. 735–756, 2013.

[143] V. K. Narayanaswamy, M. Rissdörfer, and B. Odhav, "Review on CambridgeSoft ChemBioDraw ultra 13.0 v," *International Journal of Theoretical & Applied Sciences*, vol. 5, pp. 45–49, 2013.

[144] C. A. Lipinski, "Lead- and drug-like compounds: the Rule-of-Five revolution," *Drug Discovery Today: Technologies*, vol. 1, no. 4, pp. 337–341, 2004.

[145] J. C. Dearden, "In silico prediction of ADMET properties: how far have we come?" *Expert Opinion on Drug Metabolism & Toxicology*, vol. 3, no. 5, pp. 635–639, 2007.

[146] N. S. Pagadala, K. Syed, and J. Tuszynski, "Software for molecular docking: a review," *Biophysical Reviews*, vol. 9, no. 2, pp. 91–102, 2017.

[147] D. A. Gschwend, A. C. Good, and I. D. Kuntz, "Molecular docking towards drug discovery," *Journal of Molecular Recognition*, vol. 9, no. 2, pp. 175–186, 1996.

[148] S. S. Pawar and S. H. Rohane, "Review on Discovery Studio: An important tool for molecular docking," 2021, preprint or conference paper (no journal/volume specified).

[149] D. S. Wishart, C. Knox, A. C. Guo, S. Shrivastava, M. Hassanali, P. Stothard, Z. Chang, and J. Woolsey, "DrugBank: a comprehensive resource for in silico drug discovery and exploration," *Nucleic Acids Research*, vol. 34, no. suppl_1, pp. D668–D672, 2006.

[150] J. Tibbitts, D. Canter, R. Graff, A. Smith, and L. A. Khawli, "Key factors influencing ADME properties of therapeutic proteins: A need for ADME

characterization in drug discovery and development," *mAbs*, vol. 8, no. 2, pp. 229–245, 2016.

[151] H. Van De Waterbeemd, D. A. Smith, K. Beaumont, and D. K. Walker, "Property-based design: optimization of drug absorption and pharmacokinetics," *Journal of Medicinal Chemistry*, vol. 44, no. 9, pp. 1313–1333, 2001.

[152] E. Sjögren, H. Thorn, and C. Tannergren, "In silico modeling of gastrointestinal drug absorption: predictive performance of three physiologically based absorption models," *Molecular Pharmaceutics*, vol. 13, no. 6, pp. 1763–1778, 2016.

[153] T. T. V. Tran, H. Tayara, and K. T. Chong, "Recent studies of artificial intelligence on in silico drug distribution prediction," *International Journal of Molecular Sciences*, vol. 24, no. 3, p. 1815, 2023.

[154] S. R. Kazmi, R. Jun, M.-S. Yu, C. Jung, and D. Na, "In silico approaches and tools for the prediction of drug metabolism and fate: A review," *Computers in Biology and Medicine*, vol. 106, pp. 54–64, 2019.

[155] G. Luo *et al.*, "In silico prediction of biliary excretion of drugs in rats based on physicochemical properties," *Drug Metabolism and Disposition*, vol. 38, no. 3, pp. 422–430, 2010.

[156] A. Roncaglioni, A. A. Toropov, A. P. Toropova, and E. Benfenati, "In silico methods to predict drug toxicity," *Current Opinion in Pharmacology*, vol. 13, no. 5, pp. 802–806, 2013.

[157] M. D. Segall and C. Barber, "Addressing toxicity risk when designing and selecting compounds in early drug discovery," *Drug Discovery Today*, vol. 19, no. 5, pp. 688–693, 2014.

[158] S. Vijayakumar, S. Manogar, S. Prabhu, M. Pugazhenthi, and P. Praseetha, "A pharmacoinformatic approach on Cannabinoid receptor 2 (CB2) and different small molecules: Homology modelling, molecular docking, MD simulations, drug designing and ADME analysis," *Computational Biology and Chemistry*, vol. 78, pp. 95–107, 2019.

[159] S. Durdagi, M. G. Papadopoulos, D. P. Papahatjis, and T. Mavromoustakos, "Combined 3D QSAR and molecular docking studies to reveal novel cannabinoid ligands with optimum binding activity," *Bioorganic & Medicinal Chemistry Letters*, vol. 17, no. 24, pp. 6754–6763, 2007.

[160] U. Baroroh, M. Biotek, Z. S. Muscifa, W. Destiarani, F. G. Rohmatullah, and M. Yusuf, "Molecular interaction analysis and visualization of protein-ligand docking using Biovia Discovery Studio Visualizer," *Indonesian Journal of Computational Biology (IJCB)*, vol. 2, no. 1, pp. 22–30, 2023.

[161] C. J. Bailey, "Metformin: Therapeutic profile in the treatment of type 2 diabetes," *Diabetes, Obesity and Metabolism*, vol. 26, pp. 3–19, aug 2024.

[162] P. Wang *et al.*, "A review of the botany, phytochemistry, traditional uses, pharmacology, toxicology, and quality control of the *astragalus membranaceus*," *Frontiers in Pharmacology*, vol. 14, Aug. 2023.

[163] S. Liu *et al.*, "The potential of astragalus polysaccharide for treating diabetes and its action mechanism," *Frontiers in Pharmacology*, vol. 15, Apr. 2024.

[164] P. P. Zhang *et al.*, "Astragalus membranaceus improves blood glucose and renal function in streptozotocin-induced diabetic kidney disease mice via gut microbial metabolite axis," *Fitoterapia*, Dec. 2025.

[165] Y.-C. Xiao *et al.*, "Bioactive components and clinical potential of *astragalus* species: A comprehensive review," *Frontiers in Pharmacology*, vol. 16, May 2025.

[166] HKUMed Team, "Combined therapy integrating chinese herb astragalus and methotrexate to overcome drug resistance in autoimmune diseases," HKU Med News, Jul. 2025, press release, 3 July 2025.

[167] K. Peltzer and N. a. a. T. a. t. b. a. m.-c. Pengpid, Supa, "The use of herbal medicines among chronic disease patients in thailand: A cross-sectional survey," *Therapeutic Advances in Drug Safety*, vol. 10, Jul. 2019.